# Differentiation of protective B cell responses in chronic viral infection

**Inauguraldissertation**

zur

Erlangung der Würde eines Doktors der Philosophie

vorgelegt der

Philosophisch-Naturwissenschaftlichen Fakultät

der Universität Basel

von

**Bénédict Fallet**

aus Cologny, Genf

Basel, 2017

Genehmigt von der Philosophisch-Naturwissenschaftlichen Fakultät auf Antrag von

Prof. Christoph Hess, Prof. Daniel Pinschewer, Prof. Otto Haller

Basel, den 20.09.2016

Prof. Dr. Jörg Schibler

# Table of Contents

# List of Figures

# List of Tables

# Abbreviations

| | |
|---|---|
| 7AAD | 7-aminoactinomycin D |
| Ab | Antibody |
| AID | Activation-induced cytidine deaminase |
| AM | Atypical memory |
| ANOVA | Analysis of variance |
| ART | Antiretroviral therapy |
| ASC | Antibody-secreting cell |
| BAFF | B-cell activation factor |
| BCL6 | B-cell lymphoma 6 protein |
| BCR | B cell receptor |
| BHK-21 | Baby Hamster Kidney 21 cells |
| BLIMP1 | B lymphocyte-induced maturation protein-1 |
| BM | Bone marrow |
| bnAb | broadly neutralizing Antibody |
| CCL | Chemokine ligand |
| CCR2 | C-C chemokine receptor type 2 |
| CD | Cluster of differentiation |
| CD40L | CD40 ligand |
| cDNA | complementary DNA |
| CFSE | Carboxyfluorescein succinimidyl ester |
| Cl13 | Clone-13 |
| CSR | Class switch recombination |
| CTL | Cytotoxic T lymphocyte |
| ctrl | control |
| CTV | Cell trace violet |
| CXCL13 | Chemokine (C-X-C motif) ligand 13 |
| CXCR5 | C-X-C chemokine receptor type 5 |
| DAPI | 4',6-diamidino-2-phénylindole |
| DC | Dendritic cell |
| DNA | Deoxyribonucleic acid |
| DNase | Deoxyribonuclease |
| EBV | Epstein-Barr virus |
| ELISA | Enzyme-linked immunosorbent assay |
| FACS | Fluorescence-activated cell sorting |
| FasL | Fas ligand |
| Fc | Fragment crystallizable |
| FCRL4 | Fc receptor-like protein 4 |
| FDC | Follicular dendritic cell |
| FITC | Fluorescein isothiocyanate |
| GC | Germinal center |
| GFP | Green fluorescent protein |
| GP | Glycoprotein |
| Gy | Gray |
| HBV | Hepatitis B virus |
| HCV | Hepatits C virus |
| HCMV | Human cytomegalovirus |

| | |
|---|---|
| HEK-293 | Human embryonic kidney 293 cells |
| HIV | Human immunodeficiency virus |
| HLA | Human leukocyte antigen |
| HSV | Herpes simplex virus |
| IFN | Interferon |
| IFNAR | IFN-alpha/beta receptor |
| Ig | Immunoglobulin |
| IL | Interleukin |
| iLN | inguinal Lymph node |
| InfMo | Inflammatory monocyte |
| iNOS | inducible Nitric oxide synthase |
| IRES | Internal ribosome entry site |
| IRF | Interferon regulatory factor |
| ISG | Interferon-stimulated gene |
| Jak | Janus kinase |
| KL25H | KL25 heavy chain |
| KL25HL | KL25 heavy and light chains |
| KL25L | KL25 light chain |
| LC | Light chain |
| LCMV | Lymphocytic choriomeningitis virus |
| LLPC | Long-lived plasma cell |
| LPS | Lipopolysaccharide |
| Ly6C | Lymphocyte antigen 6 complex, locus C |
| Ly6G | Lymphocyte antigen 6 complex, locus G |
| MACS | Magnetic-activated cell sorting |
| MCP1 | Monocyte chemoattractant protein 1 |
| memB | memory B cell |
| MHC | Major histocompatibility complex |
| mio | million |
| Mx | Myxovirus resistance protein |
| MZ | Marginal zone |
| nAb | neutralizing Antibody |
| Nef | Negative regulatory factor |
| NK | Natural killer cell |
| NP | Nucleoprotein |
| OAS | 2'-5'-oligoadenylate synthase |
| PAX5 | Paired box protein 5 |
| PB | Plasmablast |
| PC | Plasmacell |
| PD-1 | Programmed cell death 1 |
| pDC | plasmacytoid Dendritic cell |
| PDGFR | Platelet-derived growth factor |
| PFU | Plaque forming unit |
| PNA | Peanut agglutinin |
| RANTES | Regulated on activation, normal T cell expressed and secreted |
| rCl13 | recombinant Cl13-WE/GP |
| RNA | Ribonucleic acid |
| RNaseL | Ribonuclease L |
| RM | Resting memory |
| ROI | Region of interest |

| | |
|---|---|
| rVSV | recombinant VSV-WE/GP |
| SEM | Standard error of the mean |
| SHIV | Simian-Human immunodeficiency virus |
| SHM | Somatic hypermutation |
| SIV | Simian immunodeficiency virus |
| SPF | Specific pathogen free |
| SRBC | Sheep red blood cell |
| STAT | Signal transducer and activator of transcription |
| TD | T-dependent |
| TF | Transcription factor |
| Tfh | T follicular helper cell |
| tg | transgenic |
| Th1 | T helper 1 |
| TI | T-independent |
| TLM | Tissue-like memory |
| TLR | Toll-like receptor |
| TNF | Tumor necrosis factor |
| VSV | Vesicular stomatitis virus |
| VSVG | VSV glycoprotein |
| VV | Vaccinia virus |
| WHO | World Health Organization |
| wt | wilde type |
| XBP1 | X-box binding protein 1 |

# I Introduction

## I.1 Adaptive immune responses to acute and chronic viral infections

Acute viral infections are short-term, self-limiting infections that are readily cleared by the host immune defenses. Examples of such infections include infection with influenza and parainfluenza viruses or adenoviruses in humans, and vesicular stomatitis virus (VSV) infection in mice. Chronic viral infections are characterized by the ability of the infecting viruses to establish protracted albeit self-limiting or life-long infection. Examples thereof include infection with human immunodeficiency virus (HIV), hepatitis C virus (HCV) and in some instances hepatitis B virus (HBV). Such infections represent a major burden for global health. It is estimated that close to 40 million (mio) people are infected with HIV and that about 400 mio people suffer from chronic viral hepatitis worldwide (*1-3*). Despite several decades of research, neither curative treatments for HIV and chronic HBV infection, nor effective vaccination strategies against HIV and HCV are available.

Lymphocytic choriomeningitis virus (LCMV) is a murine prototypic viral infection model (see section 1.5). LCMV can establish either acute or chronic infection in mice, depending on the strain and dose of virus, on the route of infection, and on the host major histocompatibility complex class I (MHC-I) haplotype (*4, 5*). It has been widely used for several decades as a model to study virus-host interactions in mice.

LCMV-Armstrong infection of C57BL/6 mice leads to acute infection characterized by low-level or undetectable viremia, rapid clearance within two weeks, effective activation and differentiation of antiviral CD8$^+$ cytotoxic T lymphocytes (CTLs) (*5-7*). CTLs are critical whereas CD4$^+$ T helper cells and antiviral antibodies do not play an essential role for the clearance of acute LCMV infection (*7*). Upon infection, the CTL response occurs in three phases: the first activation and expansion phase of the CTL response is followed by a contraction phase and establishment of memory (*8*). During the initial phase of the response, virus-specific CTLs can expand up to $10^5$ fold (*9*). Similar expansion of antiviral CTLs has also been described in humans during acute viral infections (*10*). While proliferating, CTLs acquire effector functions, characterized by the production of inflammatory cytokines such as

interferon (IFN)-γ and tumor necrosis factor (TNF)-α, and by the acquisition of cytolytic activity (*11-14*). After the activation and expansion phase, antiviral CTLs enter a contraction phase during which the vast majority undergoes apoptosis, and about 5% survive and generate memory cells (*9, 15*). Finally, during the memory phase, a constant population of memory CTLs is maintained for a long period of time without antigenic stimulation. Memory CTLs display a resting phenotype but have the ability to respond rapidly to a new antigen exposure (*16, 17*).

In contrast, infection of C57BL/6 mice with LCMV Clone-13 induces chronic infection, characterized by protracted viremia and persistence of infectious virus particles in some organs for several months (*18, 19*). Such infection leads to the exhaustion of antiviral CTLs and $CD4^+$ T helper cells (*19-21*). Control of chronic LCMV infection eventually occurs after several months and relies not only on CTLs, as in the case of acute infection, but also on B cell responses, both of which depend on $CD4^+$ T cell help (*22-25*). Exhaustion of CTLs in chronic LCMV infection have been extensively studied and consist of a range of functional impairments characterized by the progressive loss of cytotoxic activity, cytokine production and proliferative capacity, and of physical loss of antiviral T cell clones (*19-21*). $CD4^+$ T cells have been shown to also display functional dysfunctions upon chronic LCMV infection (*26*). Although the mechanisms leading to $CD4^+$ T cell and CTLs exhaustion in chronic LCMV infection might differ, exhaustion is thought to result from persisting high antigen loads rather than from initial defect in priming and activation of T cells (*6, 27, 28*). Thus, high viral burden during chronic infection leads to both $CD4^+$ T cell and CTL dysfunction, which in turn favors viral persistence. Despite the described impairments of $CD4^+$ T cell and CTL responses, both cell types continue to exert antiviral effects, mediated either by the remaining antiviral activity of exhausted T cells or by a remaining pool of functional T cells (*26, 29*).

In addition to the critical role of T cells and unlike what is observed in acute infection, B cell and antibody responses play a critical role for the control of chronic LCMV infection. Indeed, virus-specific immunoglobulins M (IgMs) and IgGs have been shown to be essential to reduce viral load, thereby providing a key support to CTLs for the clearance of chronic LCMV infection (*22, 30-32*). Antiviral antibodies can be divided into neutralizing and non-neutralizing antibodies. Neutralizing antibodies (nAbs) are defined by the ability to prevent entry of viruses into target cells. In

chronic LCMV infection, the emergence of nAbs correlate with clearance of the virus (*31*). Moreover, nAb induction represent the only mechanistic correlate of protection of most currently available vaccines (*33*). In addition, nAbs have been shown to efficiently protect against infection in passive immunization experiments and recent studies even evidenced a potential curative role of nAbs in a mouse HCV model as well as in a monkey SHIV model (*34-39*). Therefore nAbs represent a very promising component of the immune response to chronic viral infection. However, unlike nAbs against acute viral pathogens, which typically arise within 2 weeks of infection, nAbs against persistent viruses only appear after long periods of protracted infection (*40-43*). Several mechanisms have been postulated to explain the weak and late nAb responses in chronic viral infection. For example, a negative impact of the massive CTL response on virus-specific B cells, structural features of persistent viruses preventing efficient neutralization such as glycosylation of the surface glycoprotein and mutational escape from neutralization have been described (*30, 31, 44-47*). Still, our understanding of the mechanisms underlying the emergence of nAbs in chronic viral infection remains incomplete and the induction of nAbs by vaccination against HIV or HCV remains unsuccessful. Unlike nAbs, non-neutralizing virus-specific antibodies appear early in the course of chronic LCMV infection as well as in HIV infection in humans (*41, 48, 49*). Several studies have shown that non-neutralizing Abs also exert antiviral effects and can act via complement-mediated functions and Fc receptors (*30, 50-53*). Despite the now well-recognized role of neutralizing and non-neutralizing antibodies in control of chronic viral infection, there is little insight into the mechanisms underlying B cell responses in chronic viral infections. Recently, B cell dysfunctions have been observed in several persistent microbial infections but remain mechanistically ill defined and will be discussed in section I.3.

## I.2 B cell responses

B cell responses to pathogens can be divided into T-dependent (TD) and T-independent (TI) responses. As the name suggests, TD antigens require T cells to induce B cell responses whereas TI antigens do not. Follicular B cells typically respond to TD antigen. Circulating naïve B cells enter the lymphoid follicles of the spleen and lymph nodes (also called B cell zone), attracted by chemokine (C-X-C

motif) ligand 13 (CXCL13), which binds to C-X-C chemokine receptor type 5 (CXCR5) expressed by naïve B cells and is secreted by stromal cells and follicular dendritic cells (FDCs) found in the follicles (*54*). There, naïve follicular B cells might enter in contact with their cognate antigen either directly as soluble antigen or as antigen bound by macrophages, FDCs or dendritic cells (DCs). (*55-58*). After engagement of the B cell receptor (BCR), B cells migrate to the border of the T cell and B cell zones (T-B border) of the spleen or lymph nodes where they interact with cognate CD4^{+} T cells leading to reciprocal activation (*59, 60*). The recognition of a peptide by CD4^{+} T cells on the MHC-II of a B cell leads to increased expression of cell-surface molecules and cytokines such as CD40L and interleukin-4 (IL-4) that in turn induce activation and proliferation of B cells (*61, 62*). In the next few days some B cells migrate to the follicle border in the lymph nodes or to the T cell zone-red pulp border, bridging channels and red pulp of the spleen, forming primary foci of expanding B cells. Some of the proliferating B cells differentiate into short-lived plasmablasts (PBs) secreting low affinity antibodies mostly of the IgM isotype although some might undergo isotype class switching. This initial extrafollicular response rapidly provides specific antibodies, mostly unmutated IgMs (*63-65*). In parallel some B cells and T cells continue to interact at the T-B border and migrate together to the follicle where they keep proliferating and start forming a germinal center (GC). GCs are specialized structures composed of 90% of proliferating B cells surrounded by CD4^{+} T cells providing help to B cells. In the GCs, B cells undergo extensive proliferation and undergo class-switch recombination (CSR) and somatic hypermutation (SHM) through the action of the enzyme activation-induced cytidine deaminase (AID). As B cells proliferate and undergo SHM, they accumulate mutation in the variable regions of the Ig genes that might alter binding to antigen. Competition for help from CD4^{+} T cells will select B cells with higher affinity for the antigen, a processed known as affinity maturation. The GC reaction thus leads to the production of high affinity, isotype-switched B cells that eventually differentiate into plasma cells (PCs) or memory B cells (memB). The GC then shrinks and eventually disappears once the infection is cleared. GCs typically last for 3 to 4 weeks but can persist much longer in the context of chronic infections (*66-75*). Characteristic features of PCs include expression of the surface marker CD138, cessation of proliferation, and high synthesis and secretion of Igs with down regulation of surface Igs. PCs exit the GCs and home to peripheral tissues, medullary cord of lymph nodes

or red pulp of the spleen. A subset of PCs migrates to survival niches mostly in the bone marrow (BM) where they survive as long-lived plasma cells (LLPCs) for extended periods of time (*76-78*). In addition to LLPCs, memB represent the end-product of the GC reaction. They do not divide or only very slowly and express surface Ig but do not secrete antibodies, however they respond rapidly and robustly to secondary exposure to antigen providing protection against previously encountered pathogens (*78-83*). Although memB have classically been thought to be the product exclusively of GC reactions it is now recognized that memB can also arise in a GC-independent manner. Such GC-independent memB are thought to be produced early in the course of humoral responses and to require only BCR and CD40 signaling without the need for cytokine signals (*63, 74*). Since CSR but not SHM might occur at this stage of the response, GC-independent memB are thought to have BCR specificities similar to initially responding B cells and to be mostly of IgM isotype although some might have undergone CSR. (*63, 64, 84-86*). The mechanisms that lead to the differentiation of GC B cells into LLPCs or memB are not fully understood although several hypotheses have been proposed. For instance, it has been postulated that cytokines such as IL-5 or CD40-CD40L interaction could influence the differentiation of PCs versus memB (*87*). Other studies suggested that B cell differentiation into distinct phenotypes might be controlled by BCR affinity for the antigen, or that it could follow a stochastic process (*78, 87, 88*). More recent evidence suggests that LLPCs and memB might be produced at different time points during the GC reaction (*74*). At the molecular level, PC differentiation is orchestrated by 5 major transcription factors: paired box protein 5 (PAX5), B-cell lymphoma 6 protein (BCL6), interferon regulatory factor 4 (IRF4), B lymphocyte-induced maturation protein-1 (BLIMP1) and X-box binding protein 1 (XBP1). PAX5 and BCL6 act as B cell promoting factors whereas IRF4, BLIMP1 and XBP1 are important to repress B cell-associated genes and to activate and maintain the plasma cell program. As plasma cell differentiation is initiated, expression of PAX5 and BCL6 is thus inhibited while expression of IRF4, BLIMP1 and XBP1 is induced (*77, 89-96*).

As mentioned before, TI antigens do not require the help of T cells to initiate a B cell response. Marginal zone B cells (MZB), a specific subset of B cells, have been shown to be particularly important to mediate responses to TI antigens (*97*). Some TI antigens such as lipopolysaccharide (LPS) and bacterial deoxyribonucleic acid (DNA)

can induce unspecific B cell proliferation and differentiation through recognition by Toll-like receptors (TLRs) (*98, 99*). Other TI antigens such as polysaccharides of bacterial capsules can activate B cells via extensive cross-linking of the BCR due to their repetitive structure (*100*). Therefore, such non-protein compounds, which cannot be recognized by T cells, can still induce B cell responses. Although TI antigens can induce robust proliferation and long-lasting antibody production in mice, responses to TI antigens have been shown to be restrained mostly to extrafollicular foci and to induce abortive GCs (*85, 101, 102*). Accordingly, low levels of SHM have been observed in response to TI antigens (*84*). Although CSR is classically thought to occur in GCs and extrafollicular responses have been shown to induce mostly IgM expression, production of IgGs and IgAs in response to TI antigens has been observed (*63, 85, 103, 104*). Recently, T-independent mechanisms leading to AID activation and CSR have been described (*105*). Moreover, despite the extrafollicular nature of TI responses, generation of memory B cells has been observed in response to TI antigens. However, TI memory B cells have been shown to differ greatly from TD memory B cells and to resemble naïve B cells with regards to the quality of their response (*106*). Responses to TI antigens are thought to be important to fight against blood born pathogens such as encapsulated bacteria (*107*).

Most of our understanding of B cell responses is based on observations made in the context of immunization with non-replicative immunogens such as sheep red blood cells or soluble proteins. Although some of the concepts described above might apply to B cell responses to invading pathogens, abnormal B cell populations and antibody responses have been observed in infectious context and in particular in persistent microbial infections, and will be discussed in section I.3.


## I.3 Immune subversion mechanisms of viruses and other pathogens

Immune subversion represents a hallmark of persistent viral infections. In order to persist in their host, viruses have developed countless mechanisms targeting virtually all steps of the innate and the adaptive immune responses. For instance cytokine production and signaling, MHC class I and class II expression, natural killer (NK) cell mediated killing, and the humoral immune response are all targets of viral immune subversion mechanisms (*108-126*). Indeed, several viruses such as HCV, measles

virus or human cytomegalovirus (HCMV) have been shown to prevent IFN-I signaling (*108-112*). HCMV, has also been shown to decrease the availability of chemokine ligand 2 (CCL2, also known as monocyte chemoattractant protein 1, MCP1) and chemokine ligand 5 (CCL5, also known as regulated on activation, normal T cell expressed and secreted, RANTES), two potent chemoattractants for monocytes, by producing chemokine receptor analogs (*113*). Down regulation of MHC-I expression is another frequently used mechanism to escape immune control. For example, the HIV protein Nef can induce MHC-I endocytosis (*114*). Several reports have shown that viruses, such as herpes simplex virus type 1 (HSV-1), Epstein-Barr virus (EBV) or HCMV also developed strategies to prevent MHC-II expression or presentation (*115-117*). Although down regulation of MHC-I expression can protect infected cells from CTL mediated killing, this mechanism might lead to the lysis of cells with low surface MHC-I expression by NK cells. However viruses also developed strategies to prevent NK cell cytotoxicity. For instance, HIV has been shown to take advantage of the different specificities of MHC-I molecules. Indeed, while the Nef protein of HIV is thought to facilitate degradation of human leukocyte antigen (HLA)-A and HLA-B it does not affect the expression of HLA-C and HLA-E, know to bind to inhibitory receptors on NK cells, thereby reducing NK cell mediated killing (*118*). Similarly, several lines of evidence suggest that HCV has developed several strategies to reduce NK cell response, for example through the stabilization of HLA-E expression or binding to CD81 (*119-121*). Subversion of the complement system is a strategy used by several viruses including HSV and HIV. The glycoprotein (gC) of HSV-1 and HSV-2 has been shown to interact with the component C3b of the complement cascade thereby protecting from complement-mediated lysis (*122*). Several reports indicate that HIV also interferes with complement activation by inducing a down-regulation of the expression of several complement receptors (*123-125*).

Mutational escape from T cell and antibody control is another important mechanism of immune evasion used by persistent viruses such as HIV in humans and LCMV in mice (*30, 31, 47, 127-133*). LCMV escape from nAb control has been observed in conditions of increased nAb pressure such as CTL deficiency and several neutralization-resistant variants have been characterized (*30, 31*). Moreover, escape variants with mutations in the immunodominant CTL epitopes of the nucleoprotein

and glycoprotein have been repeatedly observed. Although CTL responses against nonimmunodominant epitopes of such variants can still lead to viral clearance, mutational escape from CTL control is thought to contribute to viral persistence (*128-130*). In the course of natural HIV infection, mutants escaping nAb control have also been observed and have been shown to acquire mutations in the neutralizing epitopes of the envelope glycoproteins under the selection pressure exerted by nAbs (*47, 132, 133*). Similarly, emergence of CTL escape variants has been observed in HIV-infected patients (*131*). Although the nAb response constantly evolves and can lead to the emergence broadly neutralizing antibodies (bnAbs) after several years of infection in a small fraction of HIV infected patients, viral variants still escape the most potent bnAbs (*42, 134, 135*).

In addition to mutational escape, other factors that have been suggested to negatively impact B cell responses in chronic viral infection include: structural features of the HIV and LCMV surface glycoproteins that prevent neutralization, the massive CTL response, polyclonal B cell activation, and high antigen load (*44-46, 136-139*). Indeed, the immunopathology associated with the CTL response to chronic LCMV infection and the ensuing destruction of the secondary lymphoid organ architecture has been proposed to negatively impact B cell responses (*44*). Alternatively, it had been suggested that CTL might directly kill infected nAb-producing B cells although this was not found to be reproducible subsequently (*140-142*). Hypergammaglobulinemia has been reported in several persistent-prone infections such as HIV, HCV and LCMV infections and is thought to result from non-specific polyclonal B cell activation, which might contribute to the poor nAb response observed in those infections (*136, 143, 144*). Lastly, while high antigen load is believed to lead to CTL exhaustion the impact of antigen load on B cells is less clear. It has been reported that a high antigen to B cell ratio early in LCMV infection might induce terminal differentiation of virus-specific B cells into short-lived IgM-producing antibody-secreting cells (ASCs), thereby preventing effective nAb responses (*139*). However the observation that mice with impaired CTL responses, which display elevated virus load, show increased nAb responses argues against this hypothesis (*31, 44*).

While T cell exhaustion in chronic viral infection and specifically in chronic LCMV infection has been extensively studied and although some factors mentioned above

have been shown to influence antibody responses, still little is know on the mechanism directly regulating B cell responses in chronic infections. B cell exhaustion in persistent-prone viral and also bacterial and parasitic infections has become a topic of interest and recent data strongly support that persistent pathogens can induce B cell dysfunction (*145-158*). B cell dysfunction is now recognized as a major feature of HIV infection affecting mostly the memB compartment but also GC B cells and MZ B cells and impairing both the virus-specific as well as the non-HIV-specific B cell responses (*145-155*). For instance, a loss of MZ B cells associated with increased plasmablasts has been observed in HIV patients and SIV infected macaques (*153, 156*). In humans, classical memory B cells (or resting memory B cells, RM) are characterized by the capacity to persist for extended period of time and to rapidly respond to BCR stimulation, by high frequencies of SHM, and by the expression of CD27 and CD21 (*83, 146-148*). In healthy humans, RM B cells represent the vast majority of circulating memB. However abnormal memB populations constitute the majority of the memB pool in HIV viremic patients. Notably, $CD21^{lo}$ $CD27^{-}$ tissue-like memory B cells (TLM) and $CD21^{lo}$ $CD27^{+}$ activated memory B cells (AM) have been described (*146-148*). TLM express the inhibitory receptor Fc receptor-like protein 4 (FCRL4) together with other inhibitory receptors and have been shown to be unresponsive to BCR stimulation, features that are reminiscent of previously described exhausted CTLs (*146, 159*). Moreover, TLM have been shown to harbor reduced SHM frequencies as compared to RM, that correlates with weaker neutralizing capacity of antibodies produced by TLM (*148*). While the increased frequencies of PBs in blood of HIV-infected patients correlating with hypergammaglobulinemia mostly reflect alteration of non HIV-specific B cells, HIV-specific B cells have been shown to be enriched in TLM and AM populations (*146, 151, 152*). Dysfunctions in the HIV non-specific B cell compartment are thought to play a role in the increased frequency of autoimmune diseases as well as in the poor response to vaccine of HIV patients (*149, 152, 153, 160, 161*). Other infections in which abnormal B cell populations have been described include Plasmodium, Schistosoma haematobium, Mycobacterium tuberculosis, Salmonella, HCV and HBV infections (*157, 158*). In Plasmodium infection for example, $CD21^{lo}$ $CD27^{-}$ $FCRL4^{+}$ memB have also been observed. Despite similarities with the TLM B cells described in HIV infection, it has been recently reported that the AM B cells observed in malaria infection display signs of activation and antibody secretion, and might in fact

resemble PBs rather than unresponsive memB. They might therefore contribute to immunity to malaria instead of representing an exhausted B cell population (*157*). Although our understanding of the role of B cells in persistent viral infection has improved dramatically in recent years, the mechanisms underlying B cell responses in persistent viral infection still remain incomplete.

## I.4 IFN-I in acute and chronic viral infections

IFN-I was first described in 1957 for its ability to interfere with replication of influenza virus *in vitro* and is now recognized as a key first line defense mechanism against viral infections (*162*). More recently, however, detrimental effects of IFN-I in viral infections and in particular during persistent viral infections have been brought to light (*145, 163-174*). IFN-I is a large family comprising in humans 13 IFN-α subtypes, IFN-β and several other subtypes. All IFN-I proteins bind to one common cell surface receptor know as IFN-alpha/beta receptor (IFNAR), made of the IFNAR1 and IFNAR2 chains (*175*). Downstream signaling occurs via the Janus kinase (Jak) - Signal Transducer and Activator of Transcription (STAT) pathway leading to the activation of STAT1, STAT2 and Interferon regulatory factor 9 (IRF9) although other STATs such as STAT3 and STAT4 can be activated in specific cell types and conditions (*176-180*). IFN-I signaling results in the expression of hundreds of IFN-stimulated genes (ISGs), whose protein products exert numerous direct and indirect antiviral effects as well as immunomodulatory functions (*181-195*). Direct antiviral effects of ISG protein products target virtually all steps of viral replication and can, for example, induce viral ribonucleic acid (RNA) degradation, block viral transcription or modify protein function (*182, 183, 195*). For instance, myxovirus resistance protein 1 (Mx1) and MxA proteins have been shown to interfere with influenza virus replication in mice and humans respectively, and 2'-5'-oligoadenylate synthase (OAS) proteins have been shown to induce viral RNA degradation via the activation of ribonuclease L (RNaseL) (*182, 183*). In addition to those direct antiviral effects, IFN-I also has many immunomodulatory functions. For example, IFN-I can enhance expression of MHC-I molecules. Furthermore, T cell intrinsic IFN-I signaling has been shown to provide co-stimulatory effects on CTLs and to protect them from NK-mediated cytotoxicity (*185-188*). IFN-I was also shown to promote

NK cell function and survival in numerous viral infection settings (*189-191*). Similarly, several reports have shown that B cell activation and antibody production is promoted by IFN-I signaling in several acute viral infections (*192-194*). The critical antiviral role of IFN-I is well illustrated by the increased susceptibility of IFNAR$^{-/-}$ mice to several viral infections such as VSV, vaccinia virus (VV) and LCMV infections (*196*). In humans, IRF7 deficiency leads to reduced IFN-I production and life threatening influenza infection, further illustrating the critical role of IFN-I in antiviral defense (*197*).

Despite the important antiviral role of IFN-I described above, detrimental effects of IFN-I signaling in several viral infections have recently been brought to light (*145, 163-174*). In acute infection it is globally recognized that IFN-I has a beneficial effect although it was recently reported that IFNAR deficiency in Sv129 mice decreased morbidity and improved survival upon acute influenza infection (*163*). However, the dichotomy between beneficial and detrimental roles of IFN-I in chronic viral infections is much more pronounced. For instance, while IFN-I treatment early in SIV infection has been shown to prevent disease progression, sustained IFN-I administration accelerated progression of the disease (*164*). Furthermore, non-pathogenic SIV infection of African green monkey or sooty mangabeys is associated with initially high but rapidly controlled IFN-I response, whereas pathogenic infection of rhesus macaques induces sustained IFN-I signatures associated with chronic immune activation (*165, 166*). Similarly, elevated IFN-I signatures have been reported in HIV-infected progressor (*198*). Moreover, IFN-I signaling has been proposed to contribute to CD4$^+$ T cell loss and to B cell dysfunction in HIV infected patients (*145, 167*). Likewise, while pegylated IFN-α in combination with Ribavirin has been a standard treatment for patient with HCV until recently, HCV has been shown to be relatively resistant to IFN-I antiviral activity and elevated IFN-I signatures have been observed in humans and chimpanzees chronically infected with HCV (*168-170*). Finally, studies in mice chronically infected with LCMV showed that IFN-I signaling blockade reduced immune suppression and led to accelerated viral clearance despite initially elevated viral load (*171, 172*). The work by Sandler *et al*. suggests that IFN-I effects may vary depending on the stage of the infection (*164*). Moreover, it has been suggested that specific IFN-I subtypes might play different roles in controlling vs. promoting viral persistence (*173*). However, how the

beneficial and detrimental effects of IFN-I are balanced during infection and how they can be influenced to favor immune control rather than immunopathology is still not fully understood. The impact of IFN-I signaling specifically on B cell responses also requires further investigations.

## I.5 The lymphocytic choriomeningitis virus model

LCMV belongs to the Arenaviridae family. The name of the family was given because of the sandy appearance of the viruses in electron microscopy due to the incorporation of cellular ribosomes during virion formation (*199*). Arenaviruses are divided in two groups, based on geographical and genetic characteristics. The Old World group includes LCMV, which is distributed worldwide and Lassa virus found in West Africa. Viruses from the New World group comprise Junin, Machupo and Guanarito viruses found in South America and Whitewater Arroyo virus in North America (*200-203*). Natural hosts of arenaviruses are mainly rodents (*199*). The LCMV reservoir in mice is established by congenital or transplacental transmission of the virus from mother to offspring, leading to asymptomatic lifelong infection. Transmission between adult mice may occur via the saliva, urine or feces but usually does not lead to chronic infection. LCMV infection of humans can occur upon exposure to fresh urine, feces, saliva and nesting material or following accidental laboratory exposure. Clinical manifestations range from mild flu-like disease to aseptic meningitis. Other Arenaviruses such as Lassa, Junin or Guanarito viruses can cause severe hemorrhagic fever in humans (*200, 204-206*).

Since its discovery in the early 1930s, LCMV has become a widely used tool in the field of viral immunology and has contributed to the understanding of several key principles of viral pathogenesis and immunity (*207-210*). Hence, abundant specific tools and knowledge have been developed over almost a century and represent a great advantage of research using the LCMV model. Notably, reverse genetic techniques have been developed by our group and others and allow us to manipulate viruses according to our experimental needs (*211, 212*). The LCMV genome contains two negative single stranded RNA segments and encodes for four proteins. The nucleoprotein (NP) and the glycoprotein (GP) are found on the short segment (S) whereas the viral polymerase (L) and the matrix protein (Z) are located on the large

segment (L) (*213-215*). Virions are spherical enveloped particles, containing the genome segments encapsidated with the NP protein associated with the polymerase L (*216*). The matrix protein is thought to be important for the virus budding (*217*). The GP protein mediates attachment of the virions to the target cells and membrane fusion in the endosomes. It is the only surface determinant of LCMV and its outer globular domain (GP-1) is the only target of nAbs (*218*). Our group and others first described a reverse genetic technique to recover infectious LCMV entirely from cDNA in 2006 (*211, 212*). Briefly, the S and L viral genome segments are introduced on polymerase I driven plasmids and the NP and L proteins are encoded on polymerase II driven plasmids. Transfection of the four plasmids provides the viral genome as well as the necessary trans-acting factors for genome transcription and replication ultimately leading to production of infectious LCMV particles. Recovery of LCMV entirely from plasmid DNA opens the possibility to introduce mutations in the viral genome and to exchange viral proteins according to our experimental purposes.

The WE strain of LCMV (LCMV-WE) has been the most widely used strain to study antibody responses to LCMV. Thus, many tools have been developed to study B cell and antibody responses to this strain. Specifically, potent monoclonal nAbs specific for WE-GP such as KL25 have been identified and characterized (*219*). Genetically engineered BCR-transgenic mice expressing the KL25 heavy chain (KL25H) and the KL25 light chain (KL25L) respectively have been generated and are described in the materials and methods section (*220*). By intercrossing KL25H and KL25L mice, KL25HL mice with a virtually monoclonal B cell repertoire specific for WE-GP have been generated in our laboratory and represent a very powerful tool to study antiviral B cell responses. However, LCMV-WE establishes only transient infection in C57BL/6 mice. As discussed above, LCMV-Cl13 is a frequently used model of chronic viral infection and can persist for several months in organs of infected C57BL/6 mice (*5*). In order to benefit from the existing tools specific to the WE strain in a context of chronic infection, our laboratory has generated a recombinant LCMV-Cl13 expressing the WE-GP (rCl13) according to the technique described above (*211, 212, 221*).

# II Interferon-driven decimation of antiviral B cells at the onset of chronic infection

Benedict Fallet[1*], Kerstin Narr[1*], Yusuf I. Ertuna[1], Melissa Remy[1], Rami Sommerstein[2], Karen Cornille[1], Mario Kreutzfeldt[2,3], Nicolas Page[2], Gert Zimmer[4], Tobias Straub[5], Hanspeter Pircher[5], Kevin Larimore[6,7], Philip D. Greenberg[6,7], Doron Merkler[2,3] & Daniel D. Pinschewer[1,#]


**Affiliations**

[1] Department of Biomedicine, Division of Experimental Virology, University of Basel, 4003 Basel, Switzerland.

[2] Department of Pathology and Immunology, Geneva Faculty of Medicine, 1211 Geneva 4, Switzerland.

[3] Division of Clinical Pathology, University Hospital Geneva, 1 rue Michel Servet, 1211 Geneva 4, Switzerland

[4] Institute of Virology and Immunology IVI, 3147 Mittelhäusern, Switzerland.

[5] Institute for Immunology, Department for Medical Microbiology and Hygiene, University Medical Center Freiburg, 79104 Freiburg, Germany

[6] Fred Hutchinson Cancer Research Center, University of Washington, Seattle, WA 98109, USA.

[7] Department of Immunology, University of Washington, Seattle, Washington, WA 98109, USA.

*B.F. and K.N. contributed equally to this work
#Correspondence: daniel.pinschewer@unibas.ch

## II.1 Abstract

Immune subversion represents a hallmark of persistent infection, but microbial suppression of B cell responses remains mechanistically ill-defined. Adoptive transfer experiments in a chronic viral infection model evidenced the rapid and profound decimation of B cells that responded to virus or to concomitantly administered protein. Decimation affected naïve and memory B cells and resulted from biased differentiation into short-lived antibody-secreting cells. It was driven by type I interferon (IFN-I) signaling to several cell types including dendritic cells, T cells and myeloid cells. Durable B cell responses were restored upon IFN-I receptor blockade or, partially, when depleting myeloid cells or key IFN-I-induced cytokines. B cell decimation represents a molecular mechanism of humoral immune subversion and reflects an unsustainable "all-in" response of B cells in IFN-I-driven inflammation.

## II.2 One-sentence summary

Interferon-driven inflammation at the onset of chronic viral infection orchestrates unsustainable antibody production and decimation of antiviral B cell populations.

## II.3 Results and discussion

Humoral immunity represents a cornerstone of antimicrobial host defense and vaccine protection. Infection-induced suppression of humoral immune defense is therefore predicted to further microbial persistence and pathogenesis, with the potential to thwart B cell-based vaccination efforts. Perturbed or dysfunctional B cell compartments represent a hallmark of persistent microbial diseases including HIV, hepatitis B, hepatitis C, malaria, schistosomiasis and tuberculosis (*222-226*). Besides delayed and inadequate antibody responses to the causative agent itself (*227-229*), consequences can consist in a generalized suppression of vaccine responses and B cell memory (*149, 230, 231*). In comparison to T cell exhaustion, however, the molecular mechanisms leading to viral subversion of the B cell system have remained less well defined.

Here we compared B cell responses to protracted LCMV infection (rCl13) and to recombinant vesicular stomatitis virus (rVSV) vaccine vectors. The two viruses were engineered to express the same surface glycoprotein (GP) as neutralizing antibody target, but served as prototypic models of chronic viremic and acute infection, respectively (Fig. 1A). To study antiviral B cell responses in mice, we adoptively transferred oligoclonal, traceable (CD45.1$^+$) KL25H B cells, which contain ~2% GP-specific cells owing to an immunoglobulin heavy chain knock-in (Fig. S1A). The transferred KL25H cells mounted only transient GP-specific antibody responses to rCl13, whereas rVSV-induced responses were durable and of higher titer (Fig. 1B). Moreover, KL25H B cell numbers at four weeks after rVSV immunization were ~20-fold higher than after rCl13 infection (Fig. 1C). We obtained analogous results, both in spleen and inguinal lymph nodes (iLN), when adoptively transferring quasi-monoclonal KL25HL B cells (~85% GP-specific, Fig. S1A, B), which express the matching immunoglobulin light chain transgene in addition to the heavy chain knock-in (Fig. 1D, S1C). Four weeks after infection, KL25HL B cells populated the germinal centers (GCs) of rVSV-immunized mice but not of rCl13-infected animals (Fig. 1E). When studying KL25HL B cells in the first week of rCl13 infection, they proliferated vigorously and acquired a blast-like morphology within the first three days, but disappeared almost completely by day 6 (Fig. 1F, G). On day three, the majority of proliferating (CFSE$^{low}$) KL25HL B cells in rCl13-infected mice were apoptotic (7AAD$^+$AnnexinV$^+$, Fig. 1H), whereas KL25HL B cells responding to

rVSV remained mostly viable. These observations suggested a near-complete apoptotic loss (referred to as "decimation") of virus-neutralizing KL25HL B cells within days after the onset of rCl13 infection. By analogy to T cells (*27*), high antigen loads in rCl13 but not rVSV infection could have accounted for antiviral B cell decimation. Counter to this hypothesis, adoptive transfer of KL25HL B cells into neonatally infected immunologically tolerant rCl13 carrier mice (*232*) resulted in robust B cell and plasmablast/plasma cell (antibody-secreting cell, ASC) formation despite high-level viremia (Fig. 1I and S1D; B cells and ASCs jointly referred to as "B cell progeny"). Furthermore, KL25HL B cell transfer on day 3 of rCl13 infection, when viremia had set in, yielded ~20-fold more B cell progeny than transfer at the onset of infection (Fig. 1J, K (*139*)). Day 3 transfer of KL25HL B cells resulted also in substantially higher neutralizing antibody (nAb) responses and in a more potent antiviral effect than transfer on the day of infection (Fig. 1L, M).

These observations argued against antigen overload as the root cause of KL25HL B cell decimation, suggesting rather that the inflammatory milieu at the onset of infection was unfavorable to sustained B cell responses. Intriguingly, this 3-day time window coincided with the strong systemic type I interferon (IFN-I) response in rCl13 infection (Fig. 2A). Moreover, rCl13-induced serum IFN-I responses clearly exceeded those induced by rVSV, and IFN-I was below technical backgrounds in rCl13 carriers, altogether suggesting an inverse correlation between systemic IFN-I levels and sustained antiviral B cell responses. IFN-I transcriptome signatures characterize chronic hepatitis C virus, pathogenic immunodeficiency virus infection and chronic active tuberculosis (*233-236*), and IFN-I can exert detrimental effects on antiviral T cell responses (*171, 172*). Hence we speculated that rCl13-induced IFN-I accounted for antiviral B cell decimation. Antibody-based blockade of the type I interferon receptor (αIFNAR) resulted in ~20-fold more KL25HL progeny on day 3 of rCl13 infection (Fig. 2B, C). By day 15, αIFNAR blockade yielded >100-fold higher numbers of KL25HL memory B cells (memB) and GC B cells, both in spleen and iLN, and comparably elevated KL25HL progeny were found in bone marrow (BM, Fig. 2D and S2A). By immunohistochemistry we detected KL25HL B cells in GCs of IFNAR-blocked mice but not of control-treated animals (Fig. 2E). To investigate whether also antigen-experienced B cells were sensitive to IFN-I-driven decimation, we expanded KL25H B cells *in vivo* (~50% GP-specific, Fig. S2B) and

transferred them to naïve recipients, followed by rCl13 challenge. αIFNAR blockade yielded significantly more KL25H PCs and memB on day 8 and day 67 after rCl13 challenge, respectively (Fig. 2F and S2C). Performing immunohistochemistry on day 67, we readily detected KL25H B cells in GCs of IFNAR-blocked but not control-treated recipients (Fig. 2G). We extended these adoptive transfer experiments to polyclonal LCMV-experienced B cells of GFP-transgenic mice. On day 7 after rCl13 challenge, IFNAR-blocked recipients contained ~30-fold higher numbers of LCMV nucleoprotein (NP) -binding GFP$^+$ memB cell progeny than control-treated animals (Fig. 2H and S2D). Altogether, this documented that not only primary responses of LCMV-specific KL25H and KL25HL B cells but also recall responses of antigen-experienced LCMV-specific B cells, both oligoclonal (KL25H) and polyclonal, were subject to IFN-I-driven decimation. Next we tested whether B cells of unrelated specificity, when activated concomitantly with rCl13 infection ("activated bystander B cells"), were similarly affected. We transferred traceable (CD45.2$^+$) vesicular stomatitis virus glycoprotein (VSVG) -specific B cells (VI10) into syngeneic (CD45.1$^+$) wt recipients. Subsequent immunization with VSVG triggered robust proliferation (CFSE dilution) and expansion of virtually all VSVG-binding VI10 B cells. This response was markedly reduced by concomitant rCl13 infection but completely rescued by αIFNAR, extending the concept of IFN-I-driven decimation to activated bystander B cells (Fig. 2I). The use of (non-replicating) VSVG protein in these experiments corroborated that cognate antigen loads could not readily explain rCl13-driven B cell decimation.

αIFNAR prevented KL25HL B cell apoptosis as determined by flow cytometry (AnnexinV/7AAD binding) and by active caspase-3 staining in histology (Fig. 3A-C). To better understand IFN-I-driven B cell decimation, we performed whole genome RNA sequencing on KL25HL B cells recovered on day 3 of rCl13 infection. A pronounced antibody-secreting cell signature (*89*) in control-treated cells was largely reversed by αIFNAR blockade (Fig. 3D). This effect was also evident in αIFNAR-mediated suppression of ASC-related transcription factors (TF, Fig. S3A). Conversely, IFNAR blockade promoted/restored TF expression profiles, which are typical for mature B cell stages prior to ASC differentiation, and modulated also GC B cell-specific TFs (Fig. S3B, C). In line with its effects on the cells' ASC gene signature, αIFNAR altered the expression of 10 out of 13 genes, which have been

linked to terminal B cell differentiation in human HIV infection (Fig. S3D, (*145*)). Flow cytometric analyses corroborated that IFNAR blockade impeded rCl13-induced ASC differentiation. As hallmarks of ASC differentiation, most KL25HL B cells in control-treated recipients lost B220, CD22 and CD23 expression as they proliferated (Fig. 3E). When IFNAR was blocked, a significantly higher proportion of KL25HL progeny cells retained these markers. Conversely, fewer KL25HL cells up-regulated the ASC marker CD138$^+$, and their intracellular IgM levels were lower (Fig. 3E). Altogether these observations indicated that IFNAR blockade prevented specific B cell decimation by countering short-lived plasmablast differentiation.

To differentiate between B cell-intrinsic and –extrinsic IFNAR effects on B cell decimation we used IFNAR-deficient and –sufficient KL25HL B cells for adoptive transfer. Both B cell types expanded vigorously when challenged with rCl13 in *ifnar$^{-/-}$* recipients but yielded low progeny numbers when responding in wt recipients (Fig. 4A). This suggested B cell-extrinsic IFN-I effects as the root cause of rCl13-induced B cell decimation. We extended these observations to activated bystander B cells. IFNAR-deficient and –sufficient VI10 B cells responded similarly to VSVG protein immunization, and both responses were equally suppressed by concomitant rCl13 infection (Fig. 4B). When using reciprocal wt and *ifnar$^{-/-}$* BM chimeras as recipients we found that hematopoietic IFNAR expression was decisive for KL25HL B cell decimation (Fig. 4C). To dissect how IFNAR signaling in various immune cell types contributed to B cell decimation we exploited cell type-specific IFNAR deletion models. KL25HL B cell progeny were significantly more numerous when recipients lacked IFNAR in either T cells, dendritic cells (DCs) or myeloid cells. IFNAR deletion in the recipient's B cells only modestly augmented KL25HL ASCs, and neither of the above cell-type specific IFNAR deletion models fully phenocopied plain *ifnar$^{-/-}$* recipients (Fig. 4D). Taken together, IFNAR signaling in several cell types, namely in DCs, myeloid cells and T cells contributed to rCl13-induced B cell decimation. The essential antiviral role of IFN-I may preclude the success of αIFNAR-based immunomodulatory therapy ((*164, 171, 172*), Fig. S4A). Also T cells and DCs are widely recognized as essential components of antiviral immune defense (*237, 238*), but inhibition or depletion of myeloid cells can be pursued to combat persistent infection and cancer (*239, 240*). Hence we tested whether, by analogy to myeloid cell-specific IFNAR deficiency, myeloid cell depletion could rescue

KL25HL B cell responses. Albeit less dramatically than αIFNAR, also αGr-1 (Ly6C/G) antibody depletion, a widely used means to deplete myeloid cells in mice, augmented KL25HL progeny (Fig 4E). Of note, αGr-1 depletion did not substantially affect viral loads or serum IFN-I kinetics (Fig. S4A,B), attesting to the potential utility of myeloid cell-targeting strategies for countering B cell decimation. In accordance with earlier reports, however, αGr-1 depleted not only inflammatory monocytes (InfMo) and neutrophils but also eosinophils, plasmacytoid dendritic cells (pDCs) and Ly6C$^{high}$ CD8$^+$ T cells (Fig. S4C, D). Yet, the individual depletion of neutrophils, eosinophils or pDCs did not increase KL25HL B cell progeny, and $cd8^{-/-}$ mice yielded only modestly elevated numbers of KL25HL ASCs (Fig. S4E). NK cell depletion (*185, 186*) did not augment KL25HL progeny either (Fig. S4F). To address a potential role of InfMo in B cell decimation we used both InfMo-deficient $ccr2^{-/-}$ and $klf4^{fl/fl}xVav1$-icre mice recipients (Fig. S4G-I and (*241*)). Neither model phenocopied the αGr-1 effect, and αGr-1 depletion improved KL25HL progeny recovery also in InfMo-deficient $ccr2^{-/-}$ recipients (Fig S4I). Hence, the B cell-sparing effect of αGr-1 depletion likely represented its combined impact on multiple myeloid and perhaps even non-myeloid cell subsets. Thus we speculated that both αGr-1 and αIFNAR countered antiviral B cell decimation by altering virus-induced inflammation. When profiling the expression of 248 inflammation-related genes in spleen, 128 were altered upon rCl13 infection, and αIFNAR attenuated or prevented a majority of these inflammatory gene expression changes (Fig. 4F, S5A, B, Tbl. SI). αGr-1 exerted analogous albeit more modest effects, which were largely overlapping with those of αIFNAR. Similar results were obtained from BM, indicating that treatment-related anti-inflammatory effects were not confined to lymphoid organs (Fig. S5C,D, Tbl. SI). In a serum cytokine panel analysis, 19 out of 31 tested chemokines and cytokines increased at 24 and 72 hours after rCl13 infection, respectively, and were at least 4-fold suppressed by αIFNAR (Fig. 4G, Table. SII). Nine of these 19 were also significantly suppressed, albeit less potently, in αGr-1-treated animals. Taken together, IFNAR deficiency and, to a lesser extent also αGr-1, modulated rCl13-induced systemic inflammation, and most if not all αGr-1 effects on inflammation were comprised in the αIFNAR effect.

These observations raised the possibility that the IFN-I-induced inflammatory milieu in rCl13 infection caused B cell decimation by altering B cell survival and/or

differentiation signals. This hypothesis predicted that i) the supplementation of survival signals and also ii) the depletion of deleterious inflammatory mediators or blockade of death pathways should augment specific B cell responses in rCl13 infection. In line with prediction i), KL25HL B cell transfer and rCl13 infection yielded ~10-fold more progeny when performed in transgenic recipients overexpressing the B cell survival factor BAFF (Fig. 4H). In attempting to test prediction ii) we used knock-out mouse models and antibody depletion approaches to assess the individual contribution of IL-1β, IL-4, IL-6, IL-10, IL-12, TNF-α, iNOS and FasL to rCl13-induced KL25HL B cell decimation. KL25HL B cells yielded significantly more progeny when challenged with rCl13 in IL-10-deficient or TNF-α-blocked recipient mice (Fig 4I). Interestingly, IL-10 as well as TNF-α have been linked to B cell dysfunction in HIV-1 infection (*242, 243*). While we failed to detect a statistically significant individual role for IL-1β, IL-4, IL-6, IL-12, iNOS or FasL in B cell decimation (Fig. S6A,B), contributive effects of some of these and other IFN-I-induced factors and pathways (*145, 243, 244*) remain likely, and may vary between infection settings. Accordingly, only their combined suppression alongside with IL-10 and TNF-α may account for the potent B cell-sparing effect of IFNAR blockade.

IFN-I driven B cell decimation reflects apparently an "all in" strategy of the humoral immune system when facing antigen in a highly inflammatory context. In acute life-threatening infections, this ASC differentiation bias may augment survival chances by maximizing early immunoglobulin production. It thus seems desirable from an evolutionary standpoint. Conversely, B cell decimation puts at risk the sustainability of humoral responses, both of naïve and immunized hosts, when confronted with persistence-prone pathogens. Repertoire replenishment by new bone marrow emigrants (*139, 245*) and GC-driven evolution of low-affinity clones are predicted to eventually compensate for early repertoire decimation. But these processes take time, and the sustained IFN-I transcriptome signatures in active tuberculosis, chronic hepatitis C virus and pathogenic immunodeficiency virus infection raise the possibility that B cell decimation extends into the chronic phase of infection (*233-236*). In summary, IFN-I-driven B cell decimation offers a molecular mechanism for humoral immune subversion under conditions of microbial inflammation.

## II.4 Materials and Methods

### II.4.1 Viruses, virus titrations, infections and immunizations

Reverse genetically engineered LCMV strain Clone 13 expressing the LCMV strain WE glycoprotein (rCl13) has been described (*221*). A recombinant vesicular stomatitis virus vector expressing the LCMV strain WE glycoprotein instead of VSVG (rVSV) was generated following established procedures and strategies (*246*). rCl13 and rVSV were grown on BHK-21 cells and were titrated in viral stocks and blood samples as previously described (*40*). Unless specified otherwise, rCl13 and rVSV were administered to mice intravenously (i.v.) at doses of $2 \times 10^6$ and $8 \times 10^6$ plaque-forming units (PFU), respectively. Adult infections were performed 30 min. after adoptive B cell transfer. To establish an immunologically tolerant neonatal rCl13 carrier status, mice were administered $6 \times 10^5$ PFU rCl13 into the skull within 24 hours after birth. VSV glycoprotein (VSVG) for immunization was produced in SF9 cells using a recombinant baculovirus as previously described (*247*). For VSVG immunization, 20 µg whole cell lysate was administered to mice i.v..

### II.4.2 Flow cytometry and FACS sorting

To prepare single cell suspensions, tibiae were flushed and spleens were enzymatically digested using collagenase D (Roche) and DNAseI (Sigma-Aldrich). All cell media were adjusted to mouse osmolarity (*248*). Single cell suspensions were stained with fluorophore- or biotin-conjugated antibodies to detect the following markers and molecules: CD138 (clone 281-2), B220 (clone RA3-6B2), IgD (clone 11-26c.2a), CD45.1 (clone A20), CD45.2 (clone 104), CD22 (clone OX-97), CD23 (clone B3B4), CD8a (clone 53-6.7), Ly-6C (clone HK1.4), CD11b (clone M1/70), CD11c (clone HL3), CCR3 (clone J073E5), SiglecH (clone 551), NK1.1 (clone PK136), Thy1.2 (clone 30-H12) and CD19 (clone 6D5) from BioLegend; IgM (clone II/41), GL-7 (clone GL-7) and Ly-6G (clone 1A8) from eBioscience; CD95 (clone Jo2) and SiglecF (clone E50-2440) from BD Biosciences. Biotin-conjugated antibodies were detected using fluorophore-conjugated streptavidin (BioLegend). Dead cells were excluded using the Zombie UV™ Fixable viability kit (BioLegend). AnnexinV/7AAD staining (BD Biosciences) was performed to detect apoptotic cells

by flow cytometry. To label GP-binding B cells for flow cytometric detection we used a recombinant fusion protein (GP-Strep-tag, (*45*)) consisting of the GP extracellular domain, fused to a C-terminal streptag (Twin-Strep-tag, IBA GmbH). Detection was performed using Strep-Tactin-PE (IBA Biosciences). To label VSVG-binding VI10 cells we used a recombinant fusion protein consisting of the VSVG ectodomain (sVSVG), fused to a C-terminal trimerization motif derived from T4 fibritin (foldon). sVSVG-binding cells were identified using Alexa647-labelled anti-VSVG antibody VI7 (*249*). GP-Strep-tag and sVSVG were produced by transient transfection in HEK-293 cells. For the identification of NP-binding B cells in flow cytometry we used bacterially derived and Alexa647-labelled recombinant NP (*45*). The cells were measured on Gallios (Beckman Coulter) and LSRFortessa (Becton Dickinson, BD) flow cytometers and data were analyzed with FlowJo software (Tree Star). For sorting of KL25HL B cells progeny, labeled with CFSE prior to transfer and rCl13 challenge, splenocyte suspensions were stained with antibodies to B220, CD45.1 and CD45.2. We sorted $CD45.1^{+}CD45.2^{-}CFSE^{lo}B220^{int/hi}$ cells directly into TRI Reagent LS (Sigma-Aldrich) using an FACSAria II (Becton Dickinson, BD) cell sorter at the Flow Cytometry Core Facility of the University of Basel. RNA was extracted using the Direct-zol$^{TM}$ RNA MicroPrep kit (Zymo research).

## II.4.3 Immunohistochemistry and image analysis

For immunohistochemical staining, tissues were fixed in HEPES-glutamic acid buffer-mediated organic solvent protection effect (HOPE, DCS Innovative) fixative as previously described (*250*) and embedded in paraffin. Immunostaining was performed on 3 μm thick sections using antibodies against active caspase-3 (9661T, Cell Signaling) and CD45.1 (clone A20, FITC-labeled, BioLegend). Bound caspase-3 antibodies were visualized using tyramide signal amplification (Thermo-Fisher). Bound CD45.1 antibodies were visualized using rabbit anti-FITC antibody followed by incubation with Alexa-fluor goat-anti-rabbit antibody (Life-Technologies). Germinal centers were visualized using FITC-labeled Peanut agglutinin (PNA; Life technologies). Nuclei were stained with 4',6-diamidino-2-phenylindole (DAPI, Invitrogen).

Stained sections were scanned using a Panoramic Digital Slide Scanner 250 FLASH II (3DHISTECH) at 200x magnification. For representative images, contrast was linearly enhanced using the tools "levels", "curves", "brightness" and "contrast" in Photoshop CS6 (Adobe).

Whole slide images were analyzed with a custom made rule-set using Developer Definiens XD software (Definiens, Munich). Briefly, the regions of interests (ROIs) were drawn manually and CD45.1 as well as caspase-3 signal was automatically detected based on corresponding spectral channels in conjunction with the DAPI signal. Following detection, CD45.1+ cells were classified into caspase-3-positive and, -negative cells depending on cellular collocalisation with caspase-3. The total ROI area and cell quantification results were exported in CSV-format for further analysis.

### II.4.4 Whole-genome RNA sequencing and low-density inflammatory gene expression profiling

For RNA sequencing of sorted KL25HL B cells, RNA was extracted using the Direct-zol™ RNA MicroPrep kit (Zymo research) according to the manufacturer's instructions. Library preparation was performed with a TruSeq kit (Illumina) according to the provider's protocol and sequencing was performed by 50 bp single-end reads on an Illumina HiSeq 2000 at the Microarray and Deep-Sequencing Core Facility, University Medical Center, Göttingen, Germany. Analysis was performed at the Bioinformatics Core Facility of the University of Basel as follow: Reads were mapped against the mouse genome (version mm9; NCBI build 37) using the spliced-read aligner STAR (*251*). Raw reads and mapping quality was assessed by the qQCReport function from the R package QuasR (*252, 253*). Expression of RefSeq genes (UCSC version downloaded 2013-07-25) was quantified by counting reads mapping into exons using the qCount function of QuasR. The R package edgeR (*254*) was used for detecting differentially expressed genes between conditions. P-values for the contrasts of interest were calculated by likelihood ratio tests and adjusted for multiple testing by controlling the expected FDR.

For low density inflammatory gene expression profiling, spleen and BM from naïve mice and from rCl13-infected mice treated with αGr-1, αIFNAR or control antibody

were harvested on day 3. RNA was extracted using Direct-zol™ RNA MicroPrep kit (Zymo research) according to the manufacturer's instructions. Expression profiling was done using the nCounter Nanostring Mouse Inflammation v2 assay (NanoString Technologies) at the iGE3 genomics platform of the University of Geneva. Analysis was performed at the Bioinformatics Core Facility of the University of Basel as follow: Raw counts were scale-normalized using the TMM method of the R package limma (*255*). The transformed counts (log-CPM values) were subsequently used for linear modelling. Differential gene expression between conditions was evaluated using the lmFit and eBayes functions of limma. P-values of the moderated t-tests were adjusted for multiple testing by controlling the expected false discovery rate (FDR).

Heatmaps were generated using the ComplexHeatmap R package (*256*). Heatmaps employing the Nanostring data show genes with an absolute log2-fold change (log2FC) bigger than 0.5 and an FDR-controlled p-value smaller than 0.05. No thresholding was used for heatmaps showing pre-defined gene lists.


**II.4.5 Mice**

KL25L transgenic mice were generated using a construct as schematically described in Fig. S1B. It encoded for the rearranged KL25 V and J segments as well as for the light chain kappa constant domain. Additionally, for the efficient screening of transgene-expressing founder mice by FACS, a downstream internal ribosome entry site (IRES) controlled expression of a cell surface reporter protein consisting of the Thy1.1 ectodomain fused to the transmembrane and cytoplasmic domains of the mouse PDGF receptor. The complete expression cassette was released from the vector using appropriate restriction enzymes and was purified and injected into C57BL/6 embryos using standard techniques.

KL25H and VI10 mice carry an immunoglobulin heavy chain knock-in (KI) derived from the neutralizing GP-specific and VSVG-specific KL25 and VI10 antibodies, respectively (*220*). KL25H and KL25L mice were intercrossed to obtain KL25HL mice, and were brought onto a CD45.1 congenic background for adoptive transfer experiments. Intercrosses of KL25HL and VI10 mice with *ifnar*$^{-/-}$ (*196*) mice yielded KL25HL x *ifnar*$^{-/-}$ (CD45.1) and VI10 x *ifnar*$^{-/-}$ (CD45.2) mice, respectively.

Wt C57BL/6J mice were purchased from Charles River Laboratories, iNOS-deficient *nos2*$^{-/-}$ (*257*) and *Fasl*$^{gld}$ mutant mice (*258*) on C57BL/6 background were bought from the Jackson Laboratories. *ccr2*$^{-/-}$ mice (*259*) were generously provided by S. LeibundGut-Landmann, *ifnar*$^{fl/fl}$ mice (*260*) by U. Kalinke, *Baff-tg* mice (*261*) by T. Rolink, *klf4*$^{fl/fl}$ *x Vav1-icre* mice (*241*) by R. Tussiwand, *il1β*$^{-/-}$ mice (*262*) by N. Schaeren-Wiemers, *il4*$^{-/-}$ mice (*263*) by A. Teubner and *il6*$^{-/-}$ mice (*264*) by M. Recher. *cd19-cre* mice (*265*) were kindly provided by A. Oxenius with authorization from the MGC foundation. CD45.1-congenic C57BL/6, *il10*$^{-/-}$(*266*), *cd8*$^{-/-}$(*267*), *il12p40*$^{-/-}$ (*268*), *cd4-cre* (*269*), *cd11c-cre* (*270*), *LysM-cre* (*271*), *ifnar*$^{-/-}$ (*196*) and *ubc-gfp* mice (*272*) were from the Swiss Immunological Mouse Repository (SwImMR). *ifnar*$^{fl/fl}$ mice were crossed onto B cell-specific (*cd19-cre*), dendritic cell-specific (*cd11c-cre*), myeloid cell-specific (*LysM-cre*) and T cell-specific (*cd4-cre*) Cre deleter strains to obtain the respective "B-*ifnar*$^{-/-}$" (*cd19-cre x ifnar*$^{fl/fl}$), "DC-*ifnar*$^{-/-}$" (*cd11c-cre x ifnar*$^{fl/fl}$), "myeloid-*ifnar*$^{-/-}$" (*LysM-cre x ifnar*$^{fl/fl}$) and "T-*ifnar*$^{-/-}$" (*cd4-cre x ifnar*$^{fl/fl}$) strains.


## II.4.6 Animal experiments

All mice were kept under specific-pathogen-free (SPF) conditions for colony maintenance and experiments, and were housed at the Laboratory Animal Services Center (LASC) of the University of Zurich and at the Universities of Geneva and Basel. Experiments were performed at the Universities of Geneva and Basel, in accordance with the Swiss law for animal protection and with authorization by the respective Cantonal authorities.


## II.4.7 *In vivo* cell depletion and antibody blockade

IFNAR-blocking antibody (MAR1-5A3, BioXCell) was administered intraperitoneally (i.p.) at a dose of 1 mg on day -1 of infection. TNF-α-blocking antibody (XT3.11; BioXCell) was given at doses of 500 μg i.p. on day -1 and day 1 of infection. To deplete myeloid cells, we administered 500 μg of anti-Gr-1 (Ly6C/G) antibody (RB6-8C5, BioXCell) each on day -2.5 and day -0.5 of infection i.p.. Depletion of neutrophils was performed by means of a single i.p. injection of 1mg

anti-Ly6G antibody (1A8, BioXCell) on day -1 of infection. Eosinophils were depleted by i.p. injections of 20 μg anti-SiglecF (clone 238047, R&D Systems) on day -1 and day 1 of infection. The obtained results were independently confirmed in experiments relying on the combined administration of 500 μg anti-IL5 antibody (Trfk5, BioXCell) and 250 μg of anti-CCR3 antibody (6S2-19-4 (*273*), generously provided by Dr. J. J. Lee) each on day -2.5 and day -0.5 of infection. Plasmacytoid dendritic cell depletion was performed by administering 500 μg of anti-mPDCA-1 antibody (JF05-1C2.4.1, Miltenyi Biotec) i.v. on day -1 and day 0 of infection. MOPC-21 mouse IgG1, LTF-2 rat IgG2b, HPRN rat IgG1 and 2A3 rat IgG2a (all from BioXCell) were administered as isotype control antibodies.

## II.4.8 Generation of bone marrow-chimeric mice

To generate bone marrow chimeric mice, wt and *ifnar*$^{-/-}$ recipients were lethally irradiated with a fractionated dose of twice 5.5 gray (Gy) at a 6-hour interval. One day later, the recipients were given 100 μg of anti-Thy1 antibody (clone T24, BioXcell) intraperitoneally to deplete remaining T cells and were reconstituted with ~$10^7$ wt or *ifnar*$^{-/-}$ BM cells. The animals were then rested for eight weeks before entering cell transfer and infection experiments.

## II.4.9 Adoptive cell transfer and fluorescent cell labeling

For adoptive transfer of naïve B cells and subsequent analysis by flow cytometry, splenocyte suspensions (2-4x$10^6$ per recipient) in balanced salt solution were administered i.v. For histological assessments, MACS-purified B cells (Miltenyi Biotec Pan B cell isolation kit, for untouched B cells) were also used. Syngeneic C57BL/6J mice served as recipients, except for long-term (>1 week) transfer of KL25HL cells, which were performed in KL25L recipients to avoid anti-idiotypic responses. To assess *in vivo* proliferation, splenocyte populations were labeled with Carboxyfluorescein succinimidyl ester (CFSE, Sigma-Aldrich) or CellTraceViolet (CTV, Life Technologies) according to the manufacturer's instructions.

**II.4.10 Generation of antigen-experienced KL25H B cells for adoptive transfer**

To generate antigen-experienced GP-specific KL25H B cells, a sequential *in vivo* transfer system was used. We infected C57BL/6J primary recipients with 200 PFU rCl13 i.v. and six days later we transferred $2-4\times10^6$ MACS-purified untouched naïve B cells from CD45.1$^+$ KL25H mice (purified with the Pan B cell isolation kit of Miltenyi Biotec according to the provider instructions). $\geq$3 weeks later we sacrificed the primary recipients and purified antigen-experienced KL25H B cells from spleen, which at this stage were enriched to ~50% GP-binding by FACS (Fig S2B). These antigen-experienced KL25H B cells were isolated using the Pan B cell isolation kit, followed by CD45.2 MACS-based negative selection (both from Miltenyi Biotec) according to the manufacturer's instructions. $2-4\times10^4$ CD45.1$^+$ KL25H memory B cells ($\geq$95% CD45.1$^+$B220$^+$) were transferred intravenously into naïve C57BL/6J wt secondary recipient mice to study the cells' behavior upon rCl13 challenge.

**II.4.11 Generation of polyclonal LCMV-experienced B cells for adoptive transfer**

To generate polyclonal LCMV-specific memory B cells, we infected GFP-transgenic UBC-GFP mice (*272*) with $10^5$ PFU rCl13 i.v.. Fourty days later we isolated untouched splenic B cells using the Pan B cell isolation kit (Miltenyi Biotec) according to the provider's instructions. Upon CTV labeling, $2\times10^6$ of these LCMV-experienced B cells (>95% pure) were transferred into naïve syngeneic C57BL/6J recipients to study their behavior upon rCl13 challenge.

**II.4.12 Antibody, interferon-α and cytokine/chemokine panel measurements**

To assess GP-specific serum antibodies in ELISA we used a recombinant fusion protein consisting of the outer globular GP-1 domain, fused to the human IgG1 constant domain (GP1-Fc) as described previously (*41*). To discriminate responses of adoptively transferred KL25H B cells from endogenous responses in ELISA, background GP-1 antibody titers in control mice without KL25H cell transfer were determined and were subtracted.

GP-specific neutralizing antibodies (nAbs) were measured by immunofocus reduction assays using rCl13 as a test article (*274*). IFN-α concentrations in mouse sera were

determined by ELISA using the VeriKine Mouse Interferon Alpha ELISA Kit (PBL Assay Science). To profile inflammatory responses in mouse serum we used a laser bead-based 31-plex cytokine and chemokine array (Eve Biotechnologies).

## II.4.13 Statistical analysis

For comparison of one parameter between two groups, unpaired two-tailed Student's *t* tests were performed. One-way analysis of variance (ANOVA) was used to compare one parameter between multiple groups, two-way ANOVA for comparison of multiple parameters between two or more groups. ANOVA was followed by Bonferroni's post-test for multiple comparisons. Dunnett's post-test was used to compare multiple groups to a control group. With the exception of percentages, values were log-converted to obtain a near-normal distribution for statistical analysis. Data were analyzed using Graphpad Prism software (version 6.0h). *P* values $>0.05$ were considered not significant (ns), *p* values $<0.05$ were considered significant (*,#) and *p* values $<0.01$ highly significant (**,##).

## II.5 Figures
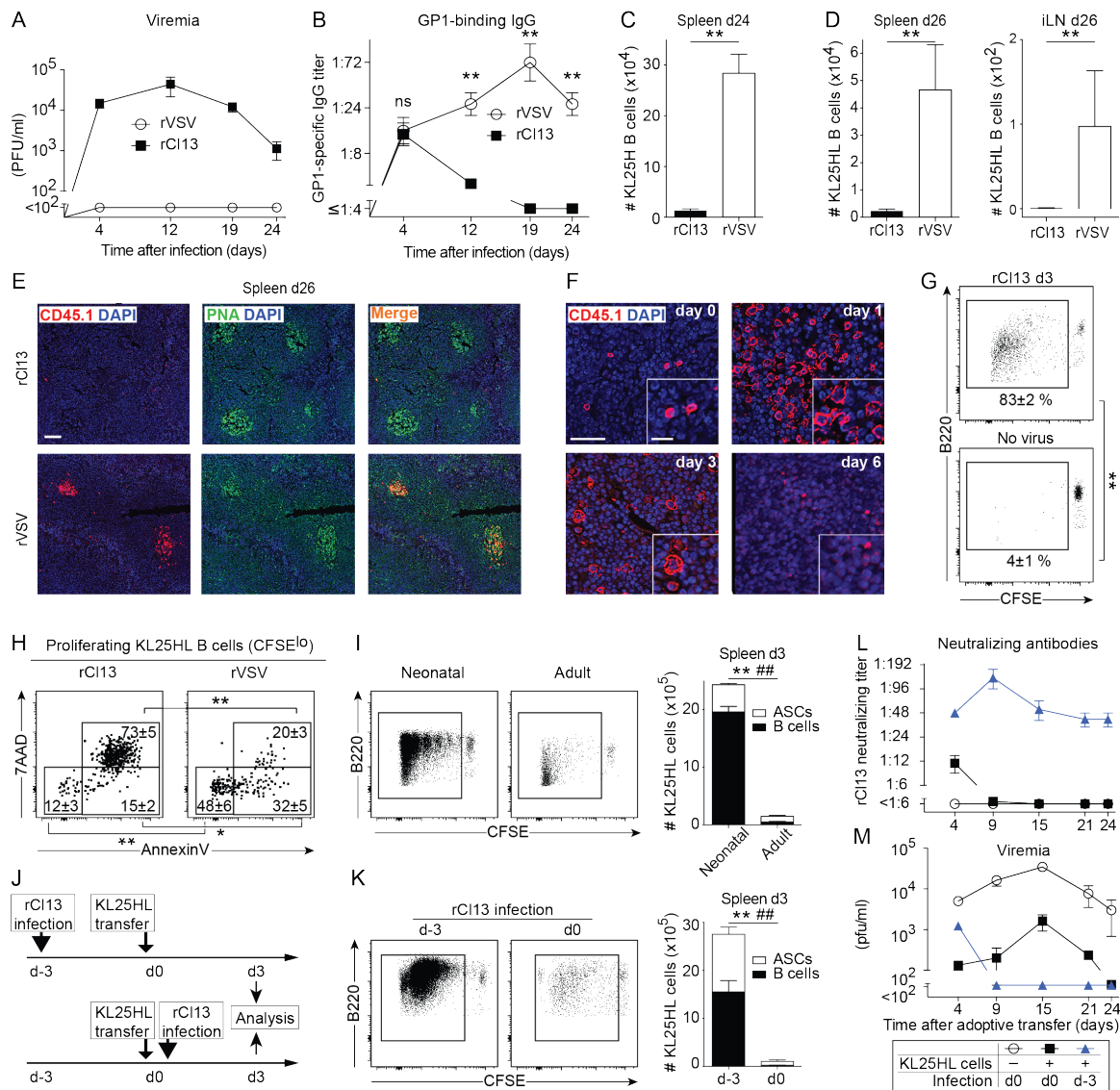


Fig. 1: Decimation of naïve and memory B cells in rCl13 but not rVSV infection.

A-H: We adoptively transferred KL25H (A-C) or KL25HL cells (D-H) into naïve syngeneic recipients, followed by rCl13 or rVSV challenge. On the indicated days, viremia (A) and KL25H-derived GP1-binding IgG (B) were determined. Progeny B cells were enumerated by flow cytometry in spleen and iLN (C,D). KL25HL B cells (CD45.1[+]) in germinal centers (E, bar 100 μm) and their abortive expansion following rCl13 infection (F, bars 50 μm, inset 20 μm) by histology. Proliferation (CFSE dilution) of d3 rCl13-challenged but not unchallenged KL25HL B cells (G). Apoptotic (AnnexinV/7AAD[+]) KL25HL B cells on d3 of rCl13 or rVSV challenge (H). I: Proliferation and resulting KL25HL B cell progeny in neonatally infected rCl13 carriers or adult rCl13-infected mice. J-M: Upon KL25HL transfer and rCl13 infection, timed as outlined (J), we measured KL25HL B cell proliferation and

expansion (K), nAb responses (L) and viremia (M). Symbols and bars represent means±SEM. $n$= 3-4, $N$=2-3. FACS plots are gated on CD45.1$^+$B220$^+$ lymphocytes. B cells and ASCs gating is shown in Fig. S1D. Numbers in FACS plots indicate percentages (mean±SEM). *,#: $p$<0.05; **,##: $p$<0.01. *,** compare B cells; #,## compare ASCs.
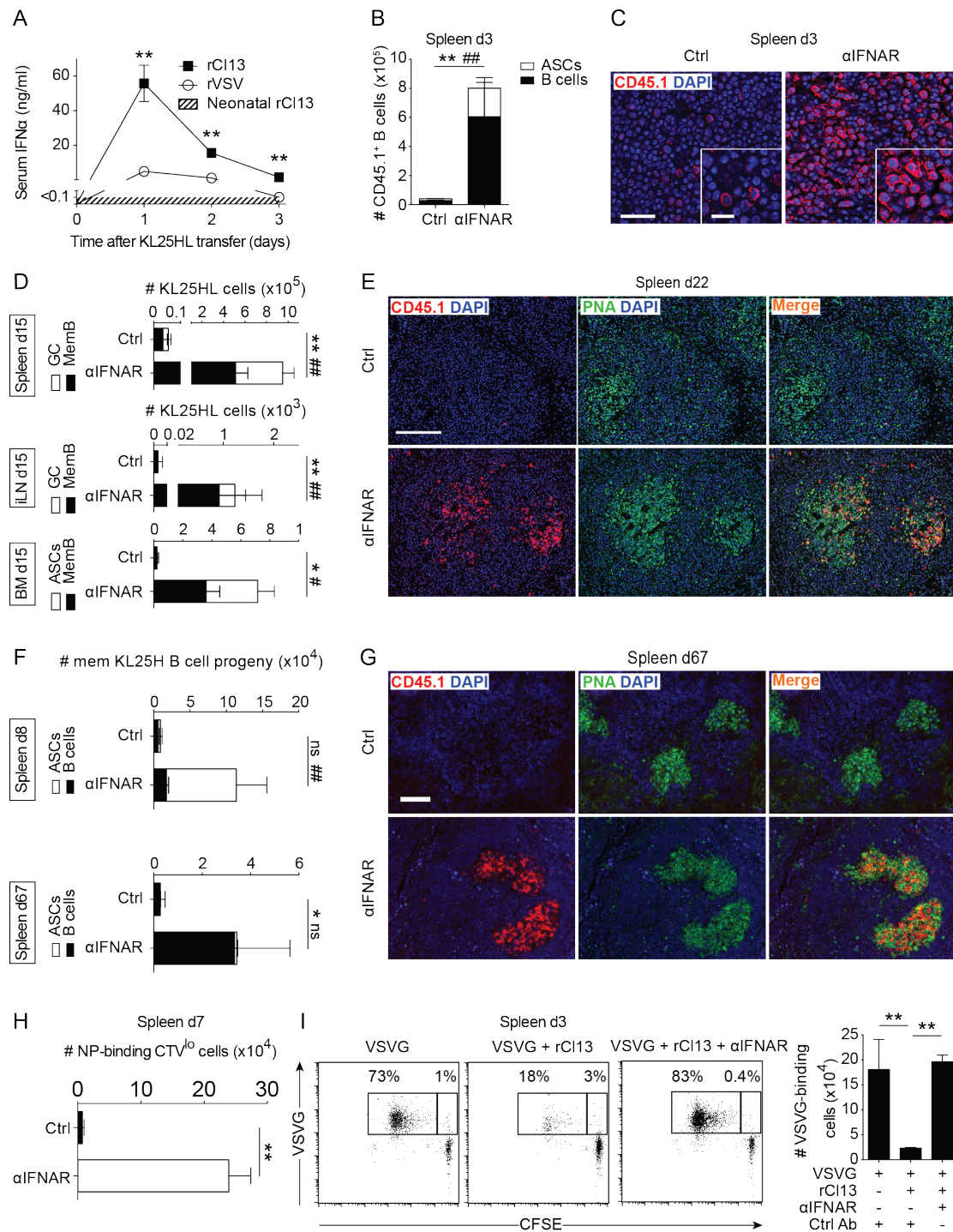
Fig. 2: IFNAR blockade restores B cell expansion and GC differentiation in rCl13 infection.

A: Serum IFN-α in KL25HL cell recipients, infected with rCl13 at birth or on d0, or infected with rVSV on d0.
B-G: We transferred naïve KL25HL cells (B-E), antigen-experienced KL25H B cells (F-G) or antigen-experienced polyclonal GFP$^+$ B cells (H) to αIFNAR- or control-treated wt recipients, followed by rCl13 infection. B cell progeny in the indicated organs were detected by FACS (B,D,F,H) and histology (C,E,G). Note progeny of naïve KL25HL cells (E) and of antigen-experienced KL25H cells (G) in GCs of

IFNAR-blocked recipients. Magnification bars: 50 µm, inset 20 µm (C); 200 µm (E); 100 µm (G). Numbers in (H) represent LCMV-NP-binding, proliferated (CellTraceViolet/CTV$^{lo}$) polyclonal donor (GFP$^+$) B cell progeny (CTV$^{lo}$GFP$^+$LCMV-NP$^+$ lymphocytes, compare Fig. S2D).

I: We transferred naïve VI10 cells to αIFNAR- or control-treated recipients, followed by VSVG immunization, alone or in combination with rCl13 infection. Proliferated (CFSE$^{lo}$) VSVG-binding VI10 B cells were enumerated by FACS. Plots are gated on CD45.2$^+$B220$^+$ lymphocytes. Bars represent the mean±SEM. *n*= 3-4, *N*=2-3. ns: not significant; *,#: *p*<0.05; **,##: *p*<0.01. *,** compare total or GC B cells; #,## compare ASCs or memB, respectively.
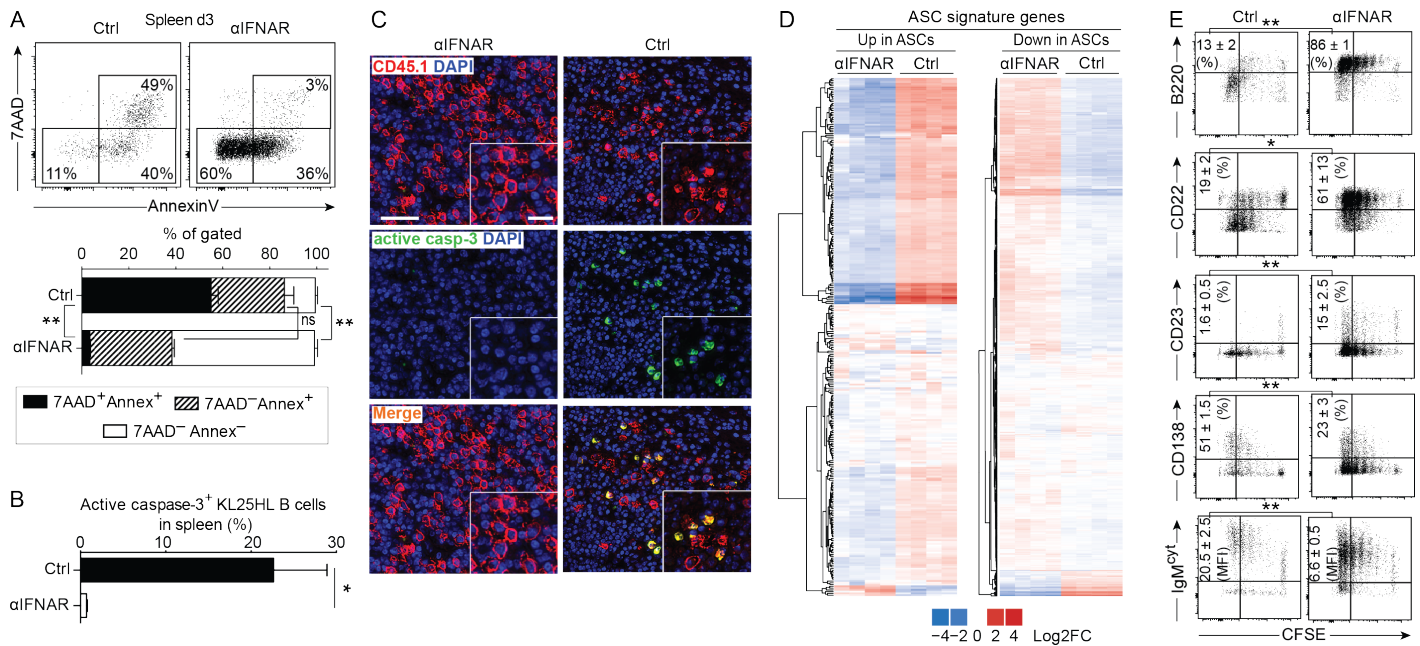
**Fig. 3: IFN-I-induced short-lived plasmablast differentiation in rCl13 infection.**

We transferred naïve KL25HL cells to αIFNAR- or control-treated recipients, followed by rCl13 infection and analysis in spleen on day 3. Apoptotic KL25HL B cell were identified in FACS based on AnnexinV/7AAD-binding (A) and by histology based on expression of active caspase-3 (B,C, magnification bar 50 μm, inset 20 μm). Proliferated KL25HL B cell progeny (CD45.1⁺B220⁺CFSE^lo) were FACS-sorted and total RNA was processed for RNAseq (D). Heat maps show expression profiles of ASC signature genes known to be upregulated (left) or downregulated (right) upon ASC differentiation, respectively (*89*). Plasmablast differentiation of proliferated (CFSE^lo) KL25HL B cell progeny was determined by flow cytometry (E). Numbers in FACS plots indicate the percentage of cells falling into the respective gate (A, representative FACS plots, gated as shown in Fig. S1D), the percentage of CFSE^lo cells expressing the respective marker (E) or the MFI of cytoplasmic IgM within IgM^cyt+CFSE^lo cells. Numbers and bars show means±SEM. n=3-4, *N*=2-3 (A-C,E). ns: not significant; *: *p*<0.05; **: *p*<0.01.
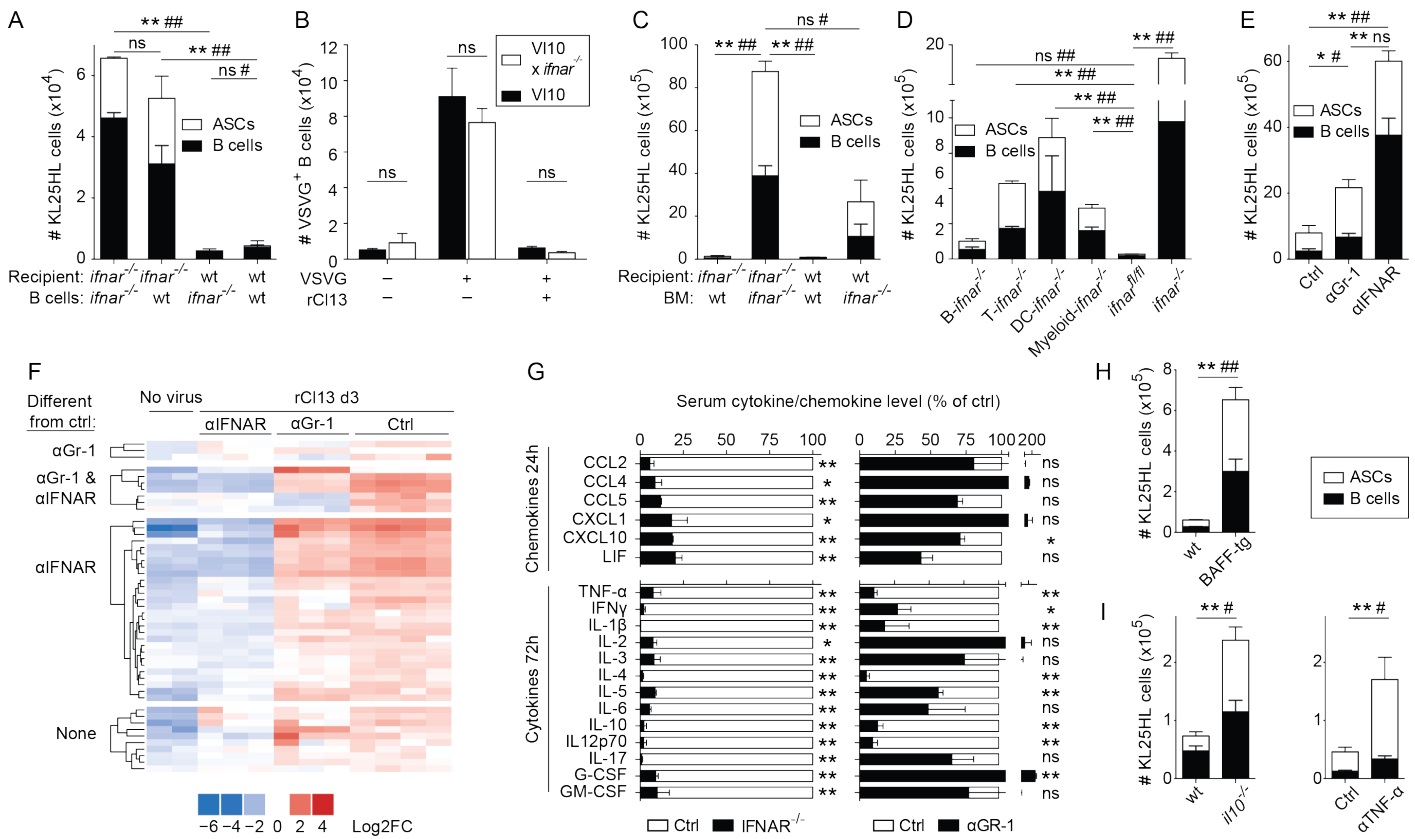
**Fig. 4: Impact of cell type-specific IFNAR signaling, IFN-I-induced inflammation and BAFF overexpression on rCl13-induced B cell decimation.**

A: We transferred KL25HL cells, either wt or *ifnar*^{-/-}, into wt or *ifnar*^{-/-} recipients and enumerated splenic KL25HL B cell progeny on d3 after rCl13.

B: We transferred VI10 cells into wt recipients, followed by VSVG immunization and rCl13 infection as indicated, and enumerated splenic VSVG-binding VI10 B cells on d3.

C-D: We transferred KL25HL cells into reciprocal wt and *ifnar*^{-/-} BM chimeras (C) or into recipients with cell type-specific, conditional or complete IFNAR deficiency (D) and enumerated splenic KL25HL B cell progeny on d3 after rCl13.

E: We transferred KL25HL cells into wt recipients, treated with αGr-1, αIFNAR or control, and enumerated splenic KL25HL B cell progeny on d3 after rCl13.

F: Low density inflammatory gene expression profiling in spleen of naïve or d3 rCl13-infected KL25HL recipients. Heat maps shows the 48 genes significantly up-regulated upon rCl13 infection.

G: Serum chemokines and cytokines were profiled at 24h and 72h after rCl13, respectively. *ifnar*^{-/-} and αGr-1-treated wt mice are expressed as percentage of control-treated wt mice. Only those 19/31 profiled chemokines and cytokines are displayed, which were ≥4-fold lower in *ifnar*^{-/-} than wt controls (Tbl. SII).

H-I: We transferred KL25HL cells into BAFF-transgenic (H), *il-10*^{-/-} or into wt recipients, treated with αTNF-α or control (I), and enumerated splenic KL25HL B cell progeny on d3 after rCl13.

B cells and ASCs were gated as shown in Fig. S1D. Bars show means±SEM. n=3-4. *N*=2-3 (A-E, H). ns: not significant; *,#: $p<0.05$; **,##: $p<0.01$. *,** compare B cells; #,## compare ASCs.

# II.6 Supplementary Figures and Tables

A



B      KL25 LC transgene cassette



C



D
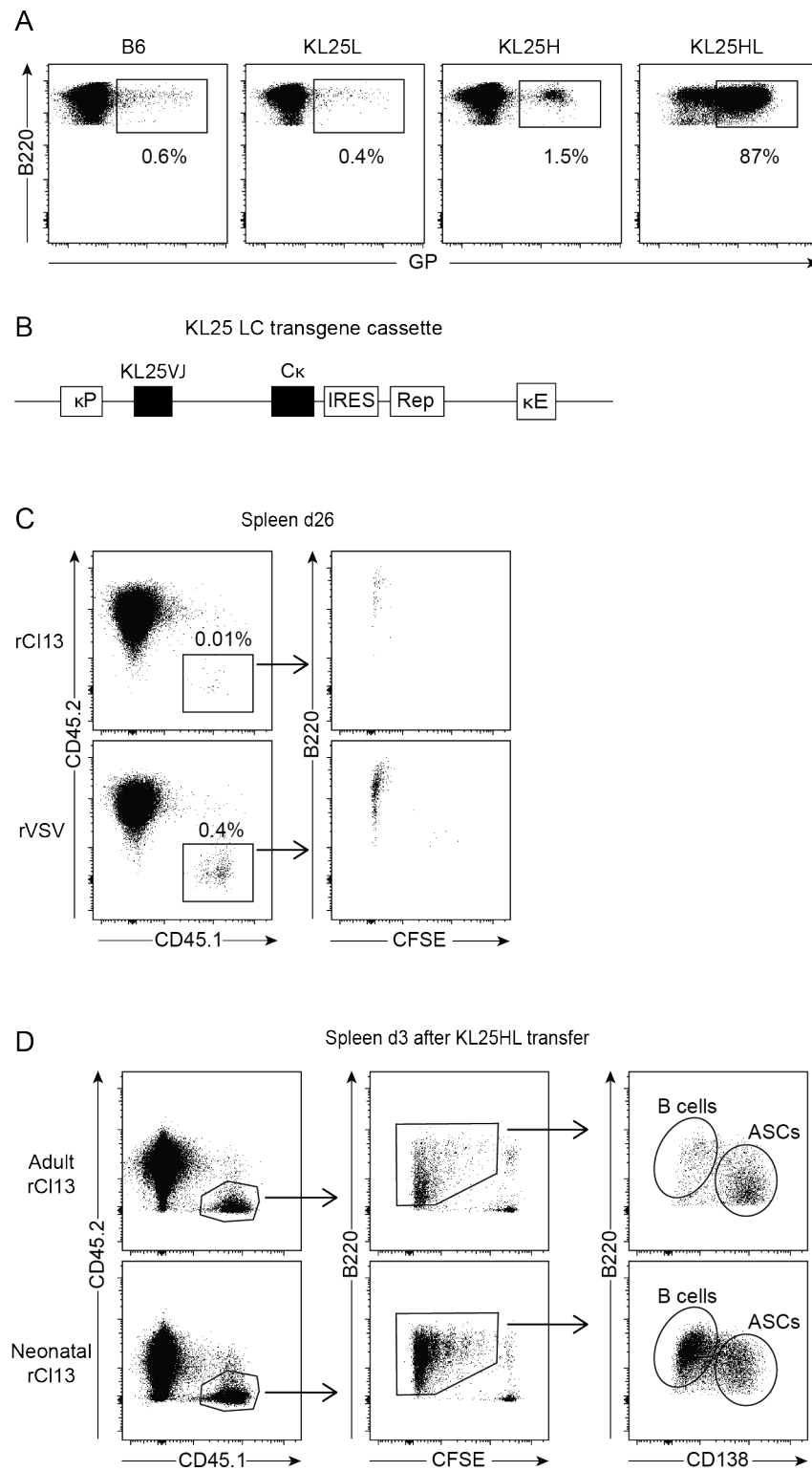
**Fig. S1: Characterization of KL25H and KL25HL mice, and FACS gating strategy pursued to analyze the respective B cell progeny in adoptive transfer experiments.**

A: GP-binding by B cells in peripheral blood of wt, KL25L (KL25 antibody light chain transgenic), KL25H (KL25 antibody heavy chain knock-in) and KL25HL mice (cross of KL25L and KL25H). Numbers in plots indicate the percentage of GP-binding cells amongst total B cells (gated on B220$^+$ lymphocytes).

B: KL25 light chain (LC) transgene construct. κP: Genomic immunoglobulin kappa (Igκ) chain promoter; KL25VJ: rearranged KL25 V and J segments, including leader and intron; Cκ: light chain kappa constant domain; IRES: internal ribosome entry site; Rep: cell surface reporter protein consisting in the murine Thy1.1 ectodomain fused to the transmembrane and cytoplasmic domains of the mouse PDGF receptor; κE: genomic Igκ locus enhancer element.

C: Gating strategy to Fig. 1D. We adoptively transferred CFSE-labeled KL25HL cells into naïve syngeneic recipients, followed by rCl13 or rVSV challenge and measured KL25HL progeny B cells on day 26. FACS plots on the left are pre-gated on B cells (B220$^+$ lymphocytes). Percentages of gated cells are indicated. Representative FACS plots are shown.

D: Gating strategy to enumerate "KL25HL B cell progeny", i.e. progeny KL25HL B cells and ASCs. On d0 we transferred KL25HL cells into adult syngeneic recipients, infected with rCl13 since birth (i.e. as neonates) or on the day of cell transfer (d0) and assessed B cell progeny (B cells and ASCs) on day 3. FACS plots on the left are pre-gated on lymphocytes. Representative FACS plots are shown.
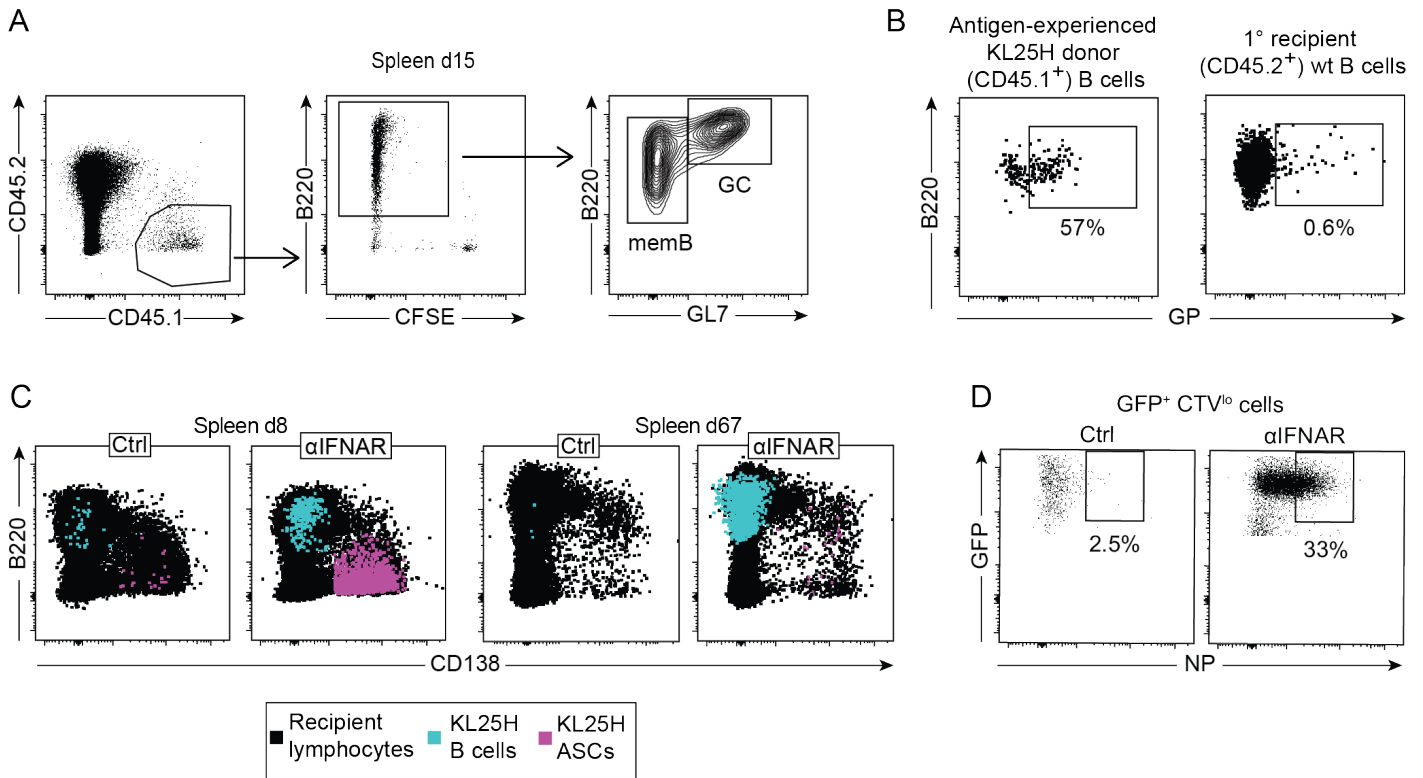
**Fig. S2: Gating strategy and representative FACS plots for adoptively transferred LCMV-experienced B cells.**

A: Gating strategy to enumerate memB and GC B cells in Fig. 2D. We adoptively transferred CFSE-labeled KL25HL cells into naïve syngeneic recipients, treated with αIFNAR or control antibody, followed by rCl13 infection and analysis on day 15. FACS plots on the left are pre-gated on lymphocytes. Representative FACS plots are shown.

B: Characterization of antigen-experienced KL25H B cells as used for adoptive transfer in Fig. 2F,G. LCMV-reactive KL25H B cells were expanded *in vivo*, and 3-4 weeks later were purified from spleen (see Materials and Methods). Such antigen-experienced KL25H cells from 10 primary recipients were pooled for adoptive transfer into secondary recipients. An aliquot thereof was analyzed for purity (~95% CD45.1$^+$B220$^+$, not shown) and was compared to B cells of the primary CD45.2$^+$ recipient (from the MACS flow-through) for GP-binding. Note the infection-induced enrichment of GP-binding KL25H donor B cells from ~2% at baseline (Fig. S1A) to >50% on the day of secondary transfer. Plots are gated on either CD45.1$^+$ or CD45.2$^+$ B220$^+$ lymphocytes, as indicated. Numbers show the percentage of gated cells. N=3.

C: Illustrative FACS plots to Fig. 2F. On the indicated days after rCl13 challenge, progeny B cells and ASCs of antigen-experienced KL25H B cell were gated as outlined in Fig. S1D. These populations were superimposed on the recipient's lymphocytes for display.

D: Illustrative FACS plot to Fig. 2H. GFP-transgenic polyclonal LCMV-experienced B cells were generated *in vivo* and purified from spleen (see Materials and Methods). On d7 after transfer into naïve recipients and rCl13 challenge we analyzed NP-binding by adoptively transferred (GFP$^+$) B cell progeny. A representative FACS plot is shown, gated on CTV$^{lo}$GFP$^+$ lymphocytes.
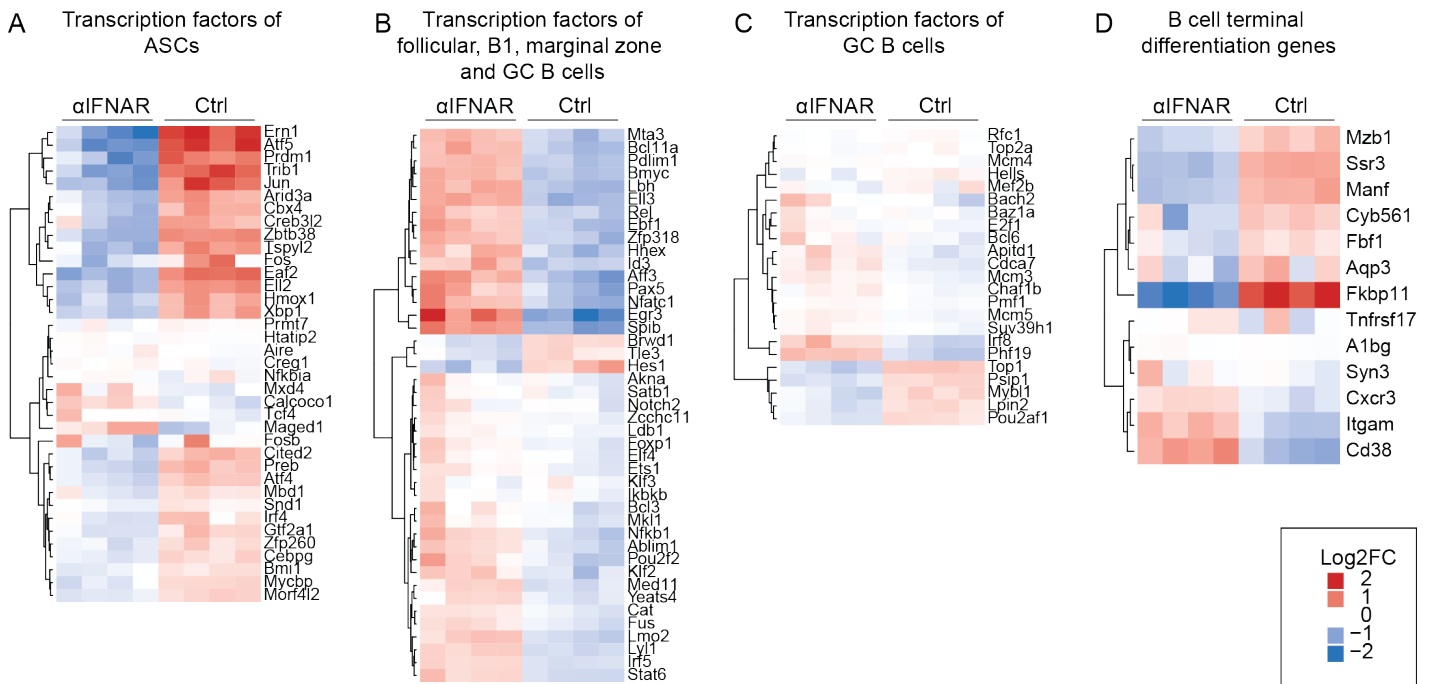
**Fig. S3: IFNAR blockade alters transcription factor and terminal differentiation profiles of B cells in rCl13 infection.**

We transferred naïve KL25HL cells to αIFNAR- or control-treated recipients, followed by rCl13 infection. On day 3, proliferated (CFSE^lo) KL25HL B cells were sorted from spleen and RNA was processed for RNAseq (same samples as in Fig. 3D). Heat maps show transcription factors associated with the indicated B cell differentiation stages (A-C, (*89*)) and genes associated with terminal B cell differentiation in HIV patients (D, (*145*)).
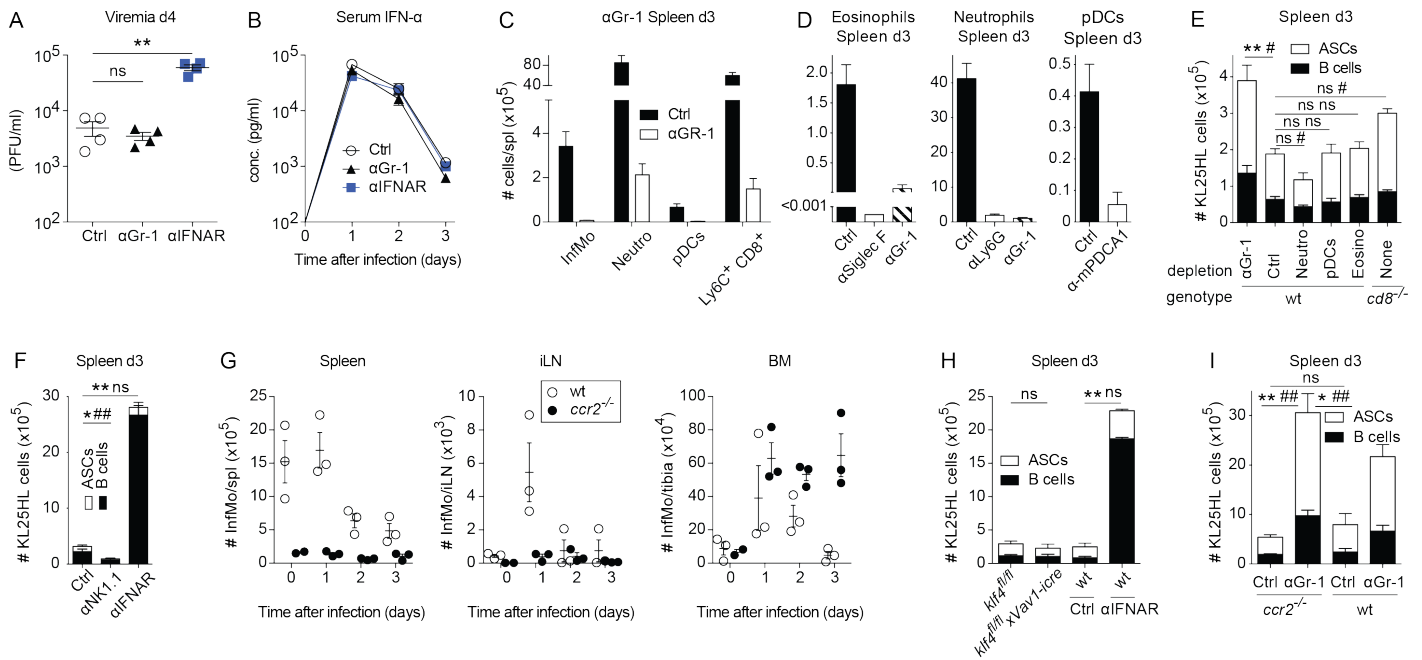
**Fig. S4: Effects of depletion antibodies on serum IFN-α, virus loads, myeloid cell population and KL25HL B cell recovery, and impact of genetic InfMo deficiency on KL25HL B cell recovery.**

A-B: We treated wt mice with αGr-1, αIFNAR or control antibody and infected them with rCl13. Viremia (A) and IFN-α concentrations in serum (B) were assessed on the indicated days.

C-E: We adoptively transferred KL25HL cells into wt (C,D) or wt and $cd8^{-/-}$ recipients (E), followed by rCl13 infection. Recipients were treated with either αGR-1 (pan-myeloid depletion), αSiglecF (selective eosinophil depletion), αLy6G (selective neutrophil depletion), α-mPDCA1 (selective pDC depletion) or control antibody. C,D: We enumerated InfMo (Thy1.2$^-$NK1.1$^-$CD19$^-$CD11b$^+$Ly6G$^-$Ly6C$^{hi}$, (*275*)), neutrophils (Thy1.2$^-$NK1.1$^-$CD19$^-$CD11b$^+$Ly6G$^{hi}$Ly6C$^{int}$ cells (*275*)), pDCs (Thy1.2$^-$NK1.1$^-$CD19$^-$CD11b$^-$Ly6C$^+$Siglec-H$^+$B220$^+$CD11c$^+$) and Ly6C$^+$ CD8$^+$ T cells (CD8$^+$Ly6C$^+$ lymphocytes) on d3 in spleen (C,D). Note that cell type-specific agents depleted their respective cell population similarly efficiently as αGr-1. KL25HL B cell progeny in spleen on d3 were enumerated (E) based on the gating strategy shown in Fig. S1D.

F: We adoptively transferred KL25HL cells into wt recipients, treated with NK cell-depleting antibody (αNK1.1), αIFNAR or control antibody, followed by rCl13 infection. KL25HL B cell progeny were enumerated on day 3 in spleen as in (E).

G: $ccr2^{-/-}$ and wt control mice were infected with rCl13 and InfMo numbers in spleen, iLN and BM were determined in spleen over time as described for (C,D).

H: We transferred KL25HL cells into $klf4^{fl/fl}$ x Vav1-icre and control $klf4^{fl/fl}$ followed by rCl13 infection. Groups of wt mice treated with αIFNAR or control antibody, served as high- and low-control groups, respectively. KL25HL B cell progeny were enumerated from spleen on d3 as in (E).

I: We adoptively transferred KL25HL cells into $ccr2^{-/-}$ and wt mice, treated with αGR-1 or control antibody as indicated, followed by rCl13 infection. KL25HL B cell progeny were enumerated from spleen on d3 as in (E). Same data set as Fig. 4E.

Symbols and bars represent means±SEM. *n*=3-4. *N*=2 (A-F, H-I). ns: not significant; *,#: *p*<0.05; **,##: *p*<0.01. *,** compare B cells; #,## compare ASCs.
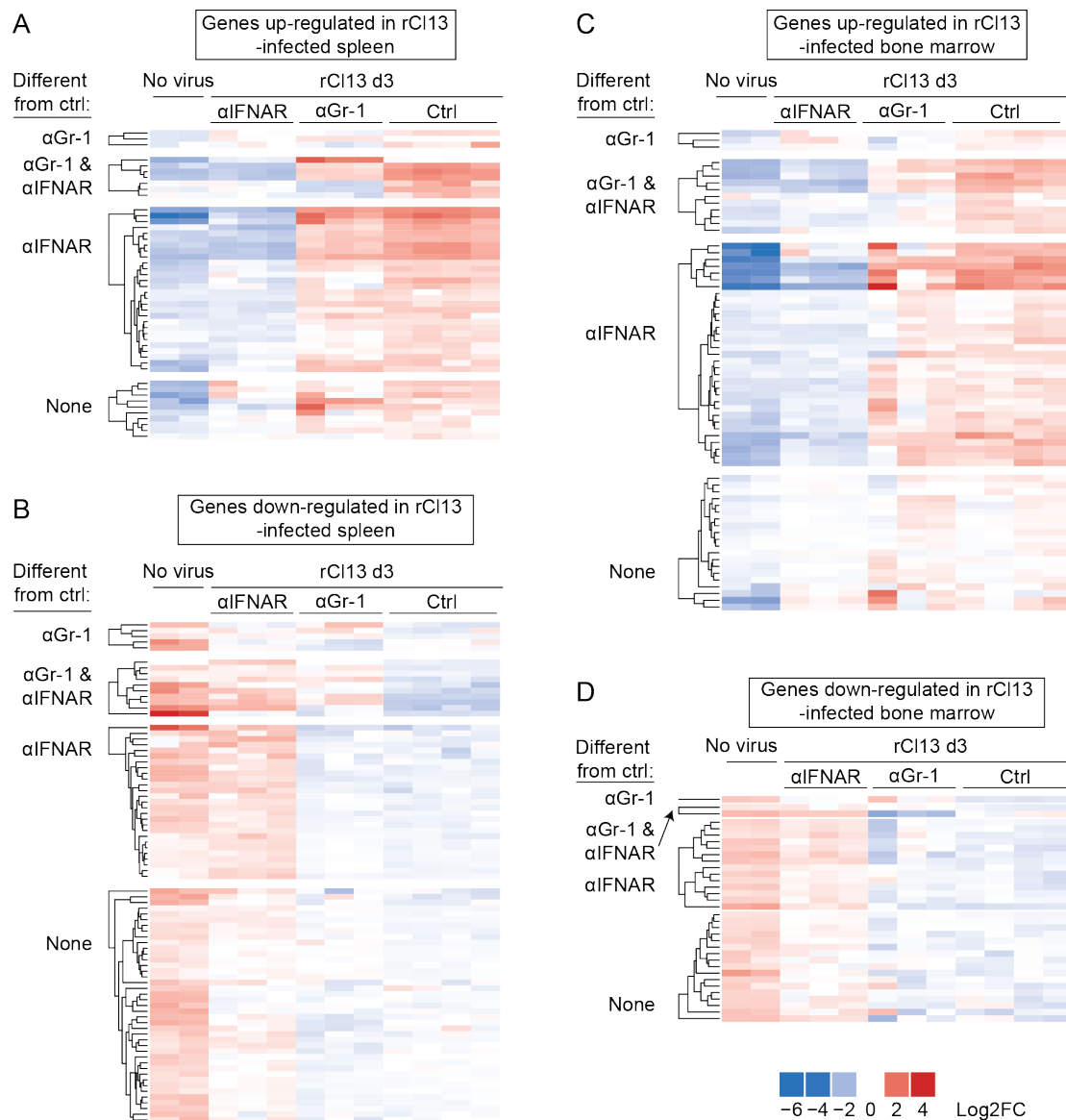
**Fig. S5: Impact of αGr-1 and αIFNAR on inflammatory gene expression profiles in spleen and bone marrow.**

We transferred KL25HL cells into wt recipients, treated with αGR-1, αIFNAR or control antibody, followed by rCl13 infection. Additional animals were left uninfected (no virus). On day 3 we processed spleen and BM for low-density expression profiling of 248 inflammatory genes. Heat maps show all those genes, which were significantly different between rCl13-infected control-treated mice and uninfected animals. Genes, which were up- (A,C) or down-regulated (B,D) in spleen (A,B) and BM (C,D) are shown separately, and were grouped according to whether αGR-1, αIFNAR or both treatments interfered with the infection-induced gene expression change. Columns represent individual mice, lanes individual genes (individually listed in Tbl. SI). Same data set as Fig. 4F.
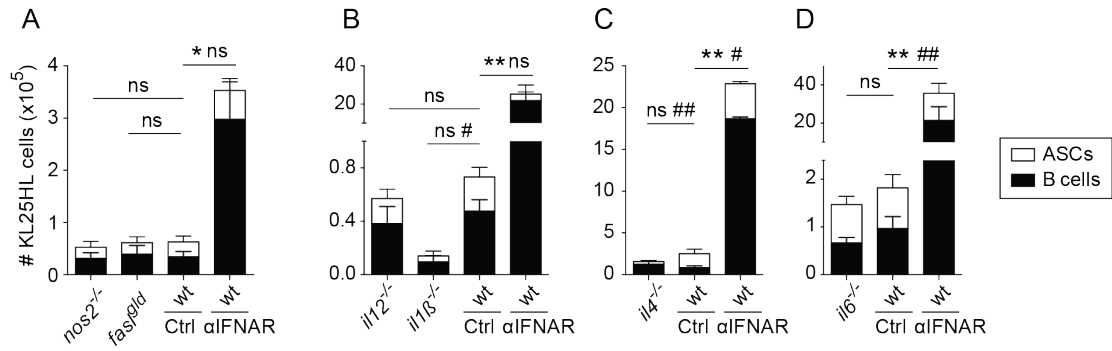
**Fig. S6: Individual impact of iNOS, FasL, IL-1β, IL-4, IL-6 and IL-12 on KL25HL B cell decimation.**

A-D. We transferred KL25HL cells into wt, iNOS-deficient $nos2^{-/-}$,FasL-mutant $fasl^{gld}$ , $il12p40^{-/-}$, $il1\beta^{-/-}$, $il4^{-/-}$ and $il6^{-/-}$ mice, followed by rCl13 infection. Groups of wt mice treated with αIFNAR or control antibody, served as high- and low-control groups, respectively. KL25HL B cell progeny in spleen on d3 were enumerated based on the gating strategy shown in Fig. S1D. B, same data set as Fig. 4I. C, same data set as Fig. S4H. Bars represent means±SEM. $n$=3-4, $N$=2. ns: not significant; *,#: $p$<0.05; **,##: $p$<0.01. *,** compare B cells; #,## compare ASCs.

**Table SI: Profound impact of IFNAR blockade and, more limited but largely overlapping, of αGr-1 depletion on inflammatory gene expression profiles in spleen and BM.**

| Gene expression change[1] | Different from ctrl Ab in: | EntrezID | Symbol | GeneName | no virus vs rCl13 + ctrl Ab[6] log2FC | adj.P.Val | rCl13 + αIFNAR vs rCl13 + ctrl Ab[7] log2FC | adj.P.Val | rCl13 + αGR-1 vs rCl13 + ctrl Ab[8] log2FC | adj.P.Val |
|---|---|---|---|---|---|---|---|---|---|---|
| up-regulated in rCl13-infected spleen[2] | αGR-1[9] | 16163 | Il13 | interleukin 13 | 0.91 | 0.03 | -0.68 | 0.07 | **-1.05** | **0.01** |
| | | 18783 | Pla2g4a | phospholipase A2, group IVA (cytosolic, calcium-dependent) | 0.70 | 0.00 | 0.05 | 0.78 | **0.51** | **0.01** |
| | | 16362 | Irf1 | interferon regulatory factor 1 | 1.15 | 0.00 | -0.47 | 0.04 | **-0.59** | **0.02** |
| | αGR-1 & αIFNAR[10] | 17392 | Mmp3 | matrix metallopeptidase 3 | 2.22 | 0.00 | **-0.63** | **0.00** | **2.04** | **0.00** |
| | | 12768 | Ccr1 | chemokine (C-C motif) receptor 1 | 1.45 | 0.00 | **-1.07** | **0.01** | **-1.90** | **0.00** |
| | | 15958 | Ifit2 | interferon-induced protein with tetratricopeptide repeats 2 | 3.31 | 0.00 | **-3.15** | **0.00** | **-0.83** | **0.00** |
| | | 15959 | Ifit3 | interferon-induced protein with tetratricopeptide repeats 3 | 2.94 | 0.00 | **-2.97** | **0.00** | **-0.71** | **0.03** |
| | | 16176 | Il1b | interleukin 1 beta | 0.82 | 0.02 | **-1.01** | **0.00** | **-1.84** | **0.00** |
| | | 227288 | Cxcr1 | chemokine (C-X-C motif) receptor 1 | 0.73 | 0.03 | **-1.11** | **0.00** | **-1.30** | **0.00** |
| | | 231655 | Oasl1 | 2'-5' oligoadenylate synthetase-like 1 | 2.46 | 0.00 | **-2.89** | **0.00** | **-0.75** | **0.01** |
| | αIFNAR[11] | 12263 | C2 | complement component 2 (within H-2S) | 1.42 | 0.01 | **-1.39** | **0.00** | 0.21 | 0.72 |
| | | 12267 | C3ar1 | complement component 3a receptor 1 | 1.35 | 0.00 | **-0.95** | **0.01** | 0.35 | 0.43 |
| | | 13163 | Daxx | Fas death domain-associated protein | 0.55 | 0.00 | **-0.96** | **0.00** | -0.31 | 0.10 |
| | | 14103 | Fasl | Fas ligand (TNF superfamily, member 6) | 0.83 | 0.04 | **-1.11** | **0.00** | -0.16 | 0.75 |
| | | 14962 | Cfb | complement factor B | 2.24 | 0.00 | **-0.89** | **0.00** | 0.47 | 0.10 |
| | | 15945 | Cxcl10 | chemokine (C-X-C motif) ligand 10 | 2.04 | 0.00 | **-1.62** | **0.00** | -0.77 | 0.16 |
| | | 15957 | Ifit1 | interferon-induced protein with tetratricopeptide repeats 1 | 2.78 | 0.00 | **-2.99** | **0.00** | -0.43 | 0.19 |
| | | 15977 | Ifnb1 | interferon beta 1, fibroblast | 1.19 | 0.00 | **-0.67** | **0.02** | -0.22 | 0.49 |
| | | 15978 | Ifng | interferon gamma | 1.37 | 0.00 | **-1.03** | **0.00** | -0.59 | 0.09 |
| | | 16153 | Il10 | interleukin 10 | 1.36 | 0.00 | **-1.22** | **0.00** | -0.16 | 0.64 |
| | | 16168 | Il15 | interleukin 15 | 0.64 | 0.02 | **-0.71** | **0.00** | -0.09 | 0.80 |
| | | 16181 | Il1rn | interleukin 1 receptor antagonist | 1.97 | 0.00 | **-0.84** | **0.02** | 0.10 | 0.84 |
| | | 17392 | Mmp3 | matrix metallopeptidase 3 | 2.22 | 0.00 | **-0.63** | **0.00** | 2.04 | 0.00 |
| | | 17857 | Mx1 | MX dynamin-like GTPase 1 | 0.64 | 0.01 | **-1.29** | **0.00** | -0.31 | 0.18 |
| | | 17858 | Mx2 | MX dynamin-like GTPase 2 | 1.41 | 0.00 | **-2.93** | **0.00** | -0.47 | 0.07 |
| | | 20296 | Ccl2 | chemokine (C-C motif) ligand 2 | 4.23 | 0.00 | **-2.20** | **0.00** | 0.06 | 0.93 |
| | | 20302 | Ccl3 | chemokine (C-C motif) ligand 3 | 2.38 | 0.00 | **-0.91** | **0.00** | 0.30 | 0.34 |
| | | 20303 | Ccl4 | chemokine (C-C motif) ligand 4 | 1.87 | 0.00 | **-1.22** | **0.00** | -0.12 | 0.80 |
| | | 20306 | Ccl7 | chemokine (C-C motif) ligand 7 | 5.67 | 0.00 | **-3.10** | **0.00** | -0.05 | 0.94 |
| | | 20846 | Stat1 | signal transducer and activator of transcription 1 | 1.53 | 0.00 | **-0.63** | **0.01** | -0.36 | 0.16 |
| | | 20847 | Stat2 | signal transducer and activator of transcription 2 | 1.31 | 0.00 | **-1.51** | **0.00** | -0.37 | 0.10 |
| | | 50909 | C1ra | complement component 1, r subcomponent A | 0.78 | 0.00 | **-0.92** | **0.00** | 0.20 | 0.35 |
| | | 54123 | Irf7 | interferon regulatory factor 7 | 3.13 | 0.00 | **-2.91** | **0.00** | -0.09 | 0.75 |
| | | 76933 | Ifi27l2a | interferon, alpha-inducible protein 27 like 2A | 2.05 | 0.00 | **-2.29** | **0.00** | -0.08 | 0.88 |
| | | 99899 | Ifi44 | interferon-induced protein 44 | 4.18 | 0.00 | **-3.46** | **0.00** | -0.06 | 0.88 |
| | | 170743 | Tlr7 | toll-like receptor 7 | 0.62 | 0.00 | **-1.00** | **0.00** | 0.06 | 0.80 |
| | | 246728 | Oas2 | 2'-5' oligoadenylate synthetase 2 | 2.54 | 0.00 | **-3.12** | **0.00** | -0.55 | 0.10 |
| | | 246730 | Oas1a | 2'-5' oligoadenylate synthetase 1A | 2.23 | 0.00 | **-2.22** | **0.00** | -0.25 | 0.44 |
| | | 625018 | C4a | complement component 4A (Rodgers blood group) | 0.75 | 0.01 | **-1.02** | **0.00** | 0.27 | 0.37 |
| | none[12] | 13198 | Ddit3 | DNA-damage inducible transcript 3 | 0.80 | 0.00 | -0.49 | 0.05 | 0.33 | 0.23 |
| | | 14825 | Cxcl1 | chemokine (C-X-C motif) ligand 1 | 2.04 | 0.03 | -1.39 | 0.10 | 0.85 | 0.40 |
| | | 16193 | Il6 | interleukin 6 | 1.05 | 0.03 | -0.32 | 0.48 | 0.06 | 0.91 |
| | | 16476 | Jun | jun proto-oncogene | 0.76 | 0.01 | -0.43 | 0.10 | 0.16 | 0.63 |
| | | 17329 | Cxcl9 | chemokine (C-X-C motif) ligand 9 | 2.16 | 0.01 | -0.39 | 0.62 | -0.13 | 0.89 |
| | | 19225 | Ptgs2 | prostaglandin-endoperoxide synthase 2 | 3.12 | 0.00 | -0.56 | 0.24 | -0.30 | 0.62 |
| | | 20307 | Ccl8 | chemokine (C-C motif) ligand 8 | 2.45 | 0.00 | -0.96 | 0.08 | 1.19 | 0.05 |
| | | 20310 | Cxcl2 | chemokine (C-X-C motif) ligand 2 | 1.17 | 0.04 | -0.55 | 0.30 | 0.19 | 0.80 |
| | | 60440 | Iigp1 | interferon inducible GTPase 1 | 2.66 | 0.00 | -0.47 | 0.34 | -0.53 | 0.35 |
| | | 257632 | Nod2 | nucleotide-binding oligomerization domain containing 2 | 0.58 | 0.05 | -0.32 | 0.24 | -0.41 | 0.18 |

| Gene expression change[1] | Different from ctrl Ab in: | EntrezID | Symbol | Gene Name | no virus vs rCl13 + ctrl Ab[6] | | rCl13 + αIFNAR vs rCl13 + ctrl Ab[7] | | rCl13 + αGR-1 vs rCl13 + ctrl Ab[8] | |
|---|---|---|---|---|---|---|---|---|---|---|
| | | | | | log2FC | adj.P.Val | log2FC | adj.P.Val | log2FC | adj.P.Val |
| down-regulated in rCl13-infected spleen[3] | αGR-1[9] | 16196 | Il7 | interleukin 7 | -1.57 | 0.00 | 0.15 | 0.72 | **1.38** | **0.00** |
| | | 21812 | Tgfbr1 | transforming growth factor, beta receptor I | -0.79 | 0.00 | 0.47 | 0.00 | **0.60** | **0.00** |
| | | 53603 | Tslp | thymic stromal lymphopoietin | -0.61 | 0.05 | 0.45 | 0.11 | **0.86** | **0.01** |
| | | 21947 | Cd40lg | CD40 ligand | -1.37 | 0.00 | -0.50 | 0.13 | **-0.72** | **0.05** |
| | | 12053 | Bcl6 | B cell leukemia/lymphoma 6 | -1.36 | 0.00 | 0.15 | 0.53 | **-0.53** | **0.04** |
| | αGR-1 & αIFNAR[10] | 11936 | Fxyd2 | FXYD domain-containing ion transport regulator 2 | -2.27 | 0.00 | **1.64** | **0.00** | **0.90** | **0.03** |
| | | 12274 | C6 | complement component 6 | -1.14 | 0.01 | **1.17** | **0.00** | **1.41** | **0.00** |
| | | 12771 | Ccr3 | chemokine (C-C motif) receptor 3 | -2.45 | 0.00 | **2.25** | **0.00** | **2.09** | **0.00** |
| | | 15289 | Hmgb1 | high mobility group box 1 | -0.50 | 0.00 | **1.15** | **0.00** | **0.58** | **0.00** |
| | | 17346 | Mknk1 | MAP kinase-interacting serine/threonine kinase 1 | -0.61 | 0.00 | **0.55** | **0.00** | **0.64** | **0.00** |
| | | 17533 | Mrc1 | mannose receptor, C type 1 | -2.21 | 0.00 | **1.75** | **0.00** | **1.78** | **0.00** |
| | | 18829 | Ccl21a | chemokine (C-C motif) ligand 21A (serine) | -3.65 | 0.00 | **0.64** | **0.01** | **0.57** | **0.04** |
| | | 19224 | Ptgs1 | prostaglandin-endoperoxide synthase 1 | -1.19 | 0.00 | **0.75** | **0.00** | **0.89** | **0.00** |
| | | 20299 | Ccl22 | chemokine (C-C motif) ligand 22 | -2.36 | 0.00 | **0.94** | **0.01** | **1.04** | **0.01** |
| | | 93671 | Cd163 | CD163 antigen | -3.01 | 0.00 | **2.31** | **0.00** | **1.04** | **0.00** |
| | αIFNAR[11] | 11687 | Alox15 | arachidonate 15-lipoxygenase | -0.99 | 0.01 | **0.88** | **0.01** | -0.19 | 0.67 |
| | | 11848 | Rhoa | ras homolog gene family, member A | -0.64 | 0.00 | **0.61** | **0.00** | 0.40 | 0.03 |
| | | 11909 | Atf2 | activating transcription factor 2 | -0.60 | 0.00 | **0.51** | **0.00** | 0.28 | 0.02 |
| | | 12048 | Bcl2l1 | BCL2-like 1 | -1.05 | 0.00 | **0.73** | **0.01** | 0.38 | 0.18 |
| | | 14784 | Grb2 | growth factor receptor bound protein 2 | -0.90 | 0.00 | **0.53** | **0.01** | 0.14 | 0.56 |
| | | 14969 | H2-Eb1 | histocompatibility 2, class II antigen E beta | -1.36 | 0.00 | **0.69** | **0.00** | -0.14 | 0.62 |
| | | 16160 | Il12b | interleukin 12b | -1.39 | 0.00 | **0.96** | **0.00** | 0.56 | 0.13 |
| | | 16189 | Il4 | interleukin 4 | -0.95 | 0.00 | **0.62** | **0.02** | -0.09 | 0.81 |
| | | 16194 | Il6ra | interleukin 6 receptor, alpha | -1.57 | 0.00 | **0.92** | **0.04** | 0.04 | 0.94 |
| | | 17134 | Mafg | v-maf musculoaponeurotic fibrosarcom oncog. fam., prot. G (avian) | -0.98 | 0.00 | **0.92** | **0.00** | 0.13 | 0.63 |
| | | 18751 | Prkcb | protein kinase C, beta | -1.24 | 0.00 | **0.61** | **0.02** | 0.18 | 0.55 |
| | | 19219 | Ptger4 | prostaglandin E receptor 4 (subtype EP4) | -1.03 | 0.00 | **0.67** | **0.00** | 0.25 | 0.10 |
| | | 20416 | Shc1 | src homology 2 domain-containing transforming protein C1 | -0.58 | 0.00 | **0.86** | **0.00** | 0.36 | 0.06 |
| | | 22154 | Tubb5 | tubulin, beta 5 class I | -0.54 | 0.02 | **0.86** | **0.00** | 0.11 | 0.68 |
| | | 26398 | Map2k4 | mitogen-activated protein kinase kinase 4 | -0.57 | 0.00 | **0.72** | **0.00** | 0.36 | 0.02 |
| | | 26409 | Map3k7 | mitogen-activated protein kinase kinase kinase 7 | -0.53 | 0.00 | **0.64** | **0.00** | 0.28 | 0.02 |
| | | 26416 | Mapk14 | mitogen-activated protein kinase 14 | -1.15 | 0.00 | **0.81** | **0.00** | 0.38 | 0.05 |
| | | 26419 | Mapk8 | mitogen-activated protein kinase 8 | -0.84 | 0.00 | **0.63** | **0.00** | 0.30 | 0.03 |
| | | 53791 | Tlr5 | toll-like receptor 5 | -1.58 | 0.00 | **1.06** | **0.00** | 0.25 | 0.49 |
| | | 54473 | Tollip | toll interacting protein | -0.61 | 0.00 | **0.64** | **0.00** | 0.30 | 0.01 |
| | | 71609 | Tradd | TNFRSF1A-associated via death domain | -0.91 | 0.00 | **0.52** | **0.04** | -0.08 | 0.81 |
| | | 73086 | Rps6ka5 | ribosomal protein S6 kinase, polypeptide 5 | -1.47 | 0.00 | **0.68** | **0.01** | 0.20 | 0.48 |
| | | 97165 | Hmgb2 | high mobility group box 2 | -0.57 | 0.03 | **1.38** | **0.00** | 0.21 | 0.47 |
| | | 237310 | Il22ra2 | interleukin 22 receptor, alpha 2 | -3.13 | 0.00 | **1.55** | **0.00** | 0.08 | 0.88 |
| | | NA | Gpr44 | NA | -0.72 | 0.04 | **1.06** | **0.00** | 0.14 | 0.75 |
| | | NA | Hras1 | NA | -1.25 | 0.00 | **1.04** | **0.00** | 0.19 | 0.52 |
| | | 329251 | Ppp1r12b | protein phosphatase 1, regulatory (inhibitor) subunit 12B | -0.71 | 0.01 | **0.89** | **0.00** | 0.40 | 0.13 |
| | none[12] | 11684 | Alox12 | arachidonate 12-lipoxygenase | -1.89 | 0.01 | 0.77 | 0.27 | 0.76 | 0.35 |
| | | 12504 | Cd4 | CD4 antigen | -1.19 | 0.00 | -0.05 | 0.74 | -0.02 | 0.90 |
| | | 12767 | Cxcr4 | chemokine (C-X-C motif) receptor 4 | -0.75 | 0.03 | 0.15 | 0.67 | -0.55 | 0.13 |
| | | 12773 | Ccr4 | chemokine (C-C motif) receptor 4 | -1.01 | 0.01 | 0.44 | 0.24 | -0.08 | 0.88 |
| | | 12775 | Ccr7 | chemokine (C-C motif) receptor 7 | -1.17 | 0.00 | 0.11 | 0.70 | -0.57 | 0.06 |
| | | 12912 | Creb1 | cAMP responsive element binding protein 1 | -1.01 | 0.00 | 0.26 | 0.10 | 0.03 | 0.88 |
| | | 13136 | Cd55 | CD55 molecule, decay accelerating factor for complement | -1.35 | 0.01 | 0.19 | 0.68 | 0.33 | 0.52 |
| | | 13712 | Elk1 | ELK1, member of ETS oncogene family | -0.88 | 0.00 | 0.44 | 0.02 | 0.22 | 0.34 |
| | | 14683 | Gnas | GNAS (guanine nucleot. bind. Prot., alpha stim.) complex locus | -0.80 | 0.01 | 0.50 | 0.08 | 0.00 | 1.00 |
| | | 14815 | Nr3c1 | nuclear receptor subfamily 3, group C, member 1 | -0.72 | 0.00 | 0.12 | 0.43 | 0.05 | 0.82 |
| | | 15139 | Hc | hemolytic complement | -1.51 | 0.00 | 0.83 | 0.08 | -0.19 | 0.78 |
| | | 15962 | Ifna1 | interferon alpha 1 | -0.62 | 0.00 | 0.15 | 0.44 | -0.40 | 0.06 |
| | | 16155 | Il10rb | interleukin 10 receptor, beta | -0.61 | 0.00 | 0.17 | 0.27 | 0.35 | 0.04 |

52

| | | 16177 | Il1r1 | interleukin 1 receptor, type I | -0.65 | 0.04 | 0.19 | 0.51 | 0.56 | 0.09 |
|---|---|---|---|---|---|---|---|---|---|---|
| | | 16183 | Il2 | interleukin 2 | -0.73 | 0.04 | -0.22 | 0.51 | -0.26 | 0.51 |
| | | 16885 | Limk1 | LIM-domain containing, protein kinase | -0.64 | 0.00 | 0.40 | 0.01 | 0.21 | 0.18 |
| | | 16994 | Ltb | lymphotoxin B | -0.74 | 0.01 | -0.20 | 0.43 | -0.21 | 0.49 |
| | | 17131 | Smad7 | SMAD family member 7 | -1.24 | 0.00 | -0.14 | 0.37 | 0.12 | 0.51 |
| | | 17135 | Mafk | v-maf musculoaponeurot. fibrosarcoma oncog. Fam., prot. K (avian) | -0.62 | 0.00 | 0.44 | 0.00 | -0.25 | 0.13 |
| | | 17195 | Mbl2 | mannose-binding lectin (protein C) 2 | -0.83 | 0.01 | 0.10 | 0.76 | -0.27 | 0.48 |
| | | 17258 | Mef2a | myocyte enhancer factor 2A | -0.55 | 0.03 | 0.26 | 0.25 | 0.37 | 0.15 |
| | | 17261 | Mef2d | myocyte enhancer factor 2D | -1.04 | 0.00 | 0.19 | 0.34 | -0.08 | 0.80 |
| | | 18021 | Nfatc3 | nuclear factor of activated T cells, cytoplasm., calcineurin dep. 3 | -0.54 | 0.03 | 0.15 | 0.51 | 0.02 | 0.93 |
| | | 18033 | Nfkb1 | nuclear factor of kappa light polypep. gene enha. in B cells 1, p105 | -0.62 | 0.01 | 0.25 | 0.27 | 0.24 | 0.35 |
| | | 19353 | Rac1 | RAS-related C3 botulinum substrate 1 | -0.51 | 0.00 | 0.50 | 0.00 | 0.47 | 0.00 |
| | | 19697 | Rela | v-rel reticuloendotheliosis viral oncogene homolog A (avian) | -0.59 | 0.00 | 0.48 | 0.00 | 0.16 | 0.17 |
| | | 19698 | Relb | avian reticuloendotheliosis viral (v-rel) oncogene related B | -0.70 | 0.01 | 0.15 | 0.52 | 0.26 | 0.34 |
| | | 19878 | Rock2 | Rho-associated coiled-coil containing protein kinase 2 | -0.53 | 0.00 | 0.20 | 0.22 | 0.35 | 0.05 |
| | | 21390 | Tbxa2r | thromboxane A2 receptor | -1.30 | 0.00 | -0.14 | 0.72 | 0.01 | 0.99 |
| | | 21413 | Tcf4 | transcription factor 4 | -0.51 | 0.00 | 0.14 | 0.35 | 0.45 | 0.01 |
| | | 21803 | Tgfb1 | transforming growth factor, beta 1 | -0.85 | 0.00 | 0.49 | 0.00 | 0.49 | 0.00 |
| | | 22030 | Traf2 | TNF receptor-associated factor 2 | -0.62 | 0.00 | 0.18 | 0.10 | 0.03 | 0.84 |
| | | 26399 | Map2k6 | mitogen-activated protein kinase kinase 6 | -1.52 | 0.00 | 0.44 | 0.11 | 0.26 | 0.42 |
| | | 26401 | Map3k1 | mitogen-activated protein kinase kinase kinase 1 | -0.80 | 0.00 | 0.15 | 0.40 | -0.10 | 0.63 |
| | | 26408 | Map3k5 | mitogen-activated protein kinase kinase kinase 5 | -0.53 | 0.00 | 0.19 | 0.24 | -0.05 | 0.81 |
| | | 26417 | Mapk3 | mitogen-activated protein kinase 3 | -0.90 | 0.01 | 0.54 | 0.09 | 0.36 | 0.34 |
| | | 27056 | Irf5 | interferon regulatory factor 5 | -1.00 | 0.00 | 0.32 | 0.27 | 0.17 | 0.64 |
| | | 54131 | Irf3 | interferon regulatory factor 3 | -0.94 | 0.00 | 0.45 | 0.11 | -0.09 | 0.82 |
| | | 11596 | Ager | advanced glycosylation end product-specific receptor | -1.12 | 0.00 | 0.27 | 0.35 | -0.35 | 0.32 |
| | | 208727 | Hdac4 | histone deacetylase 4 | -0.60 | 0.01 | 0.10 | 0.67 | -0.25 | 0.34 |
| | | 338372 | Map3k9 | mitogen-activated protein kinase kinase kinase 9 | -1.11 | 0.03 | 0.05 | 0.92 | 0.16 | 0.81 |

| Gene expression change[1] | Different from ctrl Ab in: | EntrezID | Symbol | Gene Name | no virus vs rCl13 + ctrl Ab[6] log2FC | adj.P.Val | rCl13 + αIFNAR vs rCl13 + ctrl Ab[7] log2FC | adj.P.Val | rCl13 + αGR-1 vs rCl13 + ctrl Ab[8] log2FC | adj.P.Val |
|---|---|---|---|---|---|---|---|---|---|---|
| | αGR-1[9] | 12504 | Cd4 | CD4 antigen | 0.92 | 0.00 | -0.19 | 0.24 | **-0.62** | **0.00** |
| | | 16362 | Irf1 | interferon regulatory factor 1 | 2.04 | 0.00 | -0.40 | 0.09 | **-0.81** | **0.00** |
| | | 257632 | Nod2 | nucleotide-binding oligomerization domain containing 2 | 1.21 | 0.00 | 0.11 | 0.75 | **-0.88** | **0.01** |
| | αGR-1 & αIFNAR[10] | 15958 | Ifit2 | interferon-induced protein with tetratricopeptide repeats 2 | 3.81 | 0.00 | **-2.78** | **0.00** | **-0.95** | **0.00** |
| | | 15959 | Ifit3 | interferon-induced protein with tetratricopeptide repeats 3 | 3.97 | 0.00 | **-2.47** | **0.00** | **-1.43** | **0.00** |
| | | 16153 | Il10 | interleukin 10 | 0.62 | 0.04 | **-0.78** | **0.01** | **-0.99** | **0.00** |
| | | 17858 | Mx2 | MX dynamin-like GTPase 2 | 2.19 | 0.00 | **-2.60** | **0.00** | **-0.60** | **0.04** |
| | | 20846 | Stat1 | signal transducer and activator of transcription 1 | 2.32 | 0.00 | **-0.77** | **0.00** | **-0.77** | **0.00** |
| | | 20847 | Stat2 | signal transducer and activator of transcription 2 | 1.98 | 0.00 | **-1.54** | **0.00** | **-0.86** | **0.00** |
| | | 21897 | Tlr1 | toll-like receptor 1 | 1.93 | 0.00 | **-1.06** | **0.00** | **-0.70** | **0.00** |
| | | 54123 | Irf7 | interferon regulatory factor 7 | 3.46 | 0.00 | **-2.27** | **0.00** | **-0.52** | **0.04** |
| | | 107607 | Nod1 | nucleotide-binding oligomerization domain containing 1 | 1.50 | 0.00 | **-0.52** | **0.03** | **-0.89** | **0.00** |
| | | 170743 | Tlr7 | toll-like receptor 7 | 1.39 | 0.00 | **-1.22** | **0.00** | **-0.63** | **0.00** |
| | | 231655 | Oasl1 | 2'-5' oligoadenylate synthetase-like 1 | 3.25 | 0.00 | **-3.30** | **0.00** | **-0.85** | **0.00** |
| | αIFNAR[11] | 12259 | C1qa | complement component 1, q subcomponent, alpha polypeptide | 1.79 | 0.00 | **-1.25** | **0.00** | -0.20 | 0.22 |
| | | 12260 | C1qb | complement component 1, q subcomponent, beta polypeptide | 2.30 | 0.00 | **-1.49** | **0.00** | -0.47 | 0.00 |
| | | 12263 | C2 | complement component 2 (within H-2S) | 1.37 | 0.01 | **-0.94** | **0.05** | 0.20 | 0.73 |
| | | 12267 | C3ar1 | complement component 3a receptor 1 | 3.72 | 0.00 | **-2.83** | **0.00** | -0.69 | 0.11 |
| | | 12524 | Cd86 | CD86 antigen | 1.17 | 0.00 | **-0.93** | **0.00** | -0.22 | 0.21 |
| | | 13163 | Daxx | Fas death domain-associated protein | 1.70 | 0.00 | **-1.53** | **0.00** | -0.39 | 0.05 |
| | | 14103 | Fasl | Fas ligand (TNF superfamily, member 6) | 1.82 | 0.00 | **-0.89** | **0.02** | 0.25 | 0.57 |
| | | 14433 | Gapdh | glyceraldehyde-3-phosphate dehydrogenase | 1.02 | 0.00 | **-0.62** | **0.00** | 0.18 | 0.30 |
| | | 14962 | Cfb | complement factor B | 5.52 | 0.00 | **-2.37** | **0.00** | -0.45 | 0.14 |
| | | 15945 | Cxcl10 | chemokine (C-X-C motif) ligand 10 | 5.17 | 0.00 | **-3.03** | **0.00** | -1.03 | 0.07 |
| | | 15957 | Ifit1 | interferon-induced protein with tetratricopeptide repeats 1 | 3.44 | 0.00 | **-2.09** | **0.00** | -0.27 | 0.41 |
| | | 16173 | Il18 | interleukin 18 | 1.39 | 0.00 | **-1.39** | **0.00** | -0.42 | 0.04 |
| | | 16476 | Jun | jun proto-oncogene | 1.73 | 0.00 | **-1.49** | **0.00** | -0.05 | 0.88 |
| | | 17329 | Cxcl9 | chemokine (C-X-C motif) ligand 9 | 5.67 | 0.00 | **-1.65** | **0.03** | -0.40 | 0.65 |
| | | 17857 | Mx1 | MX dynamin-like GTPase 1 | 1.18 | 0.00 | **-1.02** | **0.00** | -0.07 | 0.82 |
| | | 17869 | Myc | myelocytomatosis oncogene | 1.00 | 0.00 | **-0.78** | **0.00** | 0.30 | 0.21 |
| | | 17874 | Myd88 | myeloid differentiation primary response gene 88 | 1.39 | 0.00 | **-0.67** | **0.01** | -0.21 | 0.41 |
| | | 20296 | Ccl2 | chemokine (C-C motif) ligand 2 | 5.84 | 0.00 | **-3.87** | **0.00** | -0.93 | 0.16 |
| | | 20302 | Ccl3 | chemokine (C-C motif) ligand 3 | 1.66 | 0.00 | **-1.37** | **0.00** | -0.10 | 0.79 |
| | | 20303 | Ccl4 | chemokine (C-C motif) ligand 4 | 2.24 | 0.00 | **-1.32** | **0.00** | -0.41 | 0.30 |
| | | 20306 | Ccl7 | chemokine (C-C motif) ligand 7 | 6.43 | 0.00 | **-4.75** | **0.00** | -0.32 | 0.69 |
| | | 21898 | Tlr4 | toll-like receptor 4 | 1.24 | 0.00 | **-0.61** | **0.02** | -0.34 | 0.21 |
| | | 50868 | Keap1 | kelch-like ECH-associated protein 1 | 0.81 | 0.00 | **-0.64** | **0.00** | -0.02 | 0.91 |
| | | 58861 | Cysltr1 | cysteinyl leukotriene receptor 1 | 2.12 | 0.00 | **-1.23** | **0.02** | -0.44 | 0.44 |
| | | 60440 | Iigp1 | interferon inducible GTPase 1 | 5.33 | 0.00 | **-1.36** | **0.01** | -1.12 | 0.05 |
| | | 76933 | Ifi27l2a | interferon, alpha-inducible protein 27 like 2A | 3.18 | 0.00 | **-1.58** | **0.00** | -0.48 | 0.22 |
| | | 81897 | Tlr9 | toll-like receptor 9 | 1.70 | 0.00 | **-1.46** | **0.00** | -0.66 | 0.06 |
| | | 99899 | Ifi44 | interferon-induced protein 44 | 5.47 | 0.00 | **-4.20** | **0.00** | -0.35 | 0.26 |
| | | 142980 | Tlr3 | toll-like receptor 3 | 1.46 | 0.00 | **-1.06** | **0.00** | -0.27 | 0.28 |
| | | 209488 | Hsh2d | hematopoietic SH2 domain containing | 1.10 | 0.00 | **-0.96** | **0.00** | -0.49 | 0.04 |
| | | 246728 | Oas2 | 2'-5' oligoadenylate synthetase 2 | 2.97 | 0.00 | **-1.57** | **0.00** | -0.48 | 0.17 |
| | | 246730 | Oas1a | 2'-5' oligoadenylate synthetase 1A | 3.36 | 0.00 | **-1.82** | **0.00** | -0.38 | 0.21 |
| | | 625018 | C4a | complement component 4A (Rodgers blood group) | 2.49 | 0.00 | **-1.43** | **0.00** | -0.28 | 0.37 |
| up-regulated in rCl13-infected bone marrow[4] | none[12] | 12608 | Cebpb | CCAAT/enhancer binding protein (C/EBP), beta | 1.34 | 0.00 | -0.49 | 0.14 | -0.45 | 0.22 |
| | | 15251 | Hif1a | hypoxia inducible factor 1, alpha subunit | 0.74 | 0.00 | -0.42 | 0.05 | 0.32 | 0.18 |
| | | 16155 | Il10rb | interleukin 10 receptor, beta | 0.57 | 0.00 | -0.32 | 0.05 | -0.04 | 0.87 |
| | | 16885 | Limk1 | LIM-domain containing, protein kinase | 0.81 | 0.00 | -0.27 | 0.07 | 0.27 | 0.10 |
| | | 16992 | Lta | lymphotoxin A | 0.58 | 0.04 | -0.02 | 0.94 | -0.18 | 0.55 |
| | | 17087 | Ly96 | lymphocyte antigen 96 | 0.86 | 0.00 | -0.32 | 0.08 | -0.15 | 0.46 |
| | | 17164 | Mapkapk2 | MAP kinase-activated protein kinase 2 | 1.05 | 0.00 | -0.28 | 0.11 | 0.03 | 0.88 |
| | | 18033 | Nfkb1 | nuclear factor of kappa light polypept. gene enh. in B cells 1, p105 | 0.60 | 0.02 | -0.11 | 0.70 | 0.40 | 0.12 |
| | | 18783 | Pla2g4a | phospholipase A2, group IVA (cytosolic, calcium-dependent) | 0.78 | 0.00 | -0.47 | 0.01 | 0.07 | 0.74 |

54

| 19766 | Ripk1 | receptor (TNFRSF)-interacting serine-threonine kinase 1 | 0.61 | 0.00 | -0.14 | 0.46 | 0.23 | 0.27 |
| 20304 | Ccl5 | chemokine (C-C motif) ligand 5 | 2.50 | 0.00 | -0.30 | 0.48 | 0.02 | 0.96 |
| 20307 | Ccl8 | chemokine (C-C motif) ligand 8 | 3.60 | 0.00 | -0.27 | 0.69 | 0.12 | 0.87 |
| 20848 | Stat3 | signal transducer and activator of transcription 3 | 0.56 | 0.00 | -0.17 | 0.26 | 0.01 | 0.96 |
| 21899 | Tlr6 | toll-like receptor 6 | 0.85 | 0.00 | -0.31 | 0.18 | -0.49 | 0.06 |
| 21926 | Tnf | tumor necrosis factor | 0.61 | 0.01 | -0.18 | 0.45 | -0.38 | 0.14 |
| 24047 | Ccl19 | chemokine (C-C motif) ligand 19 | 1.48 | 0.02 | 0.20 | 0.78 | 1.10 | 0.10 |
| 26395 | Map2k1 | mitogen-activated protein kinase kinase 1 | 0.76 | 0.00 | -0.41 | 0.02 | -0.09 | 0.65 |
| 50909 | C1ra | complement component 1, r subcomponent A | 0.71 | 0.00 | -0.02 | 0.94 | 0.42 | 0.05 |
| 56221 | Ccl24 | chemokine (C-C motif) ligand 24 | 1.69 | 0.02 | -0.28 | 0.72 | -0.21 | 0.80 |
| 110006 | Gusb | glucuronidase, beta | 1.10 | 0.00 | -0.44 | 0.04 | 0.34 | 0.16 |

| Gene expression change[1] | Different from ctrl Ab in: | EntrezID | Symbol | Gene Name | no virus vs rCl13 + ctrl Ab[6] | | rCl13 + αIFNAR vs rCl13 + ctrl Ab[7] | | rCl13 + αGR-1 vs rCl13 + ctrl Ab[8] | |
|---|---|---|---|---|---|---|---|---|---|---|
| | | | | | log2FC | adj.P.Val | log2FC | adj.P.Val | log2FC | adj.P.Val |
| | αGR-1[9] | 16177 | Il1r1 | interleukin 1 receptor, type I | -1.45 | 0.00 | 0.47 | 0.11 | **1.08** | **0.00** |
| | αGR-1 & αIFNAR[10] | 11687 | Alox15 | arachidonate 15-lipoxygenase | -0.94 | 0.02 | **0.80** | **0.03** | **-2.16** | **0.00** |
| | | 15962 | Ifna1 | interferon alpha 1 | -0.68 | 0.00 | **0.67** | **0.00** | **0.52** | **0.03** |
| | αIFNAR[11] | 11596 | Ager | advanced glycosylation end product-specific receptor | -1.24 | 0.00 | **0.99** | **0.00** | 0.35 | 0.29 |
| | | 12048 | Bcl2l1 | BCL2-like 1 | -2.23 | 0.00 | **1.27** | **0.00** | 0.17 | 0.58 |
| | | 13712 | Elk1 | ELK1, member of ETS oncogene family | -0.85 | 0.00 | **0.51** | **0.01** | -0.42 | 0.06 |
| | | 17134 | Mafg | v-maf musculoaponeurotic fibrosarc. oncog. fam., protein G (avian) | -1.13 | 0.00 | **0.67** | **0.00** | -0.12 | 0.64 |
| | | 17392 | Mmp3 | matrix metallopeptidase 3 | -0.71 | 0.00 | **0.56** | **0.01** | 0.11 | 0.64 |
| | | 17906 | Myl2 | myosin, light polypeptide 2, regulatory, cardiac, slow | -1.53 | 0.00 | **1.11** | **0.01** | -0.40 | 0.39 |
| | | 18751 | Prkcb | protein kinase C, beta | -0.79 | 0.01 | **0.62** | **0.02** | -0.40 | 0.17 |
| | | 18795 | Plcb1 | phospholipase C, beta 1 | -0.77 | 0.03 | **1.09** | **0.00** | 0.12 | 0.76 |
| | | 19222 | Ptgir | prostaglandin I receptor (IP) | -0.91 | 0.00 | **0.70** | **0.01** | 0.42 | 0.14 |
| | | 19224 | Ptgs1 | prostaglandin-endoperoxide synthase 1 | -1.20 | 0.00 | **0.65** | **0.01** | 0.32 | 0.21 |
| | | 26408 | Map3k5 | mitogen-activated protein kinase kinase kinase 5 | -0.63 | 0.00 | **0.61** | **0.00** | -0.09 | 0.64 |
| | | 26417 | Mapk3 | mitogen-activated protein kinase 3 | -0.72 | 0.04 | **0.71** | **0.04** | -0.26 | 0.50 |
| | | 53791 | Tlr5 | toll-like receptor 5 | -1.32 | 0.00 | **1.09** | **0.00** | -0.26 | 0.44 |
| | | 97165 | Hmgb2 | high mobility group box 2 | -1.31 | 0.00 | **0.79** | **0.00** | 0.09 | 0.79 |
| down-regulated in rCl13-infected bone marrow[5] | none[12] | 11909 | Atf2 | activating transcription factor 2 | -0.53 | 0.00 | 0.27 | 0.02 | 0.06 | 0.65 |
| | | 12053 | Bcl6 | B cell leukemia/lymphoma 6 | -0.53 | 0.04 | 0.47 | 0.05 | -0.52 | 0.05 |
| | | 12775 | Ccr7 | chemokine (C-C motif) receptor 7 | -0.67 | 0.03 | -0.05 | 0.89 | -0.28 | 0.38 |
| | | 14683 | Gnas | GNAS (guanine nucleot. Bind. Prot., alpha stim.) complex locus | -0.83 | 0.01 | 0.50 | 0.09 | -0.38 | 0.25 |
| | | 14699 | Gngt1 | guanine nucleot. bind. protein (G prot.), gamma transd. Act. polyp. 1 | -0.73 | 0.01 | 0.30 | 0.24 | 0.31 | 0.27 |
| | | 16198 | Il9 | interleukin 9 | -0.89 | 0.03 | 0.50 | 0.18 | -0.09 | 0.87 |
| | | 17135 | Mafk | v-maf musculoaponeurotic fibrosarc. Oncog. Fam., prot. K (avian) | -0.88 | 0.00 | 0.26 | 0.08 | -0.03 | 0.88 |
| | | 17165 | Mapkapk5 | MAP kinase-activated protein kinase 5 | -0.87 | 0.03 | 0.30 | 0.44 | 0.18 | 0.68 |
| | | 18750 | Prkca | protein kinase C, alpha | -1.47 | 0.01 | 0.84 | 0.13 | 0.53 | 0.40 |
| | | 18829 | Ccl21a | chemokine (C-C motif) ligand 21A (serine) | -0.73 | 0.01 | 0.15 | 0.58 | -0.05 | 0.87 |
| | | 21390 | Tbxa2r | thromboxane A2 receptor | -0.87 | 0.04 | 0.72 | 0.07 | 0.36 | 0.41 |
| | | 26401 | Map3k1 | mitogen-activated protein kinase kinase kinase 1 | -0.53 | 0.01 | 0.16 | 0.37 | -0.18 | 0.38 |
| | | 73086 | Rps6ka5 | ribosomal protein S6 kinase, polypeptide 5 | -0.77 | 0.01 | 0.48 | 0.05 | 0.05 | 0.88 |
| | | 93671 | Cd163 | CD163 antigen | -1.86 | 0.00 | 0.50 | 0.09 | -0.34 | 0.29 |
| | | 329251 | Ppp1r12b | protein phosphatase 1, regulatory (inhibitor) subunit 12B | -0.70 | 0.01 | 0.20 | 0.42 | 0.49 | 0.07 |
| | | 338372 | Map3k9 | mitogen-activated protein kinase kinase kinase 9 | -1.22 | 0.02 | 0.90 | 0.07 | -0.55 | 0.30 |
| | | NA | Hras1 | NA | -0.83 | 0.00 | 0.42 | 0.10 | -0.14 | 0.65 |

[1] We transferred naïve KL25HL cells into wt recipients followed by rCl13 infection. Total RNA was extracted from spleen and BM on day 3 p.i. and processed for expression profiling of 248 inflammation-related genes. The table displays all those genes whose expression was significantly altered upon rCl13 infection (absolute $\log_2$ fold change (log2FC) >0.5 and adjusted $p$ value (adj.P.Val) <0.05 when comparing gene expression in uninfected animals to rCl13-infected control-treated animals.

[2] The table shows 49 genes significantly up-regulated upon rCl13 infection in spleen. These data are displayed in form of a heat map in Fig. 4F.

[3] The table displays 83 genes significantly down-regulated upon rCl13 infection in spleen.

[4] The table displays 67 genes significantly up-regulated upon rCl13 infection in BM.

[5] The table displays 34 genes significantly down-regulated upon rCl13 infection in BM.

[6] Gene expression changes as $\log_2$ fold-change (log2FC) and adjusted *p* value (adj.P.Val) when comparing uninfected (no virus) and rCl13-infected control-treated mice.

[7] Gene expression changes as $\log_2$ fold-change (log2FC) and adjusted *p* value (adj.P.Val) when comparing rCL13 infected αIFNAR-treated mice and rCl13-infected control-treated mice.

[8] Gene expression changes as $\log_2$ fold-change (log2FC) and adjusted *p* value (adj.P.Val) when comparing rCL13 infected αGr-1-treated mice and rCl13-infected control-treated mice.

[9] Genes whose expression was significantly altered in αGr-1-treated as compared to control-treated animals.

[10] Genes whose expression was significantly altered in both αGr-1-treated and αIFNAR-treated as compared to control-treated animals.

[11] Genes whose expression was significantly altered in αIFNAR-treated as compared to control-treated animals.

[12] Genes whose expression was not altered by αGr-1 nor αIFNAR treatment as compared to control-treated animals.

**Table SII: Profound impact of IFNAR blockade and, to a more limited but largely overlapping extent, of αGr-1 depletion of inflammatory chemokine and cytokine responses in serum.**

| Chemokine[3] | Experimental group[1] | | | | | |
|---|---|---|---|---|---|---|
| | ctrl Ab[2] | | αGR-1[2] | | *ifnar*[-/- 2] | |
| | mean | SEM | mean | SEM | mean | SEM |
| CCL2 | 3873.73 | 658.68 | 3118.46 | 1460.51 | 217.61 | 93.03 |
| CCL3 | 226.09 | 3.47 | 432.50 | 34.29 | 82.84 | 8.55 |
| CCL4 | 770.38 | 58.54 | 1257.12 | 64.58 | 63.90 | 31.97 |
| CCL5 | 778.74 | 113.17 | 535.88 | 30.32 | 92.33 | 4.09 |
| CCL11 | 987.74 | 41.62 | 891.78 | 33.50 | 526.14 | 52.38 |
| CXCL1 | 465.31 | 117.45 | 677.78 | 231.09 | 95.51 | 37.41 |
| CXCL2 | 231.37 | 5.84 | 165.34 | 24.87 | 153.95 | 35.92 |
| CXCL5 | 16152.36 | 830.11 | 10648.70 | 1903.08 | 17578.23 | 1945.04 |
| CXCL9 | 913.28 | 101.08 | 430.89 | 8.83 | 366.17 | 39.26 |
| CXCL10 | 1173.96 | 136.86 | 832.50 | 36.37 | 217.87 | 7.57 |
| LIF | 6.99 | 0.50 | 4.60 | 0.46 | 1.75 | 0.20 |

| Cytokine[3] | Experimental group[1] | | | | | |
|---|---|---|---|---|---|---|
| | ctrl Ab[2] | | αGR-1[2] | | *ifnar*[-/- 2] | |
| | mean | SEM | mean | SEM | mean | SEM |
| TNF-α | 68.29 | 9.97 | 7.01 | 1.59 | 5.20 | 3.04 |
| IFN-γ | 20.86 | 1.55 | 5.69 | 2.01 | <0.64 | N.A. |
| IL-1α | 293.45 | 31.74 | 409.65 | 121.65 | 147.44 | 22.68 |
| IL1-β | 281.69 | 78.77 | 50.23 | 49.91 | <0.64 | N.A. |
| IL-2 | 16.85 | 9.45 | 25.56 | 14.58 | 1.16 | 0.46 |
| IL-3 | 26.15 | 7.11 | 19.70 | 14.34 | 2.00 | 1.04 |
| IL-4 | 25.43 | 5.47 | 0.99 | 0.67 | <0.64 | N.A. |
| IL-5 | 100.21 | 9.90 | 56.80 | 3.59 | 8.67 | 0.71 |
| IL-6 | 115.56 | 30.20 | 57.10 | 30.71 | 6.27 | 1.08 |
| IL-7 | 113.62 | 26.91 | 64.80 | 5.05 | 28.81 | 6.73 |
| IL-9 | 85.86 | 35.49 | 133.78 | 71.19 | 18.83 | 3.52 |
| IL-10 | 97.96 | 24.94 | 12.65 | 3.92 | 1.87 | 1.55 |
| IL-12p40 | 74.39 | 42.89 | 182.91 | 168.07 | 26.94 | 3.87 |
| IL-12p70 | 515.30 | 128.33 | 48.73 | 17.86 | 9.53 | 9.21 |
| IL-13 | 85.90 | 23.17 | 47.53 | 13.93 | 71.33 | 10.73 |
| IL-15 | 443.36 | 151.27 | 180.02 | 27.39 | 119.71 | 24.72 |
| IL-17 | 31.33 | 1.91 | 20.79 | 4.92 | <0.64 | N.A. |
| G-CSF | 6712.20 | 587.83 | 19290.09 | 905.23 | 606.98 | 97.00 |
| GM-CSF | 104.69 | 28.14 | 82.16 | 39.27 | 8.53 | 8.21 |
| M-CSF | 55.13 | 27.95 | 129.93 | 121.08 | 12.62 | 2.91 |
| VEGF | 1.19 | 0.47 | 3.72 | 1.85 | <0.64 | N.A. |

[1] We infected mice with rCl13 and collected serum 24 and 72 hours later.
[2] The experimental groups consisted in wt mice, treated with αGr-1 or isotype control antibody, and in *ifnar*^{-/-} mice.

[3] Chemokine concentrations (pg/ml) measured at 24 hours and cytokines measured at 72 hours after infection are displayed. To calculate means and SEM ($n$=3), individual values below detection limits were set to detection limit (0.64 pg/ml). A selection of these data is displayed in Fig. 4G.

## II.7 Acknowledgments

# III Discussion

Although B cell immunity in chronic viral infection has long been paid less attention than cellular immunity, it gained a lot of interest over the last decade. Indeed, the critical role of B cells to support CTLs in the control of persistent viruses is now well recognized (*22*). However, like T cells, B cells have been shown to display dysfunctional features in chronic viral infections. While several recent studies have allowed to identify and characterize abnormal B cell populations in various persistent infectious settings, the mechanisms shaping antiviral B cell responses in chronic viral infection remain ill defined (*145-158*). Moreover, the poor nAb response to chronic viral infection represents a long-standing puzzle to immunologists that is still not fully resolved (*44-47*). With few exceptions nAbs remain the only mechanistic correlate of protection of most successful vaccine to date and their induction by vaccination against persistent viruses such as HIV and HCV remains a major goal of research (*33, 50, 276, 277*). The ambivalent role of IFN-I in chronic viral infection is well recognized. Several reports have highlighted elevated IFN-I signatures in chronic HCV infection, pathogenic SIV infection, and progressing HIV infection (*165-170, 198*). Moreover some studies have suggested that altered expression of genes linked to IFN-I signaling could have direct negative effects on $CD4^+$ T cell and B cell responses in HIV infection (*145, 167*). However, there is little understanding of how IFN-I signaling impacts B cell responses in chronic viral infections.

This work provides new mechanistic insights on antiviral B cell responses in a chronic viral infection model. We demonstrate that high levels of IFN-I induced by infection with a persistent strain of LCMV dramatically influence B cell response at the onset of chronic infection. IFN-I signaling biased the antiviral B cell response towards rapid end-stage plasmablast differentiation at the expense of memory and GC B cell formation, thereby leading to decimation of the B cell response. This observation represents a first mechanistic link between elevated IFN-I responses and B cell dysfunction in a chronic viral infection model. Importantly, intrinsic IFNAR signaling on B cells was not necessary for IFN-I driven plasmablast differentiation. Rather, IFN-I exerted its effect through signaling on several other cell types including T cells, DCs and myeloid cells. IFN-I induced profound modification of the

inflammatory milieu, which we propose altered B cell survival and differentiation. The observation that TNF-α blockade and IL-10 deficiency led to a partial rescue of the B cell response supported this hypothesis. The partial recue also observed when transferring KL25HL B cells in mice overexpressing B-cell activation factor (BAFF) further indicate that the decimation is the result of a B cell intrinsic process altering B cell differentiation and survival. However it does not allow to conclude that the IFN-I effects are mediated by alteration of BAFF signaling.

We report that T cells might contribute to IFN-I mediated B cell decimation and previous studies already outlined the deleterious effects that CTLs might exert on B cell responses, notably through the CTL-mediated immunopathologic destruction of the lymphoid microarchitecture (*44*). Although these observations might contribute to the poor nAb response and delayed GC formation observed in chronic LCMV infection, it is less likely to contribute to the IFN-I-driven B cell decimation described in the present work. Indeed the very rapid loss of antiviral B cells within three days of infection renders it very unlikely that any specific CTL response and the ensuing destruction of lymphoid organ microarchitecture might contribute to the phenomenon (*278*). The partial rescue of the B cell response seen in mice lacking IFNAR on T cells (*cd4-cre x ifnar$^{fl/fl}$*) and in *cd8$^{-/-}$* mice suggest that T cells contribute to IFN-I sensing at the onset of infection and most likely participate to the IFN-I-induced changes in the inflammatory milieu. However, the latter still needs to be specifically tested.

IFN-I has been postulated to bias CD4$^{+}$ T cell differentiation towards Th1 responses at the expense of Tfh in LCMV infection (*279*). Moreover, neutrophils have been shown to reduce humoral response to chronic LCMV infection by suppressing Tfh responses (*280*). Although it cannot be strictly excluded, a role of a lack of Tfh in B cell decimation early after chronic LCMV infection as observed in our work remains however unlikely since Tfh responses typically require longer than three days to set in (*281*). Moreover depletion of NK cells in our setting did not have an impact on B cell decimation. However, whether increased T cell help is beneficial to B cell responses is a very interesting and controversial question (*282-284*). If so, whether cognate T cell help is needed or if unspecific T cell help is sufficient, and whether *bona fide* Tfh only can provide help to B cells at the early stage of the response are still open questions.

The correlation between high antigen load and CTL exhaustion is well recognized and it has been postulated that CTL dysfunction is driven by elevated antigen levels in chronic LCMV infection (*27*). The observation that antiretroviral therapy (ART) in HIV-infected patients helps preserving B cell function suggests that high antigen load might also negatively influence B cell responses in chronic viral infection (*147, 150*). Here we show that B cell decimation at the onset of chronic LMCV infection does not correlate with virus load. Indeed, adoptive transfer of KL25HL B cells in neonatal carrier mice with persistently elevated viremia did not lead to B cell decimation in the early phase of the response. However this observation does not preclude that persistently elevated viral load might have an impact on B cell function later in the course of infection.

While several observations such as the identification of abnormal B cell populations in several persistent infections, the impact of CTL-mediated immunopathology on B cell responses, mutational escape from nAb control and structural properties of viral glycoproteins may all contribute to the late and weak nAb response observed in chronic viral infection, mechanistic explanations are still lacking (*44-47, 146, 157*). The present work describes a new mechanism that might contributes to the delayed GC and nAb responses in chronic LCMV infection. The adoptive transfer of traceable virus-specific B cells allowed to unravel mechanisms at the cellular level that are likely to apply to the rare endogenous LCMV-specific B cells present at the onset of infection. GCs would thus depend on the recruitment of naïve B cells from the bone marrow at a later stage of the infection, when IFN-I driven decimation of B cells does no longer occur, thereby delaying their formation. Though adoptive transfer experiments might represent a relatively artificial approach, oligoclonal and polyclonal B cell transfer experiments supported the concept of IFN-I induced B cell decimation in a more physiological setting and further reinforce the hypothesis that endogenous B cells might be similarly influenced by IFN-I. Moreover, this setup showed that not only naïve B cells but also antigen-experienced cells including memory B cells and GC B cells were susceptible to IFN-I driven decimation. The concept that an established B cell memory population might be lost if activated under highly inflammatory and/or elevated IFN-I signaling conditions has important implications for vaccination strategies against persistent viral diseases.

Although B cell dysfunction in persistent microbial infection is a complex phenomenon certainly ruled by more than one mechanism, the work presented here describes a new strategy that likely contributes to viral subversion of B cell response in chronic LCMV infection. We show that virus-induced IFN-I redirects the antiviral B cell response towards short-lived plasmablast differentiation thereby preventing memory and GC B cell formation in the early phase of infection. On the one hand, driving unsustainable plasmablast differentiation might be a strategy for the virus to establish persistence. On the other hand, rapid production of high numbers of ASCs might represent an all-in strategy of the host immune system to combat invading pathogens in life threatening situations. Elevated numbers of non-HIV-specific plasmablasts have been observed in blood of HIV-infected patients and, more generally, chronic viral infections have been associated with polyclonal B cell activation and hypergammaglobulinemia (*136, 143, 144, 152*). Moreover autoimmune diseases have been associated with HIV and HCV infection (*160, 161*). IFN-I driven decimation of B cells might also represent a mechanism of the host immune system to reduce the risk of self-reactive B cell activation and autoantibody formation in a very inflammatory context.

B cell and nAb responses are key components of immune defenses against persistent-prone viruses (*22*). Understanding the mechanisms underlying those responses is therefore critical to refine treatment and vaccination strategies against chronic viral infection. Taken together, our data describe a novel mechanism of immune subversion of B cell responses in highly inflammatory conditions. Strategies, such as programmed cell death 1 (PD-1) blockade, aiming at restoring T cell function represent a promising therapeutic approach against cancer and chronic viral infection (*285-287*). Treatments to preserve B cell function in chronic viral infection might also be beneficial and could represent a promising alternative or complementary strategy. Our data suggest that one such approach could reside in the modulation of the inflammatory milieu at the early stage of chronic viral infection. Several immunomodulatory strategies, such as IFN-I, PD-1, IL-10 or TNF-α blockade have been shown to ameliorate T cell function and/or viral control in mice (*171, 172, 285, 286, 288, 289*). Moreover, several immunomodulatory drugs such as TNF-α blockers already exist and are safely used in humans. However the impact of those treatments on the B cell response deserves further investigations. Our data suggest that some of

the beneficial effects of such treatments might be due to their impact on B cells. Taken together, our work suggest that strategies targeting inflammatory mediators such as IFN-I, TNF-α or IL-10 could have tremendous impact on B cell responses in chronic viral infection and have a great potential in the treatment of such infections.

# IV References and Notes

1. J. Fettig, M. Swaminathan, C. S. Murrill, J. E. Kaplan, Global epidemiology of HIV. *Infect Dis Clin North Am* **28**, 323-337 (2014).
2. J. P. Messina *et al.*, Global distribution and prevalence of hepatitis C virus genotypes. *Hepatology* **61**, 77-87 (2015).
3. J. J. Ott, G. A. Stevens, J. Groeger, S. T. Wiersma, Global epidemiology of hepatitis B virus infection: new estimates of age-specific HBsAg seroprevalence and endemicity. *Vaccine* **30**, 2212-2219 (2012).
4. R. M. Zinkernagel, C. J. Pfau, H. Hengartner, A. Althage, Susceptibility to murine lymphocytic choriomeningitis maps to class I MHC genes--a model for MHC/disease associations. *Nature* **316**, 814-817 (1985).
5. D. Moskophidis *et al.*, Role of virus and host variables in virus persistence or immunopathological disease caused by a non-cytolytic virus. *J Gen Virol* **76 ( Pt 2)**, 381-391 (1995).
6. R. Ahmed, A. Salmi, L. D. Butler, J. M. Chiller, M. B. Oldstone, Selection of genetic variants of lymphocytic choriomeningitis virus in spleens of persistently infected mice. Role in suppression of cytotoxic T lymphocyte response and viral persistence. *J Exp Med* **160**, 521-540 (1984).
7. D. Moskophidis, S. P. Cobbold, H. Waldmann, F. Lehmann-Grube, Mechanism of recovery from acute virus infection: treatment of lymphocytic choriomeningitis virus-infected mice with monoclonal antibodies reveals that Lyt-2+ T lymphocytes mediate clearance of virus and regulate the antiviral antibody response. *J Virol* **61**, 1867-1874 (1987).
8. E. J. Wherry, R. Ahmed, Memory CD8 T-cell differentiation during viral infection. *J Virol* **78**, 5535-5545 (2004).
9. J. N. Blattman *et al.*, Estimating the precursor frequency of naive antigen-specific CD8 T cells. *J Exp Med* **195**, 657-664 (2002).
10. M. F. Callan *et al.*, Large clonal expansions of CD8+ T cells in acute infectious mononucleosis. *Nat Med* **2**, 906-911 (1996).
11. S. Oehen, K. Brduscha-Riem, Differentiation of naive CTL to effector and memory CTL: correlation of effector function with phenotype and cell division. *J Immunol* **161**, 5338-5346 (1998).
12. S. M. Kaech, S. Hemby, E. Kersh, R. Ahmed, Molecular and functional profiling of memory CD8 T cell differentiation. *Cell* **111**, 837-851 (2002).
13. D. Kagi *et al.*, Cytotoxicity mediated by T cells and natural killer cells is greatly impaired in perforin-deficient mice. *Nature* **369**, 31-37 (1994).
14. M. A. Brehm, K. A. Daniels, R. M. Welsh, Rapid production of TNF-alpha following TCR engagement of naive CD8 T cells. *J Immunol* **175**, 5043-5049 (2005).
15. V. P. Badovinac, B. B. Porter, J. T. Harty, Programmed contraction of CD8(+) T cells after infection. *Nat Immunol* **3**, 619-626 (2002).
16. K. Murali-Krishna *et al.*, Counting antigen-specific CD8 T cells: a reevaluation of bystander activation during viral infection. *Immunity* **8**, 177-187 (1998).
17. E. J. Wherry *et al.*, Lineage relationship and protective immunity of memory CD8 T cell subsets. *Nat Immunol* **4**, 225-234 (2003).

18. A. Bergthaler *et al.*, Viral replicative capacity is the primary determinant of lymphocytic choriomeningitis virus persistence and immunosuppression. *Proc Natl Acad Sci U S A* **107**, 21641-21646 (2010).
19. E. J. Wherry, J. N. Blattman, K. Murali-Krishna, R. van der Most, R. Ahmed, Viral persistence alters CD8 T-cell immunodominance and tissue distribution and results in distinct stages of functional impairment. *J Virol* **77**, 4911-4927 (2003).
20. D. Moskophidis, F. Lechner, H. Pircher, R. M. Zinkernagel, Virus persistence in acutely infected immunocompetent mice by exhaustion of antiviral cytotoxic effector T cells. *Nature* **362**, 758-761 (1993).
21. A. J. Zajac *et al.*, Viral immune evasion due to persistence of activated T cells without effector function. *J Exp Med* **188**, 2205-2213 (1998).
22. A. Bergthaler *et al.*, Impaired antibody response causes persistence of prototypic T cell-contained virus. *PLoS Biol* **7**, e1000080 (2009).
23. M. Matloubian, R. J. Concepcion, R. Ahmed, CD4+ T cells are required to sustain CD8+ cytotoxic T-cell responses during chronic viral infection. *J Virol* **68**, 8056-8063 (1994).
24. M. Battegay *et al.*, Enhanced establishment of a virus carrier state in adult CD4+ T-cell-deficient mice. *J Virol* **68**, 4700-4704 (1994).
25. A. Ciurea, L. Hunziker, P. Klenerman, H. Hengartner, R. M. Zinkernagel, Impairment of CD4(+) T cell responses during chronic virus infection prevents neutralizing antibody responses against virus escape mutants. *J Exp Med* **193**, 297-305 (2001).
26. D. G. Brooks, L. Teyton, M. B. Oldstone, D. B. McGavern, Intrinsic functional dysregulation of CD4 T cells occurs rapidly following persistent viral infection. *J Virol* **79**, 10514-10527 (2005).
27. S. N. Mueller, R. Ahmed, High antigen levels are the cause of T cell exhaustion during chronic viral infection. *Proc Natl Acad Sci U S A* **106**, 8623-8628 (2009).
28. D. G. Brooks, D. B. McGavern, M. B. Oldstone, Reprogramming of antiviral T cells prevents inactivation and restores T cell activity during persistent viral infection. *J Clin Invest* **116**, 1675-1685 (2006).
29. S. Johnson *et al.*, Protective efficacy of individual CD8+ T cell specificities in chronic viral infection. *J Immunol* **194**, 1755-1762 (2015).
30. L. Hangartner *et al.*, Nonneutralizing antibodies binding to the surface glycoprotein of lymphocytic choriomeningitis virus reduce early virus spread. *J Exp Med* **203**, 2033-2042 (2006).
31. A. Ciurea *et al.*, Viral persistence in vivo through selection of neutralizing antibody-escape variants. *Proc Natl Acad Sci U S A* **97**, 2749-2754 (2000).
32. J. R. Baldridge, T. S. McGraw, A. Paoletti, M. J. Buchmeier, Antibody prevents the establishment of persistent arenavirus infection in synergy with endogenous T cells. *J Virol* **71**, 755-758 (1997).
33. S. A. Plotkin, Correlates of protection induced by vaccination. *Clin Vaccine Immunol* **17**, 1055-1065 (2010).
34. R. Shibata *et al.*, Neutralizing antibody directed against the HIV-1 envelope glycoprotein can completely block HIV-1/SIV chimeric virus infections of macaque monkeys. *Nat Med* **5**, 204-210 (1999).

35. J. R. Mascola *et al.*, Protection of Macaques against pathogenic simian/human immunodeficiency virus 89.6PD by passive transfer of neutralizing antibodies. *J Virol* **73**, 4009-4018 (1999).

36. A. Trkola *et al.*, Delay of HIV-1 rebound after cessation of antiretroviral therapy through passive transfer of human neutralizing antibodies. *Nat Med* **11**, 615-622 (2005).

37. M. Law *et al.*, Broadly neutralizing antibodies protect against hepatitis C virus quasispecies challenge. *Nat Med* **14**, 25-27 (2008).

38. Y. P. de Jong *et al.*, Broadly neutralizing antibodies abrogate established hepatitis C virus infection. *Sci Transl Med* **6**, 254ra129 (2014).

39. A. J. Hessell *et al.*, Early short-term treatment with neutralizing human monoclonal antibodies halts SHIV infection in infant macaques. *Nat Med* **22**, 362-368 (2016).

40. D. D. Pinschewer *et al.*, Kinetics of protective antibodies are determined by the viral surface antigen. *J. Clin. Invest.* **114**, 988-993 (2004).

41. B. Eschli *et al.*, Early antibodies specific for the neutralizing epitope on the receptor binding subunit of the lymphocytic choriomeningitis virus glycoprotein fail to neutralize the virus. *J Virol* **81**, 11650-11657 (2007).

42. E. S. Gray *et al.*, The neutralization breadth of HIV-1 develops incrementally over four years and is associated with CD4+ T cell decline and high viral load during acute infection. *J Virol* **85**, 4828-4840 (2011).

43. M. L. Robb *et al.*, Prospective Study of Acute HIV-1 Infection in Adults in East Africa and Thailand. *N Engl J Med* **374**, 2120-2130 (2016).

44. M. Battegay *et al.*, Impairment and delay of neutralizing antiviral antibody responses by virus-specific cytotoxic T cells. *J Immunol* **151**, 5408-5415 (1993).

45. R. Sommerstein *et al.*, Arenavirus Glycan Shield Promotes Neutralizing Antibody Evasion and Protracted Infection. *PLoS Pathog* **11**, e1005276 (2015).

46. P. D. Kwong *et al.*, HIV-1 evades antibody-mediated neutralization through conformational masking of receptor-binding sites. *Nature* **420**, 678-682 (2002).

47. X. Wei *et al.*, Antibody neutralization and escape by HIV-1. *Nature* **422**, 307-312 (2003).

48. I. Pellegrin *et al.*, Kinetics of appearance of neutralizing antibodies in 12 patients with primary or recent HIV-1 infection and relationship with plasma and cellular viral loads. *J Acquir Immune Defic Syndr Hum Retrovirol* **11**, 438-447 (1996).

49. M. M. Aasa-Chapman *et al.*, Development of the antibody response in acute HIV-1 infection. *AIDS* **18**, 371-381 (2004).

50. B. F. Haynes *et al.*, Immune-correlates analysis of an HIV-1 vaccine efficacy trial. *N Engl J Med* **366**, 1275-1286 (2012).

51. M. M. Aasa-Chapman *et al.*, Detection of antibody-dependent complement-mediated inactivation of both autologous and heterologous virus in primary human immunodeficiency virus type 1 infection. *J Virol* **79**, 2823-2830 (2005).

52. D. N. Forthal, G. Landucci, T. B. Phan, J. Becerra, Interactions between natural killer cells and antibody Fc result in enhanced antibody

neutralization of human immunodeficiency virus type 1. *J Virol* **79**, 2042-2049 (2005).

53. A. J. Hessell *et al.*, Fc receptor but not complement binding is important in antibody protection against HIV. *Nature* **449**, 101-104 (2007).

54. D. C. Hargreaves *et al.*, A coordinated change in chemokine responsiveness guides plasma cell movements. *J Exp Med* **194**, 45-56 (2001).

55. K. A. Pape, D. M. Catron, A. A. Itano, M. K. Jenkins, The humoral immune response is initiated in lymph nodes by B cells that acquire soluble antigen directly in the follicles. *Immunity* **26**, 491-502 (2007).

56. Y. R. Carrasco, F. D. Batista, B cells acquire particulate antigen in a macrophage-rich area at the boundary between the follicle and the subcapsular sinus of the lymph node. *Immunity* **27**, 160-171 (2007).

57. T. Junt *et al.*, Subcapsular sinus macrophages in lymph nodes clear lymph-borne viruses and present them to antiviral B cells. *Nature* **450**, 110-114 (2007).

58. K. Suzuki, I. Grigorova, T. G. Phan, L. M. Kelly, J. G. Cyster, Visualizing B cell capture of cognate antigen from follicular dendritic cells. *J Exp Med* **206**, 1485-1493 (2009).

59. P. Garside *et al.*, Visualization of specific B and T lymphocyte interactions in the lymph node. *Science* **281**, 96-99 (1998).

60. K. Reif *et al.*, Balanced responsiveness to chemoattractants from adjacent zones determines B-cell position. *Nature* **416**, 94-99 (2002).

61. A. I. Jaiswal, M. Croft, CD40 ligand induction on T cell subsets by peptide-presenting B cells: implications for development of the primary T and B cell response. *J Immunol* **159**, 2282-2291 (1997).

62. K. D. Shanebeck *et al.*, Regulation of murine B cell growth and differentiation by CD30 ligand. *Eur J Immunol* **25**, 2147-2153 (1995).

63. J. J. Taylor, K. A. Pape, M. K. Jenkins, A germinal center-independent pathway generates unswitched memory B cells early in the primary response. *J Exp Med* **209**, 597-606 (2012).

64. M. G. McHeyzer-Williams, M. J. McLean, P. A. Lalor, G. J. Nossal, Antigen-driven B cell differentiation in vivo. *J Exp Med* **178**, 295-307 (1993).

65. K. G. Smith, T. D. Hewitson, G. J. Nossal, D. M. Tarlinton, The phenotype and fate of the antibody-forming cells of the splenic foci. *Eur J Immunol* **26**, 444-448 (1996).

66. G. M. Griffiths, C. Berek, M. Kaartinen, C. Milstein, Somatic mutation and the maturation of immune response to 2-phenyl oxazolone. *Nature* **312**, 271-275 (1984).

67. D. McKean *et al.*, Generation of antibody diversity in the immune response of BALB/c mice to influenza virus hemagglutinin. *Proc Natl Acad Sci U S A* **81**, 3180-3184 (1984).

68. J. A. Harker, G. M. Lewis, L. Mack, E. I. Zuniga, Late Interleukin-6 Escalates T Follicular Helper Cell Responses and Controls a Chronic Viral Infection. *Science*, (2011).

69. T. A. Schwickert *et al.*, A dynamic T cell-limited checkpoint regulates affinity-dependent B cell entry into the germinal center. *J Exp Med* **208**, 1243-1252 (2011).

70. K. M. McBride *et al.*, Regulation of class switch recombination and somatic mutation by AID phosphorylation. *J Exp Med* **205**, 2585-2594 (2008).
71. A. D. Gitlin *et al.*, HUMORAL IMMUNITY. T cell help controls the speed of the cell cycle in germinal center B cells. *Science* **349**, 643-646 (2015).
72. D. Liu *et al.*, T-B-cell entanglement and ICOSL-driven feed-forward regulation of germinal centre reaction. *Nature* **517**, 214-218 (2015).
73. R. Shinkura *et al.*, Separate domains of AID are required for somatic hypermutation and class-switch recombination. *Nat Immunol* **5**, 707-712 (2004).
74. F. J. Weisel, G. V. Zuccarino-Catania, M. Chikina, M. J. Shlomchik, A Temporal Switch in the Germinal Center Determines Differential Output of Memory B and Plasma Cells. *Immunity* **44**, 116-130 (2016).
75. M. J. Shlomchik, F. Weisel, Germinal center selection and the development of memory B and plasma cells. *Immunol Rev* **247**, 52-63 (2012).
76. R. A. Manz *et al.*, Humoral immunity and long-lived plasma cells. *Curr Opin Immunol* **14**, 517-521 (2002).
77. A. Kallies *et al.*, Plasma cell ontogeny defined by quantitative changes in blimp-1 expression. *J Exp Med* **200**, 967-977 (2004).
78. S. G. Tangye, D. T. Avery, P. D. Hodgkin, A division-linked mechanism for the rapid generation of Ig-secreting cells from human memory B cells. *J Immunol* **170**, 261-269 (2003).
79. S. G. Tangye, D. T. Avery, E. K. Deenick, P. D. Hodgkin, Intrinsic differences in the proliferation of naive and memory human B cells as a mechanism for enhanced secondary immune responses. *J Immunol* **170**, 686-694 (2003).
80. C. Arpin, J. Banchereau, Y. J. Liu, Memory B cells are biased towards terminal differentiation: a strategy that may prevent repertoire freezing. *J Exp Med* **186**, 931-940 (1997).
81. V. Kindler, R. H. Zubler, Memory, but not naive, peripheral blood B lymphocytes differentiate into Ig-secreting cells after CD40 ligation and costimulation with IL-4 and the differentiation factors IL-2, IL-10, and IL-3. *J Immunol* **159**, 2085-2090 (1997).
82. N. L. Bernasconi, E. Traggiai, A. Lanzavecchia, Maintenance of serological memory by polyclonal activation of human memory B cells. *Science* **298**, 2199-2202 (2002).
83. K. L. Good, D. T. Avery, S. G. Tangye, Resting human memory B cells are intrinsically programmed for enhanced survival and responsiveness to diverse stimuli compared to naive B cells. *J Immunol* **182**, 890-901 (2009).
84. K. M. Toellner *et al.*, Low-level hypermutation in T cell-independent germinal centers compared with high mutation rates associated with T cell-dependent germinal centers. *J Exp Med* **195**, 383-389 (2002).
85. C. Garcia de Vinuesa, P. O'Leary, D. M. Sze, K. M. Toellner, I. C. MacLennan, T-independent type 2 antigens induce B cell proliferation in multiple splenic sites, but exponential growth is confined to extrafollicular foci. *Eur J Immunol* **29**, 1314-1323 (1999).
86. T. Kurosaki, K. Kometani, W. Ise, Memory B cells. *Nat Rev Immunol* **15**, 149-159 (2015).

87. J. Hasbold, L. M. Corcoran, D. M. Tarlinton, S. G. Tangye, P. D. Hodgkin, Evidence from the generation of immunoglobulin G-secreting cells that stochastic mechanisms regulate lymphocyte differentiation. *Nat Immunol* **5**, 55-63 (2004).

88. D. Paus *et al.*, Antigen recognition strength regulates the choice between extrafollicular plasma cell and germinal center B cell differentiation. *J Exp Med* **203**, 1081-1091 (2006).

89. W. Shi *et al.*, Transcriptional profiling of mouse B cell terminal differentiation defines a signature for antibody-secreting plasma cells. *Nat Immunol* **16**, 663-673 (2015).

90. K. I. Lin, C. Angelin-Duclos, T. C. Kuo, K. Calame, Blimp-1-dependent repression of Pax-5 is required for differentiation of B cells to immunoglobulin M-secreting plasma cells. *Mol Cell Biol* **22**, 4771-4780 (2002).

91. A. M. Reimold *et al.*, Plasma cell differentiation requires the transcription factor XBP-1. *Nature* **412**, 300-307 (2001).

92. A. M. Reimold *et al.*, Transcription factor B cell lineage-specific activator protein regulates the gene for human X-box binding protein 1. *J Exp Med* **183**, 393-401 (1996).

93. S. L. Nutt, P. Urbanek, A. Rolink, M. Busslinger, Essential functions of Pax5 (BSAP) in pro-B cell development: difference between fetal and adult B lymphopoiesis and reduced V-to-DJ recombination at the IgH locus. *Genes Dev* **11**, 476-491 (1997).

94. C. Duy *et al.*, BCL6 is critical for the development of a diverse primary B cell repertoire. *J Exp Med* **207**, 1209-1221 (2010).

95. C. Tunyaplin *et al.*, Direct repression of prdm1 by Bcl-6 inhibits plasmacytic differentiation. *J Immunol* **173**, 1158-1165 (2004).

96. R. Sciammas *et al.*, Graded expression of interferon regulatory factor-4 coordinates isotype switching with plasma cell differentiation. *Immunity* **25**, 225-236 (2006).

97. T. G. Phan, S. Gardam, A. Basten, R. Brink, Altered migration, recruitment, and somatic hypermutation in the early response of marginal zone B cells to T cell-dependent antigen. *J Immunol* **174**, 4567-4578 (2005).

98. A. Coutinho, E. Gronowicz, W. W. Bullock, G. Moller, Mechanism of thymus-independent immunocyte triggering. Mitogenic activation of B cells results in specific immune responses. *J Exp Med* **139**, 74-92 (1974).

99. A. M. Krieg *et al.*, CpG motifs in bacterial DNA trigger direct B-cell activation. *Nature* **374**, 546-549 (1995).

100. R. Z. Dintzis, M. Okajima, M. H. Middleton, G. Greene, H. M. Dintzis, The immunogenicity of soluble haptenated polymers is determined by molecular mass and hapten valence. *J Immunol* **143**, 1239-1244 (1989).

101. C. G. de Vinuesa *et al.*, Germinal centers without T cells. *J Exp Med* **191**, 485-494 (2000).

102. V. M. Lentz, T. Manser, Cutting edge: germinal centers can be induced in the absence of T cells. *J Immunol* **167**, 15-20 (2001).

103. A. J. Macpherson *et al.*, A primitive T cell-independent mechanism of intestinal mucosal IgA responses to commensal bacteria. *Science* **288**, 2222-2226 (2000).

104.    P. Bergqvist, A. Stensson, N. Y. Lycke, M. Bemark, T cell-independent IgA class switch recombination is restricted to the GALT and occurs prior to manifest germinal center formation. *J Immunol* **184**, 3545-3553 (2010).

105.    E. J. Pone *et al.*, BCR-signalling synergizes with TLR-signalling for induction of AID and immunoglobulin class-switching through the non-canonical NF-kappaB pathway. *Nat Commun* **3**, 767 (2012).

106.    T. V. Obukhanych, M. C. Nussenzweig, T-independent type II immune responses generate memory B cells. *J Exp Med* **203**, 305-310 (2006).

107.    M. Balazs, F. Martin, T. Zhou, J. Kearney, Blood dendritic cells interact with splenic marginal zone B cells to initiate T-independent immune responses. *Immunity* **17**, 341-352 (2002).

108.    M. H. Heim, D. Moradpour, H. E. Blum, Expression of hepatitis C virus proteins inhibits signal transduction through the Jak-STAT pathway. *J Virol* **73**, 8469-8475 (1999).

109.    F. H. Duong, M. Filipowicz, M. Tripodi, N. La Monica, M. H. Heim, Hepatitis C virus inhibits interferon signaling through up-regulation of protein phosphatase 2A. *Gastroenterology* **126**, 263-277 (2004).

110.    C. Paulus, S. Krauss, M. Nevels, A human cytomegalovirus antagonist of type I IFN-dependent signal transducer and activator of transcription signaling. *Proc Natl Acad Sci U S A* **103**, 3840-3845 (2006).

111.    P. Devaux, V. von Messling, W. Songsungthong, C. Springfeld, R. Cattaneo, Tyrosine 110 in the measles virus phosphoprotein is required to block STAT1 phosphorylation. *Virology* **360**, 72-83 (2007).

112.    D. M. Miller, Y. Zhang, B. M. Rahill, W. J. Waldman, D. D. Sedmak, Human cytomegalovirus inhibits IFN-alpha-stimulated antiviral and immunoregulatory responses by blocking multiple levels of IFN-alpha signal transduction. *J Immunol* **162**, 6107-6113 (1999).

113.    B. Bodaghi *et al.*, Chemokine sequestration by viral chemoreceptors as a novel viral escape strategy: withdrawal of chemokines from the environment of cytomegalovirus-infected cells. *J Exp Med* **188**, 855-866 (1998).

114.    O. Schwartz, V. Marechal, S. Le Gall, F. Lemonnier, J. M. Heard, Endocytosis of major histocompatibility complex class I molecules is induced by the HIV-1 Nef protein. *Nat Med* **2**, 338-342 (1996).

115.    D. M. Miller *et al.*, Human cytomegalovirus inhibits major histocompatibility complex class II expression by disruption of the Jak/Stat pathway. *J Exp Med* **187**, 675-683 (1998).

116.    M. K. Spriggs *et al.*, The extracellular domain of the Epstein-Barr virus BZLF2 protein binds the HLA-DR beta chain and inhibits antigen presentation. *J Virol* **70**, 5557-5563 (1996).

117.    G. A. Lewandowski, D. Lo, F. E. Bloom, Interference with major histocompatibility complex class II-restricted antigen presentation in the brain by herpes simplex virus type 1: a possible mechanism of evasion of the immune response. *Proc Natl Acad Sci U S A* **90**, 2005-2009 (1993).

118.    S. Le Gall *et al.*, Nef interacts with the mu subunit of clathrin adaptor complexes and reveals a cryptic sorting signal in MHC I molecules. *Immunity* **8**, 483-495 (1998).

119. J. Nattermann *et al.*, The HLA-A2 restricted T cell epitope HCV core 35-44 stabilizes HLA-E expression and inhibits cytolysis mediated by natural killer cells. *Am J Pathol* **166**, 443-453 (2005).

120. J. Nattermann *et al.*, Surface expression and cytolytic function of natural killer cell receptors is altered in chronic hepatitis C. *Gut* **55**, 869-877 (2006).

121. S. Crotta *et al.*, Inhibition of natural killer cells through engagement of CD81 by the major hepatitis C virus envelope protein. *J Exp Med* **195**, 35-41 (2002).

122. I. Kostavasili *et al.*, Mechanism of complement inactivation by glycoprotein C of herpes simplex virus. *J Immunol* **158**, 1763-1771 (1997).

123. L. G. Munson, M. E. Scott, A. L. Landay, G. T. Spear, Decreased levels of complement receptor 1 (CD35) on B lymphocytes in persons with HIV infection. *Clin Immunol Immunopathol* **75**, 20-25 (1995).

124. M. H. Jouvin, W. Rozenbaum, R. Russo, M. D. Kazatchkine, Decreased expression of the C3b/C4b complement receptor (CR1) in AIDS and AIDS-related syndromes correlates with clinical subpopulations of patients with HIV infection. *AIDS* **1**, 89-94 (1987).

125. S. M. Wahl *et al.*, HIV-1 and its envelope glycoprotein down-regulate chemotactic ligand receptors and chemotactic function of peripheral blood monocytes. *J Immunol* **142**, 3553-3559 (1989).

126. D. Tortorella, B. E. Gewurz, M. H. Furman, D. J. Schust, H. L. Ploegh, Viral subversion of the immune system. *Annu Rev Immunol* **18**, 861-926 (2000).

127. A. Ciurea *et al.*, CD4+ T-cell-epitope escape mutant virus selected in vivo. *Nat Med* **7**, 795-800 (2001).

128. D. Moskophidis, R. M. Zinkernagel, Immunobiology of cytotoxic T-cell escape mutants of lymphocytic choriomeningitis virus. *J Virol* **69**, 2187-2193 (1995).

129. H. Lewicki *et al.*, CTL escape viral variants. I. Generation and molecular characterization. *Virology* **210**, 29-40 (1995).

130. H. A. Lewicki, M. G. Von Herrath, C. F. Evans, J. L. Whitton, M. B. Oldstone, CTL escape viral variants. II. Biologic activity in vivo. *Virology* **211**, 443-450 (1995).

131. P. Borrow *et al.*, Antiviral pressure exerted by HIV-1-specific cytotoxic T lymphocytes (CTLs) during primary infection demonstrated by rapid selection of CTL escape virus. *Nat Med* **3**, 205-211 (1997).

132. D. D. Richman, T. Wrin, S. J. Little, C. J. Petropoulos, Rapid evolution of the neutralizing antibody response to HIV type 1 infection. *Proc Natl Acad Sci U S A* **100**, 4144-4149 (2003).

133. S. D. Frost *et al.*, Neutralizing antibody responses drive the evolution of human immunodeficiency virus type 1 envelope during recent HIV infection. *Proc Natl Acad Sci U S A* **102**, 18514-18519 (2005).

134. L. M. Walker *et al.*, A limited number of antibody specificities mediate broad and potent serum neutralization in selected HIV-1 infected individuals. *PLoS Pathog* **6**, e1001028 (2010).

135. C. K. Wibmer *et al.*, Viral escape from HIV-1 neutralizing antibodies drives increased plasma neutralization breadth through sequential recognition of multiple epitopes and immunotypes. *PLoS Pathog* **9**, e1003738 (2013).
136. L. Hunziker *et al.*, Hypergammaglobulinemia and autoantibody induction mechanisms in viral infections. *Nat Immunol* **4**, 343-349 (2003).
137. M. Recher *et al.*, Deliberate removal of T cell help improves virus-neutralizing antibody production. *Nat Immunol* **5**, 934-942 (2004).
138. S. M. Schnittman, H. C. Lane, S. E. Higgins, T. Folks, A. S. Fauci, Direct polyclonal activation of human B lymphocytes by the acquired immune deficiency syndrome virus. *Science* **233**, 1084-1086 (1986).
139. R. M. Zellweger, L. Hangartner, J. Weber, R. M. Zinkernagel, H. Hengartner, Parameters governing exhaustion of rare T cell-independent neutralizing IgM-producing B cells after LCMV infection. *Eur J Immunol* **36**, 3175-3185 (2006).
140. O. Planz, P. Seiler, H. Hengartner, R. M. Zinkernagel, Specific cytotoxic T cells eliminate B cells producing virus-neutralizing antibodies [corrected]. *Nature* **382**, 726-729 (1996).
141. O. Planz, P. Seiler, H. Hengartner, R. M. Zinkernagel, Specific cytotoxic T cells eliminate cells producing neutralizing antibodies. *Nature* **426**, 474 (2003).
142. N. Shinohara, M. Watanabe, D. H. Sachs, N. Hozumi, Killing of antigen-reactive B cells by class II-restricted, soluble antigen-specific CD8+ cytolytic T lymphocytes. *Nature* **336**, 481-484 (1988).
143. E. V. Tsianos, A. M. Di Bisceglie, N. M. Papadopoulos, R. Costello, J. H. Hoofnagle, Oligoclonal immunoglobulin bands in serum in association with chronic viral hepatitis. *Am J Gastroenterol* **85**, 1005-1008 (1990).
144. H. C. Lane *et al.*, Abnormalities of B-cell activation and immunoregulation in patients with the acquired immunodeficiency syndrome. *N Engl J Med* **309**, 453-458 (1983).
145. S. Moir *et al.*, Decreased survival of B cells of HIV-viremic patients mediated by altered expression of receptors of the TNF superfamily. *J Exp Med* **200**, 587-599 (2004).
146. S. Moir *et al.*, Evidence for HIV-associated B cell exhaustion in a dysfunctional memory B cell compartment in HIV-infected viremic individuals. *J Exp Med* **205**, 1797-1805 (2008).
147. S. Moir *et al.*, B cells in early and chronic HIV infection: evidence for preservation of immune function associated with early initiation of antiretroviral therapy. *Blood* **116**, 5571-5579 (2010).
148. E. Meffre *et al.*, Maturational characteristics of HIV-specific antibodies in viremic individuals. *JCI Insight* **1**,  (2016).
149. A. Malaspina *et al.*, Compromised B cell responses to influenza vaccination in HIV-infected individuals. *J Infect Dis* **191**, 1442-1450 (2005).
150. K. Titanji *et al.*, Primary HIV-1 infection sets the stage for important B lymphocyte dysfunctions. *AIDS* **19**, 1947-1955 (2005).
151. L. Kardava *et al.*, Abnormal B cell memory subsets dominate HIV-specific responses in infected individuals. *J Clin Invest* **124**, 3252-3262 (2014).
152. C. M. Buckner *et al.*, Characterization of plasmablasts in the blood of HIV-infected viremic individuals: evidence for nonspecific immune activation. *J Virol* **87**, 5800-5811 (2013).

153.   M. Hart *et al.*, Loss of discrete memory B cell subsets is associated with impaired immunization responses in HIV-1 infection and may be a risk factor for invasive pneumococcal disease. *J Immunol* **178**, 8212-8220 (2007).

154.   M. C. Levesque *et al.*, Polyclonal B cell differentiation and loss of gastrointestinal tract germinal centers in the earliest stages of HIV-1 infection. *PLoS Med* **6**, e1000107 (2009).

155.   C. Legendre *et al.*, CD80 expression is decreased in hyperplastic lymph nodes of HIV+ patients. *Int Immunol* **10**, 1847-1851 (1998).

156.   S. Peruchon *et al.*, Tissue-specific B-cell dysfunction and generalized memory B-cell loss during acute SIV infection. *PLoS One* **4**, e5966 (2009).

157.   M. F. Muellenbeck *et al.*, Atypical and classical memory B cells produce Plasmodium falciparum neutralizing antibodies. *J Exp Med* **210**, 389-399 (2013).

158.   G. Borhis, Y. Richard, Subversion of the B-cell compartment during parasitic, bacterial, and viral infections. *BMC Immunol* **16**, 15 (2015).

159.   H. W. Sohn, P. D. Krueger, R. S. Davis, S. K. Pierce, FcRL4 acts as an adaptive to innate molecular switch dampening BCR signaling and enhancing TLR signaling. *Blood* **118**, 6332-6341 (2011).

160.   M. M. Stimmler, F. P. Quismorio, Jr., W. G. McGehee, T. Boylen, O. P. Sharma, Anticardiolipin antibodies in acquired immunodeficiency syndrome. *Arch Intern Med* **149**, 1833-1835 (1989).

161.   M. Ramos-Casals *et al.*, Systemic autoimmune diseases co-existing with chronic hepatitis C virus infection (the HISPAMEC Registry): patterns of clinical and immunological expression in 180 cases. *J Intern Med* **257**, 549-557 (2005).

162.   A. Isaacs, J. Lindenmann, Virus interference. I. The interferon. *Proc R Soc Lond B Biol Sci* **147**, 258-267 (1957).

163.   S. Davidson, S. Crotta, T. M. McCabe, A. Wack, Pathogenic potential of interferon alphabeta in acute influenza infection. *Nat Commun* **5**, 3864 (2014).

164.   N. G. Sandler *et al.*, Type I interferon responses in rhesus macaques prevent SIV infection and slow disease progression. *Nature* **511**, 601-605 (2014).

165.   S. E. Bosinger *et al.*, Global genomic analysis reveals rapid control of a robust innate response in SIV-infected sooty mangabeys. *J Clin Invest* **119**, 3556-3572 (2009).

166.   B. Jacquelin *et al.*, Nonpathogenic SIV infection of African green monkeys induces a strong but rapidly controlled type I IFN response. *J Clin Invest* **119**, 3544-3555 (2009).

167.   A. R. Sedaghat *et al.*, Chronic CD4+ T-cell activation and depletion in human immunodeficiency virus type 1 infection: type I interferon-mediated disruption of T-cell dynamics. *J Virol* **82**, 1870-1883 (2008).

168.   S. Wieland *et al.*, Simultaneous detection of hepatitis C virus and interferon stimulated gene expression in infected human liver. *Hepatology* **59**, 2121-2130 (2014).

169.   L. Chen *et al.*, Hepatic gene expression discriminates responders and nonresponders in treatment of chronic hepatitis C viral infection. *Gastroenterology* **128**, 1437-1444 (2005).

170. R. Thimme *et al.*, Viral and immunological determinants of hepatitis C virus clearance, persistence, and disease. *Proc Natl Acad Sci U S A* **99**, 15661-15668 (2002).
171. E. B. Wilson *et al.*, Blockade of chronic type I interferon signaling to control persistent LCMV infection. *Science* **340**, 202-207 (2013).
172. J. R. Teijaro *et al.*, Persistent LCMV infection is controlled by blockade of type I interferon signaling. *Science* **340**, 207-211 (2013).
173. C. T. Ng *et al.*, Blockade of interferon Beta, but not interferon alpha, signaling controls persistent viral infection. *Cell Host Microbe* **17**, 653-661 (2015).
174. J. R. Teijaro, Type I interferons in viral control and immune regulation. *Curr Opin Virol* **16**, 31-40 (2016).
175. D. Novick, B. Cohen, M. Rubinstein, The human interferon alpha/beta receptor: characterization and molecular cloning. *Cell* **77**, 391-400 (1994).
176. C. Schindler, K. Shuai, V. R. Prezioso, J. E. Darnell, Jr., Interferon-dependent tyrosine phosphorylation of a latent cytoplasmic transcription factor. *Science* **257**, 809-813 (1992).
177. C. Beadling *et al.*, Activation of JAK kinases and STAT proteins by interleukin-2 and interferon alpha, but not the T cell antigen receptor, in human T lymphocytes. *EMBO J* **13**, 5605-5615 (1994).
178. S. Matikainen *et al.*, Interferon-alpha activates multiple STAT proteins and upregulates proliferation-associated IL-2Ralpha, c-myc, and pim-1 genes in human T cells. *Blood* **93**, 1980-1991 (1999).
179. J. D. Farrar, J. D. Smith, T. L. Murphy, K. M. Murphy, Recruitment of Stat4 to the human interferon-alpha/beta receptor requires activated Stat2. *J Biol Chem* **275**, 2693-2697 (2000).
180. N. Torpey, S. E. Maher, A. L. Bothwell, J. S. Pober, Interferon alpha but not interleukin 12 activates STAT4 signaling in human vascular endothelial cells. *J Biol Chem* **279**, 26789-26796 (2004).
181. S. D. Der, A. Zhou, B. R. Williams, R. H. Silverman, Identification of genes differentially regulated by interferon alpha, beta, or gamma using oligonucleotide arrays. *Proc Natl Acad Sci U S A* **95**, 15623-15628 (1998).
182. J. Pavlovic, O. Haller, P. Staeheli, Human and mouse Mx proteins inhibit different steps of the influenza virus multiplication cycle. *J Virol* **66**, 2564-2569 (1992).
183. K. Malathi, B. Dong, M. Gale, Jr., R. H. Silverman, Small self-RNA generated by RNase L amplifies antiviral innate immunity. *Nature* **448**, 816-819 (2007).
184. P. Lindahl, I. Gresser, P. Leary, M. Tovey, Interferon treatment of mice: enhanced expression of histocompatibility antigens on lymphoid cells. *Proc Natl Acad Sci U S A* **73**, 1284-1287 (1976).
185. J. Crouse *et al.*, Type I interferons protect T cells against NK cell attack mediated by the activating receptor NCR1. *Immunity* **40**, 961-973 (2014).
186. H. C. Xu *et al.*, Type I interferon protects antiviral CD8+ T cells from NK cell cytotoxicity. *Immunity* **40**, 949-960 (2014).
187. J. M. Curtsinger, J. O. Valenzuela, P. Agarwal, D. Lins, M. F. Mescher, Type I IFNs provide a third signal to CD8 T cells to stimulate clonal expansion and differentiation. *J Immunol* **174**, 4465-4469 (2005).

188. G. A. Kolumam, S. Thomas, L. J. Thompson, J. Sprent, K. Murali-Krishna, Type I interferons act directly on CD8 T cells to allow clonal expansion and memory formation in response to viral infection. *J Exp Med* **202**, 637-650 (2005).

189. K. B. Nguyen *et al.*, Coordinated and distinct roles for IFN-alpha beta, IL-12, and IL-15 regulation of NK cell responses to viral infection. *J Immunol* **169**, 4279-4287 (2002).

190. J. Martinez, X. Huang, Y. Yang, Direct action of type I IFN on NK cells is required for their activation in response to vaccinia viral infection in vivo. *J Immunol* **180**, 1592-1597 (2008).

191. I. Hwang *et al.*, Activation mechanisms of natural killer cells during influenza virus infection. *PLoS One* **7**, e51858 (2012).

192. K. Fink *et al.*, Early type I interferon-mediated signals on B cells specifically enhance antiviral humoral responses. *Eur J Immunol* **36**, 2094-2105 (2006).

193. E. S. Coro, W. L. Chang, N. Baumgarth, Type I IFN receptor signals directly stimulate local B cells early following influenza virus infection. *J Immunol* **176**, 4343-4351 (2006).

194. W. E. Purtha, K. A. Chachu, H. W. t. Virgin, M. S. Diamond, Early B-cell activation after West Nile virus infection requires alpha/beta interferon but not antigen receptor signaling. *J Virol* **82**, 10964-10974 (2008).

195. A. J. Sadler, B. R. Williams, Interferon-inducible antiviral effectors. *Nat Rev Immunol* **8**, 559-568 (2008).

196. U. Muller *et al.*, Functional role of type I and type II interferons in antiviral defense. *Science* **264**, 1918-1921 (1994).

197. M. J. Ciancanelli *et al.*, Infectious disease. Life-threatening influenza and impaired interferon amplification in human IRF7 deficiency. *Science* **348**, 448-453 (2015).

198. M. D. Hyrcza *et al.*, Distinct transcriptional profiles in ex vivo CD4+ and CD8+ T cells are established early in human immunodeficiency virus type 1 infection and are characterized by a chronic interferon response as well as extensive transcriptional changes in CD8+ T cells. *J Virol* **81**, 3477-3486 (2007).

199. C. J. Pfau *et al.*, Arenaviruses. *Intervirology* **4**, 207-214 (1974).

200. R. N. Charrel, X. de Lamballerie, Arenaviruses other than Lassa virus. *Antiviral Res* **57**, 89-100 (2003).

201. K. M. Johnson, M. L. Kuns, R. B. Mackenzie, P. A. Webb, C. E. Yunker, Isolation of Machupo virus from wild rodent Calomys callosus. *Am J Trop Med Hyg* **15**, 103-106 (1966).

202. R. B. Tesh *et al.*, Field studies on the epidemiology of Venezuelan hemorrhagic fever: implication of the cotton rat Sigmodon alstoni as the probable rodent reservoir. *Am J Trop Med Hyg* **49**, 227-235 (1993).

203. J. N. Mills *et al.*, Prevalence of infection with Junin virus in rodent populations in the epidemic area of Argentine hemorrhagic fever. *Am J Trop Med Hyg* **51**, 554-562 (1994).

204. B. E. Vanzee *et al.*, Lymphocytic choriomeningitis in university hospital personnel. Clinical features. *Am J Med* **58**, 803-809 (1975).

205. A. R. Hinman *et al.*, Outbreak of lymphocytic choriomeningitis virus infections in medical center personnel. *Am J Epidemiol* **101**, 103-110 (1975).
206. L. L. Barton *et al.*, Congenital lymphocytic choriomeningitis virus infection in twins. *Pediatr Infect Dis J* **12**, 942-946 (1993).
207. E. Traub, A Filterable Virus Recovered from White Mice. *Science* **81**, 298-299 (1935).
208. R. M. Zinkernagel, P. C. Doherty, Restriction of in vitro T cell-mediated cytotoxicity in lymphocytic choriomeningitis within a syngeneic or semiallogeneic system. *Nature* **248**, 701-702 (1974).
209. R. M. Zinkernagel, P. C. Doherty, Immunological surveillance against altered self components by sensitised T lymphocytes in lymphocytic choriomeningitis. *Nature* **251**, 547-548 (1974).
210. M. B. A. Oldstone, Biology and Pathogenesis of Lymphocytic Choriomeningitiis Virus Infection. *in Curr. Top. Microb. Immunol.* **263**, 83-117 (2002).
211. L. Flatz, A. Bergthaler, J. C. de la Torre, D. D. Pinschewer, Recovery of an arenavirus entirely from RNA polymerase I/II-driven cDNA. *Proc Natl Acad Sci U S A* **103**, 4663-4668 (2006).
212. A. B. Sanchez, J. C. de la Torre, Rescue of the prototypic Arenavirus LCMV entirely from plasmid. *Virology*, (2006).
213. M. Salvato, E. Shimomaye, P. Southern, M. B. Oldstone, Virus-lymphocyte interactions. IV. Molecular characterization of LCMV Armstrong (CTL+) small genomic segment and that of its variant, Clone 13 (CTL-). *Virology* **164**, 517-522. (1988).
214. M. Salvato, E. Shimomaye, M. B. Oldstone, The primary structure of the lymphocytic choriomeningitis virus L gene encodes a putative RNA polymerase. *Virology* **169**, 377-384. (1989).
215. M. S. Salvato, E. M. Shimomaye, The completed sequence of lymphocytic choriomeningitis virus reveals a unique RNA structure and a gene for a zinc finger protein. *Virology* **173**, 1-10. (1989).
216. B. W. Neuman *et al.*, Complementarity in the supramolecular design of arenaviruses and retroviruses revealed by electron cryomicroscopy and image analysis. *J Virol* **79**, 3822-3830 (2005).
217. M. Perez, R. C. Craven, J. C. De La Torre, The small RING finger protein Z drives arenavirus budding: Implications for antiviral strategies. *Proc Natl Acad Sci U S A* **100**, 12978-12983 (2003).
218. B. S. Parekh, M. J. Buchmeier, Proteins of lymphocytic choriomeningitis virus: antigenic topography of the viral glycoproteins. *Virology* **153**, 168-178 (1986).
219. M. Bruns, J. Cihak, G. Muller, F. Lehmann-Grube, Lymphocytic choriomeningitis virus. VI. Isolation of a glycoprotein mediating neutralization. *Virology* **130**, 247-251 (1983).
220. L. Hangartner *et al.*, Antiviral immune responses in gene-targeted mice expressing the immunoglobulin heavy chain of virus-neutralizing antibodies. *Proc Natl Acad Sci U S A* **100**, 12883-12888 (2003).
221. P. Penaloza-MacMaster *et al.*, Vaccine-elicited CD4 T cells induce immunopathology after chronic LCMV infection. *Science* **347**, 278-282 (2015).

222.	S. Moir, A. S. Fauci, B-cell exhaustion in HIV infection: the role of immune activation. *Curr Opin HIV AIDS* **9**, 472-477 (2014).
223.	B. Oliviero *et al.*, Enhanced B-cell differentiation and reduced proliferative capacity in chronic hepatitis C and chronic hepatitis B virus infections. *J Hepatol* **55**, 53-60 (2011).
224.	G. E. Weiss *et al.*, Atypical memory B cells are greatly expanded in individuals living in a malaria-endemic area. *J Immunol* **183**, 2176-2182 (2009).
225.	L. A. Labuda *et al.*, Alterations in peripheral blood B cell subsets and dynamics of B cell responses during human schistosomiasis. *PLoS Negl Trop Dis* **7**, e2094 (2013).
226.	S. A. Joosten *et al.*, Patients with Tuberculosis Have a Dysfunctional Circulating B-Cell Compartment, Which Normalizes following Successful Treatment. *PLoS Pathog* **12**, e1005687 (2016).
227.	M. Chen *et al.*, Limited humoral immunity in hepatitis C virus infection. *Gastroenterology* **116**, 135-143 (1999).
228.	M. S. Cohen, G. M. Shaw, A. J. McMichael, B. F. Haynes, Acute HIV-1 Infection. *N Engl J Med* **364**, 1943-1954 (2011).
229.	D. B. Peacock, J. V. Jones, M. Gough, The immune response to thetaX 174 in man. I. Primary and secondary antibody production in normal adults. *Clin Exp Immunol* **13**, 497-513 (1973).
230.	A. K. Wheatley, A. B. Kristensen, W. N. Lay, S. J. Kent, HIV-dependent depletion of influenza-specific memory B cells impacts B cell responsiveness to seasonal influenza immunisation. *Sci Rep* **6**, 26478 (2016).
231.	A. J. Cunnington, E. M. Riley, Suppression of vaccine responses by malaria: insignificant or overlooked? *Expert Rev Vaccines* **9**, 409-429 (2010).
232.	H. Pircher, K. Burki, R. Lang, H. Hengartner, R. M. Zinkernagel, Tolerance induction in double specific T-cell receptor transgenic mice varies with antigen. *Nature* **342**, 559-561 (1989).
233.	C. R. Bolen *et al.*, The blood transcriptional signature of chronic hepatitis C virus is consistent with an ongoing interferon-mediated antiviral response. *J Interferon Cytokine Res* **33**, 15-23 (2013).
234.	M. P. Berry *et al.*, An interferon-inducible neutrophil-driven blood transcriptional signature in human tuberculosis. *Nature* **466**, 973-977 (2010).
235.	J. N. Mandl *et al.*, Divergent TLR7 and TLR9 signaling and type I interferon production distinguish pathogenic and nonpathogenic AIDS virus infections. *Nat Med* **14**, 1077-1087 (2008).
236.	M. Rotger *et al.*, Comparative transcriptomics of extreme phenotypes of human HIV-1 infection and SIV infection in sooty mangabey and rhesus macaque. *J Clin Invest* **121**, 2391-2400 (2011).
237.	J. E. Schmitz *et al.*, Control of viremia in simian immunodeficiency virus infection by CD8+ lymphocytes. *Science* **283**, 857-860 (1999).
238.	H. C. Probst, M. van den Broek, Priming of CTLs by lymphocytic choriomeningitis virus depends on dendritic cells. *J Immunol* **174**, 3920-3924 (2005).

239. R. Wesolowski, J. Markowitz, W. E. Carson, 3rd, Myeloid derived suppressor cells - a new therapeutic target in the treatment of cancer. *J Immunother Cancer* **1**, 10 (2013).

240. B. A. Norris *et al.*, Chronic but not acute virus infection induces sustained expansion of myeloid suppressor cell numbers that inhibit viral-specific T cell immunity. *Immunity* **38**, 309-321 (2013).

241. R. Tussiwand *et al.*, Klf4 expression in conventional dendritic cells is required for T helper 2 cell responses. *Immunity* **42**, 916-928 (2015).

242. D. Macchia *et al.*, Membrane tumour necrosis factor-alpha is involved in the polyclonal B-cell activation induced by HIV-infected human T cells. *Nature* **363**, 464-466 (1993).

243. F. Muller, P. Aukrust, I. Nordoy, S. S. Froland, Possible role of interleukin-10 (IL-10) and CD40 ligand expression in the pathogenesis of hypergammaglobulinemia in human immunodeficiency virus infection: modulation of IL-10 and Ig production after intravenous Ig infusion. *Blood* **92**, 3721-3729 (1998).

244. L. Kacani, H. Stoiber, M. P. Dierich, Role of IL-15 in HIV-1-associated hypergammaglobulinaemia. *Clin Exp Immunol* **108**, 14-18 (1997).

245. D. G. Osmond, The turnover of B-cell populations. *Immunol Today* **14**, 34-37 (1993).

246. N. H. Kalhoro, J. Veits, S. Rautenschlein, G. Zimmer, A recombinant vesicular stomatitis virus replicon vaccine protects chickens from highly pathogenic avian influenza virus (H7N1). *Vaccine* **27**, 1174-1183 (2009).

247. C. Burkhart *et al.*, Localization of T helper cell epitopes in the vesicular stomatitis virus: the nucleoprotein is responsible for serotype cross-reactive T help. *Viral Immunol* **7**, 103-111 (1994).

248. N. Williams, N. Kraft, K. Shortman, The separation of different cell classes from lymphoid organs. VI. The effect of osmolarity of gradient media on the density distribution of cells. *Immunology* **22**, 885-899 (1972).

249. U. Kalinke *et al.*, The role of somatic mutation in the generation of the protective humoral immune response against vesicular stomatitis virus. *Immunity* **5**, 639-652 (1996).

250. A. Bergthaler, D. Merkler, E. Horvath, L. Bestmann, D. D. Pinschewer, Contributions of the LCMV glycoprotein and polymerase to strain-specific differences in murine liver pathogenicity. *J Gen Virol* **88**, 592-603 (2007).

251. A. Dobin *et al.*, STAR: ultrafast universal RNA-seq aligner. *Bioinformatics* **29**, 15-21 (2013).

252. D. Gaidatzis, A. Lerch, F. Hahne, M. B. Stadler, QuasR: quantification and annotation of short reads in R. *Bioinformatics* **31**, 1130-1132 (2015).

253. R. C. Team, R: A language and environment for statistical computing. R Foundation for Statistical Computing, Vienna, Austria. . http://www.R-project.org/ (2015).

254. D. J. McCarthy, Y. Chen, G. K. Smyth, Differential expression analysis of multifactor RNA-Seq experiments with respect to biological variation. *Nucleic Acids Res* **40**, 4288-4297 (2012).

255. C. W. Law, Y. Chen, W. Shi, G. K. Smyth, voom: Precision weights unlock linear model analysis tools for RNA-seq read counts. *Genome Biol* **15**, R29 (2014).

256. Z. Gu, ComplexHeatmap: Making Complex Heatmaps. R package version 1.10.2. . https://github.com/jokergoo/ComplexHeatmap (2016).

257. V. E. Laubach, E. G. Shesely, O. Smithies, P. A. Sherman, Mice lacking inducible nitric oxide synthase are not resistant to lipopolysaccharide-induced death. *Proc Natl Acad Sci U S A* **92**, 10688-10692 (1995).

258. J. B. Roths, E. D. Murphy, E. M. Eicher, A new mutation, gld, that produces lymphoproliferation and autoimmunity in C3H/HeJ mice. *J Exp Med* **159**, 1-20 (1984).

259. L. Boring *et al.*, Impaired monocyte migration and reduced type 1 (Th1) cytokine responses in C-C chemokine receptor 2 knockout mice. *J Clin Invest* **100**, 2552-2561 (1997).

260. M. Prinz *et al.*, Distinct and nonredundant in vivo functions of IFNAR on myeloid cells limit autoimmunity in the central nervous system. *Immunity* **28**, 675-686 (2008).

261. M. Kreuzaler *et al.*, Soluble BAFF levels inversely correlate with peripheral B cell numbers and the expression of BAFF receptors. *J Immunol* **188**, 497-503 (2012).

262. R. Horai *et al.*, Production of mice deficient in genes for interleukin (IL)-1alpha, IL-1beta, IL-1alpha/beta, and IL-1 receptor antagonist shows that IL-1beta is crucial in turpentine-induced fever development and glucocorticoid secretion. *J Exp Med* **187**, 1463-1475 (1998).

263. R. Kuhn, K. Rajewsky, W. Muller, Generation and analysis of interleukin-4 deficient mice. *Science* **254**, 707-710 (1991).

264. M. Kopf *et al.*, Impaired immune and acute-phase responses in interleukin-6-deficient mice. *Nature* **368**, 339-342 (1994).

265. R. C. Rickert, J. Roes, K. Rajewsky, B lymphocyte-specific, Cre-mediated mutagenesis in mice. *Nucleic Acids Res* **25**, 1317-1318 (1997).

266. R. Kuhn, J. Lohler, D. Rennick, K. Rajewsky, W. Muller, Interleukin-10-deficient mice develop chronic enterocolitis. *Cell* **75**, 263-274 (1993).

267. W. P. Fung-Leung *et al.*, CD8 is needed for development of cytotoxic T cells but not helper T cells. *Cell* **65**, 443-449 (1991).

268. J. Magram *et al.*, IL-12-deficient mice are defective in IFN gamma production and type 1 cytokine responses. *Immunity* **4**, 471-481 (1996).

269. P. P. Lee *et al.*, A critical role for Dnmt1 and DNA methylation in T cell development, function, and survival. *Immunity* **15**, 763-774 (2001).

270. M. L. Caton, M. R. Smith-Raska, B. Reizis, Notch-RBP-J signaling controls the homeostasis of CD8- dendritic cells in the spleen. *J Exp Med* **204**, 1653-1664 (2007).

271. B. E. Clausen, C. Burkhardt, W. Reith, R. Renkawitz, I. Forster, Conditional gene targeting in macrophages and granulocytes using LysMcre mice. *Transgenic Res* **8**, 265-277 (1999).

272. B. C. Schaefer, M. L. Schaefer, J. W. Kappler, P. Marrack, R. M. Kedl, Observation of antigen-dependent CD8+ T-cell/ dendritic cell interactions in vivo. *Cell Immunol* **214**, 110-122 (2001).

273. J. C. Grimaldi *et al.*, Depletion of eosinophils in mice through the use of antibodies specific for C-C chemokine receptor 3 (CCR3). *J Leukoc Biol* **65**, 846-853 (1999).

274. M. Battegay *et al.*, Quantification of lymphocytic choriomeningitis virus with an immunological focus assay in 24- or 96-well plates. *J Virol Methods* **33**, 191-198 (1991).

275. S. Rose, A. Misharin, H. Perlman, A novel Ly6C/Ly6G-based strategy to analyze the mouse splenic myeloid compartment. *Cytometry A* **81**, 343-350 (2012).

276. D. J. West, G. B. Calandra, Vaccine induced immunologic memory for hepatitis B surface antigen: implications for policy on booster vaccination. *Vaccine* **14**, 1019-1027 (1996).

277. A. Weinberg *et al.*, Varicella-zoster virus-specific immune responses to herpes zoster in elderly participants in a trial of a clinically effective zoster vaccine. *J Infect Dis* **200**, 1068-1077 (2009).

278. B. Odermatt, M. Eppler, T. P. Leist, H. Hengartner, R. M. Zinkernagel, Virus-triggered acquired immunodeficiency by cytotoxic T-cell-dependent destruction of antigen-presenting cells and lymph follicle structure. *Proc Natl Acad Sci U S A* **88**, 8252-8256 (1991).

279. J. P. Ray *et al.*, Transcription factor STAT3 and type I interferons are corepressive insulators for differentiation of follicular helper and T helper 1 cells. *Immunity* **40**, 367-377 (2014).

280. K. D. Cook, H. C. Kline, J. K. Whitmire, NK cells inhibit humoral immunity by reducing the abundance of CD4+ T follicular helper cells during a chronic virus infection. *J Leukoc Biol* **98**, 153-162 (2015).

281. M. Kitano *et al.*, Bcl6 protein expression shapes pre-germinal center B cell dynamics and follicular helper T cell heterogeneity. *Immunity* **34**, 961-972 (2011).

282. B. J. Hebeis *et al.*, Activation of virus-specific memory B cells in the absence of T cell help. *J Exp Med* **199**, 593-602 (2004).

283. A. Jegerlehner *et al.*, Carrier induced epitopic suppression of antibody responses induced by virus-like particles is a dynamic phenomenon caused by carrier-specific antibodies. *Vaccine* **28**, 5503-5512 (2010).

284. L. A. Herzenberg, T. Tokuhisa, Epitope-specific regulation. I. Carrier-specific induction of suppression for IgG anti-hapten antibody responses. *J Exp Med* **155**, 1730-1740 (1982).

285. D. L. Barber *et al.*, Restoring function in exhausted CD8 T cells during chronic viral infection. *Nature* **439**, 682-687 (2006).

286. V. Velu *et al.*, Enhancing SIV-specific immunity in vivo by PD-1 blockade. *Nature* **458**, 206-210 (2009).

287. Y. Zhang, S. Huang, D. Gong, Y. Qin, Q. Shen, Programmed death-1 upregulation is correlated with dysfunction of tumor-infiltrating CD8+ T lymphocytes in human non-small cell lung cancer. *Cell Mol Immunol* **7**, 389-395 (2010).

288. D. G. Brooks *et al.*, Interleukin-10 determines viral clearance or persistence in vivo. *Nat Med* **12**, 1301-1309 (2006).

289. M. Beyer *et al.*, Tumor-necrosis factor impairs CD4(+) T cell-mediated immunological control in chronic viral infection. *Nat Immunol* **17**, 593-603 (2016).

# Contributions to the work

The vast majority of the experiments and analyses presented here were conducted by myself with the technical assistance of Karen Cornille. The experiments contributing to the following figures were performed by Kerstin Narr in our laboratory: Figure 2H; Figure 4D and I; Figure S2D; Figure S4H; Figure S6B-D. The experiments contributing to the following figures were preformed by Yusuf Ismail Ertuna in our laboratory: Figure 1I, L and M; Figure 4H; Figure S1D and Figure S6A. Preliminary work on the KL25HL mice has been done by Melissa Remy and Rami Sommerstein, former members of our laboratory. Immunofluorescence stainings were performed and analyzed by Ingrid Wagner, Séverine Clément and Mario Kreutzfeldt in the laboratory of Professor Doron Merkler at the University of Geneva.

# Acknowledgments

This work would not have been possible without the help and support of many people, I would like to thank everyone who contributed.

Thank you Daniel for giving me the opportunity to work in your lab and for the great support you have offered. Thank you for your optimism towards our projects in almost all situations, for your encouragements, for your trust, and for the intense brain storming sessions. I am very grateful for all I've learned during the five years in your lab from molecular cloning to *in vivo* experimentation, including domestication of capricious creatures such as the Fortessa.

I would like to thank the members of my committee: Prof. Christoph Hess, thank you for accepting to be my faculty representative and for taking the time to evaluate my work. Thank you very much also to Prof. Otto Haller for travailing to Basel for my committee meetings as well as for my thesis defense and for evaluating my work.

I would like to thank all the past and present members of the lab. Especially, thank you Melissa for taking me under your wing when I first arrived in the lab. Just after graduating from medical school I had not much clue about basic research and on how to hold a pipet or a mouse. I would have been quite lost without you. Thank you for your patience (that's not a typing mistake), you always took the time to carefully explain everything you and others did in the lab and everything you knew. It was really great not only to work with you but also to hike, ski or party with you. A big thank you to the B cell team: thank you Kerstin, Karen and Yusuf, for you priceless help in this difficult project and for the very fruitful and friendly collaboration. It was also a great pleasure to work with you. Thank you Karen for your excellent work and for the good company during the many hours spent together in the mouse house or in the P2. The collagenase sessions would not have been the same without you. Thanks for being a great "binôme". Je te souhaite tout le meilleur pour la suite et beaucoup de bonheur avec ta famille qui s'agrandit. A special thank you to Sandra: it was really nice to share this adventure in the Pinschi lab with you from the beginning in Geneva to the end in Basel. Thank you for your great support and clever advices in many experimental but also social and psychological matters. Thanks a lot for the nice

# Curriculum Vitae

Bénédict Fallet                                 Date of Birth : 19.02.1985
Jungstrasse 9                                   Citizenship : Swiss
4056 Basel
076 679 40 39
Benedict.Fallet@unibas.ch

## Education

| | | |
|---|---|---|
| **2014 - 2016** | **Swiss MD-PhD program** (Swiss National Science Foundation Fellowship) *Universität Basel* | |
| **2011 – 2013** | **Swiss MD-PhD program** *Université de Genève* | |
| **2004 – 2011** | **Medical school** *Université de Genève* | |
| **2000 – 2004** | **High School** (Major: Biology & Chemistry) *Collège Calvin, Genève* | |

## Diplomas

| | | |
|---|---|---|
| **2015** | **Doctor of medicine (MD)** *Medizinische Fakultät, Universität Basel* | |
| **2011** | **Federal Diploma of Medicine** *Faculté de Médecine, Université de Genève* | |
| **2004** | **High school diploma** (Major: Biology & Chemistry) *Collège Calvin, Genève* | |

## Scientific Publications

**2016**    **Fallet B**, Narr K, Ertuna YI, Remy M, Sommerstein R, Cornille K, Kreutzfeldt M, Page N, Zimmer G, Geier F, Straub T, Pircher H, Larimore K, Greenberg PD, Merkler D, Pinschewer DD: Interferon-driven deletion of antiviral B cells at the onset of chronic infection. *Science Immunology,* Vol.1, Issue 4, DOI: 10.1126/sciimmunol.aah6817, (2016).

**2016**    Sammicheli S, Kuka M, Di Lucia P, de Oya NJ, De Giovanni M, Fioravanti J, Cristofani C, Maganuco CG, **Fallet B**, Ganzer L, Sironi L, Mainetti M, Ostuni R, Larimore K, Greenberg PD, de la Torre JC, Guidotti

LG, Iannacone M: Inflammatory monocytes hinder antiviral B cell responses. *Science Immunology,* Vol.1, Issue 4, DOI: 10.1126/sciimmunol.aah6789, (2016).

## Experience in the medical field

**2010-2011**    **Internships "Praktisches Jahr"**
- Internal Medicine (three month), *Geneva University Hospital,*
- Basic research (two month), *Division of Immunology and Allergology, Geneva University Hospital*
- Tropical medicine and global health (two month), *Division of Infectious disease, Hospital Carlos Andrade Marin, Ecuador*
- Neurology (one month), *Division of Neurology, Geneva University Hospital*
- Child and Adolescent Psychiatry, *"Office médico-pédagogique", Department of Public Education*

**Medical student placements**

**2009**
- Pediatrics, *Vivantes-Klinikum im Friedrichshain, Berlin*
- Surgery, *Charité Hospital, campus Virschow, Berlin*

**2007**
- Pediatrics*, Pediatric Medical Center Persis, Ouahigouya, Burkina Faso*

## Languages

**French**    Mother Language
**German**    Advanced
**English**    Advanced
**Spanish**    Basic knowledge